Polyoxometalates: Very Large Clusters—Nanoscale Magnets

Achim Müller* and Frank Peters

Fakultät für Chemie, Universität Bielefeld, Postfach 100131, 33501 Bielefeld, Germany

Michael T. Pope*

Department of Chemistry, Georgetown University, Box 571227, Washington, D.C. 20057, USA

Dante Gatteschi*

Dipartimento di Chimica, Universitá di Firenze, Via G. Capponi 9, 50121 Firenze, Italy

Received September 24, 1997 (Revised Manuscript Received November 17, 1997)

> I can hardly doubt that when we have some control of the arrangement of things on a small scale we will get an enormously greater range of possible properties that substances can have.
>
> *R. P. Feynman*[1]

I. Introduction

In every branch of science in which structured spatial objects have to be analyzed, essentially one and the same basic strategy is used: one decomposes, at least mentally, the given objects into elementary building blocks (e.g., polygons, polyhedra or aggregates of these) and then tries to identify and explore the local matching rules according to which the building blocks are to be assembled to yield the considered objects. Our subject, the structural chemistry of large polyoxometalate clusters, is archetypal for this basic procedure of science.

Generally speaking, the chemist, and in particular the inorganic chemist concentrating on polyoxometa-

S0009-2665(96)00394-9 CCC: $30.00
Published on Web 01/21/1998

Achim Müller, born in Detmold, Germany, studied Chemistry and Physics at the University of Göttingen and received his Ph.D. (1965) and his Habilitation (1967) there under the supervision of O. Glemser. He is now Professor of Inorganic Chemistry at the University of Bielefeld. His research interests range from problems of molecular physics (theory of mass influence on molecular constants), vibrational spectroscopy (matrix isolation spectroscopy, band contour analysis, resonance Raman effect, metal isotope effects), bioinorganic chemistry (model compounds and biological nitrogen fixation by free-living organisms), molecular metal chalcogenide complexes and clusters (synthesis, geochemical relevance, electronic and molecular structure, topological aspects, and their usage in heterogeneous catalysis), and supramolecular chemistry to aspects of philosophy of science. He has received national and international recognitions.

Frank Peters was born in Paderborn, Germany, and, after completing an apprenticeship, studied chemistry at the University of Bielefeld. Following a visit to Queen Mary and Westfield College, London, England, he received his Diploma (1995) at Bielefeld under the supervision of A. Müller. He is currently in the second year of his Ph.D. with A. Müller.

Michael T. Pope was born in Exeter, England, and was educated at Oxford University (D.Phil. with R. J. P. Williams). Following postdoctoral research at Boston University (L. C. W. Baker) he spent three years with Laporte Industries Ltd. in England. He came to Georgetown University in 1962 and has been Full Professor there since 1973 (Department Chair 1990–96). His research activities at Georgetown have focused on all aspects of the chemistry, structures, and applications of polyoxoanion complexes of the early transition metals. He is a recipient of a PRF International Award and a Senior Humboldt Award, and is author and author/editor of two books and some 150 papers and reviews on polyoxometalate chemistry.

Dante Gatteschi was born in Florence, Italy, in 1945. He graduated in Chemistry at the University of Florence in 1969. He became assistant of Professor Sacconi in the same university, and in 1980 became Professor of Inorganic Chemistry there in the Faculty of Pharmacy. His research interests lie in the electronic structure of low-symmetry transition-metal complexes, in EPR spectroscopy of transition metal ions, and more recently in molecular magnetism. During the last years he has focused on the magnetic properties of large spin clusters, stressing their role as nanosize magnets, which allowed for the first time the observation of quantum tunneling effects of magnetization in molecular clusters. He his the author of more than 300 publications in international journals, of one book on *EPR of Exchange Coupled Systems* and the editor of several books on molecular magnetism. In 1979 he was awarded by the Italian Chemical Society the Nasini prize, reserved for young inorganic chemists.

lates, is in a position to connect elementary building blocks and their derivatives in different ways, enabling him to synthesize a large variety of remarkable substances, especially those in the "nanoworld". Of particular importance in this context are the anionic-type species which have $\{MO_x\}$-type building-block units, where M stands for the d block elements in high oxidation states.[2−4]

For the chemist, three basic areas within the material world are distinguishable by the very different size of the related species: The world of small molecular systems, that of the substances, and the intervening area between these two, all of which occur within chemistry based on transition metal−oxide systems. By acidifying solutions of mononuclear oxoanions (like WO_4^{2-}), first (polynuclear) polyoxoanions (POMs) including the large and giant species reported in this review are obtained, and subsequently the oxides (like $WO_3 \cdot 2H_2O$) with typical extended solid-state structures are formed as precipitates. In this review our interest will be focused on POMs of large or extreme size with their fascinating and extensive structural variety. Their structures are based on different types of linking of $\{MO_x\}$ polyhedra, whereby the species are formed by a kind of self-assembly process.

A fascinating aspect is the self-assembly process leading to aggregates, which can be linked in different ways. This type of unit-construction principle seems to be archetypal for polyoxometalate chemistry. It is now possible to enter the "nanoworld" step-by-step by means of (directed) self-assembly processes. This designates the goal of current chemical research in this area, that of generating nanosized molecular materials deliberately from units with well-defined properties, for instance molecular magnets as reported here. Since a considerable number of very large polyoxometalate clusters have been reported in recent years, it seems worthwhile to review the present state of art.

II. General Aspects

Although the basic structural principle for polyoxovanadates, molybdates, and tungstates is the same—since the structures are governed by the principle that each metal atom occupies an $\{MO_x\}$ coordination polyhedron, in which the metal atom is displaced, as a result of M−O π bonding, toward those polyhedral vertexes that form the surface of the structure—a more detailed view of this fascinating area of chemistry shows striking differences for the three compound types also with respect to the very large cluster systems discussed here.

In contrast to the vanadate and molybdate species, the structures of very large polytungstate anions (defined for the purposes of this review as those species with 20 or more tungsten atoms) may practically all be represented in terms of subunits based on lacunary fragments of the Keggin anion (with the classical archetypal $\{W^{VI}_3O_{13}\}$ units) or its isomers. This can, in principle, be attributed to the high stability of the related species, which is probably due to the existence of extremely weak but not negligible W−W interactions in the $\{W_3\}$ triangles.[2]

An important characteristic of polyoxovanadates is the occurrence of different basic types of polyhedra ($\{VO_4\}$, $\{VO_5\}$, and $\{VO_6\}$) whereby the pyramidal $\{O{=}VO_4\}$ polyhedra show a tendency to form cluster shells or cages which have topological similarities to the fullerenes and structural relations to the layers of V_2O_5.[5,6]

Most of the very large mixed-valence polyoxomolybdates now known can be considered as being based on the same or similar building-block unit (like $\{Mo_8\}$ or $\{Mo_{17}\}$) which can be linked in different ways directly or via other coordinating centers. Using these types of linking interesting growth processes have been found, which have led to novel types of large ring or wheel-shaped systems with 154, 176, and even more Mo atoms. The classical $\{Mo_3O_{13}\}$ fragment seems to be less important and to have a much smaller formation tendency (at least with respect to reduced systems) compared to the tungstates. As the chemistry of the polyoxometalates of different early transition elements is rather variable, also the assumed lower limit for the number of metal atoms of the large clusters considered here varies (V_n, $n \geq 19$; Mo_n, $n \geq 24$; W_n, $n \geq 20$).

How is it possible to synthesize even larger molecular constructions, for example, clusters, in a range we shall call mesoscopic? (In this context it is of course a challenge to investigate the area where quantum and classical effects coexist.) A useful strategy certainly is to generate in solution relatively large, directly linkable intermediates by a self-assembly process (for instance Keggin ions with lacunary structures) and to use these as educts, e.g., together with cationic metal centers as linkers.[7,8] Generally speaking, the quasi-preorganized building blocks abundant in solution can either be combined directly or linked by cations thus forming giant species.[7,9] This step of course requires an intrinsic knowledge of the system. In general, it is important to secure high solubility of the intermediates—for instance through the high negative charge of reduced species—in order to prevent uncontrolled linking or precipitation occurring too early.

The following related model example can be pursued for demonstration: substitution of more positive by formally less positive metal centers M—for example, by replacing Mo^{VI} by V^{IV} centers in the α-Keggin-type anion $[Mo_{12}XO_{40}]^{3-}$ (X = P, As)—results in highly negatively charged (nucleophilic) intermediates. These can either be stabilized or capped by electrophilic species or connected by cations to give larger moieties.[7,10,11] In the case of $[Mo_{12}AsO_{40}]^{3-}$ the intermediate species $\{Mo^{VI}_8V^{IV}_4As^{V}O_{40}\}^{11-}$, formed according to the above formalism, can be stabilized, for example by As^{III} centers, yielding the $[As^{III}_2Mo^{VI}_8V^{IV}_4As^{V}O_{40}]^{5-}$ cluster. In the absence of As^{III} and presence of the reducing agent NH_2OH further condensation occurs.[7,11] A large $\{Mo_{17}\}$ fragment (see below) is formed as an intermediate that can, formally as a reactive, highly negatively charged and transferable ligand, be connected in various ways by metal cations or cationic groups (e.g. VO^{2+}/Fe^{III}/MoO_2^{2+}) to yield large molecular constructions. The substitution $\{MoO\}^{4+} \rightarrow \{MoNO\}^{3+}$ leads to an increase in charge of the related species or intermediates, too.[7,11]

Hydroxylamine is a reducing agent often used for the preparation of large or giant polyoxomolybdates. In this respect, but also because of its historic interest [the first large polymolybdate, the red $[Mo_{36}(NO)_4O_{108}(H_2O)_{16}]^{12-}$ species, was (very probably) prepared in 1931 by Jakób and Jezowska[12]], this type of reaction of aqueous molybdate solution with hydroxylamine is worth discussing. It can lead in general to different types of polynuclear oxo [or in the presence of S_x^{2-} ions to (poly)sulfido[13]] molybdates, whereby the hydroxylamine, besides generating the $\{MoNO\}^{3+}$ group,[14] may lead to the reduction of other Mo centers. The structure of the yellow precipitate first formed is still unknown and contains most likely a polyoxomolybdate ion with NO groups and hydroxylamine.[15] The $\{MoNO\}^{3+}$ group can, generally speaking, act as a robust unit and link sulfide/polysulfide ions[13] or polymolybdate-based fragments[9,16] (see section V.E[17]).

As an empirical rule we can state that upon increasing the size of polyoxometalates, the charge density on the anion has to be kept approximately constant (which means increasing the overall charge) in order to keep the anion in growth as a soluble,

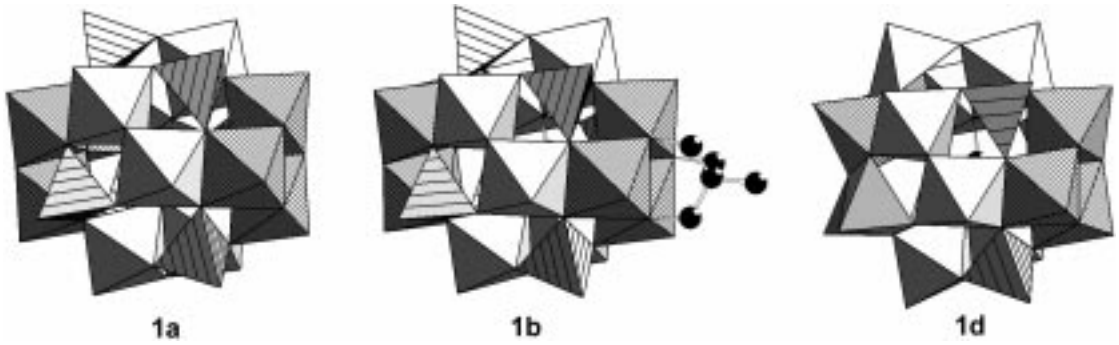

Figure 1. Structure of the clusters $[(VO_4)V_{18}O_{36}(OH)_{10}]^{7-}$ (**1a**), $[(VO_4)V_{18}O_{39}(OH)_7\{(CH_2)_3CCH_2OH\}]^{7-}$ (**1b**), and $[(VO_4)V_{18}O_{45}]^{9-}$ (**1d**) in polyhedral representation (a, $\{VO_4\}$ tetrahedra, hatched; $\{VO_6\}$ octahedra of the $\{V_3O_{13}\}$ poles, crosshatched; b, code as in a, plus carbon atoms of the organic ligand, black spheres; c, code as in a, but the left "pole"represents a $\{V_3O_{12}\}$ unit consisting of $\{VO_5\}$ square pyramids).

nonhydrolyzing entity in solution. An exception to this rule would be when the solubility of the large molecular system is due to other reasons, e.g., the presence of very many H_2O ligands. This has been proven as several very large ring-shaped hydrophilic polyoxomolybdates with more than 150 Mo atoms and a relatively low or extremely low negative charge can be isolated, even without $\{MoNO\}^{3+}$ (instead of $\{MoO\}^{4+}$) groups, which would increase the negative charge. These types of species were prepared with reducing agents such as $SnCl_2$. This means that in principle the presence of NH_2OH is not a necessary prerequisite for the formation of the very large ring-type structures mentioned in sections V.E.3 and V.E.4.[17,18]

III. Vanadates

The vanadates show more structural flexibility (based on a relatively large number of different types of $\{VO_x\}$ polyhedra, $x = 4, 5, 6$) compared for instance to the tungstates. A nice example is given by the *pure* vanadates with 19 atoms showing a range of different structures which are discussed in the next section.

A. $\{V_{19}\}$ Clusters

In the chiral anions $[(V^VO_4)V^{IV}_{12}V^V_6O_{36}(OH)_{10}]^{7-}$ (**1a**)[19,20] and $[(V^VO_4)V^{IV}_{12}V^V_6O_{39}(OH)_7\{(CH_2)_3CCH_2OH\}]^{7-}$ (**1b**)[20] two opposite $\{V^{IV}_3O_{13}\}$ units, twisted by 60° with respect to each other, form the "poles" of an ellipsoid cluster. The poles are connected by six $\{V^{IV}O_6\}$ octahedra and six $\{V^VO_4\}$ tetrahedra. The anions have approximate C_3 symmetry (D_3 without the central V atom) and are formally generated by linking twelve $\{VO_6\}$ octahedra (V^{IV}), six $\{VO_4\}$ tetrahedra (V^V), and the central $\{V^VO_4\}$ unit. All V^{IV} and V^V centers have octahedral and tetrahedral environment, respectively (Figure 1a,b).

In the racemic salt of **1a** and in the chiral salt of **1b** the V atom of the central $\{VO_4\}$ tetrahedron is disordered over two lattice sites in a ratio of 1:1. The 18 peripheral V atoms are joined by a μ_4-O and four μ_3-O atoms in the central part of the anion as well as by 12 μ_3-O and 15 μ_2-O atoms in the "outer shell". Of the latter, the nine μ_2-O atoms involved in the edge-sharing of two $\{VO_6\}$ octahedra are protonated. (The remaining six are unprotonated, each atom joining a $\{VO_6\}$ with a $\{VO_4\}$ unit.) The μ_3-O atom, located on the C_3 axis opposite the μ_4-O atom of the central tetrahedron, is protonated, too. Due to the disorder, the protonation is distributed equally over the two μ_3-O sites. In **1b**, one of the two $\{V^{IV}_3O_{13}\}$ pole units is "alkylated" by the organic tripod ligand $\{(CH_2)_3CCH_2OH\}^{3+}$, while the corresponding oxygen atoms of the corresponding opposite unit are protonated (Figure 1b).

Due to their relatively high charge density, units such as $\{V^{IV}_3O_{13}\}$ are not stable and are only abundant in condensed form in larger cluster aggregates. This is for instance the case for $[(V^VO_4)V^{IV}_{16}V^V_2O_{35}(OH)_7]^{6-}$ (**1c**) which is an α-Keggin derivative. The high charge of the unstable Keggin ion $\{(V^VO_4)V^{IV}_{12}O_{36}\}^{27-}$ is lowered by capping with six $\{VO^{2+}\}$ groups and protonation.[21] In the case of **1b**, one $\{V^{IV}_3O_{13}\}$ unit is shielded and its charge is decreased by means of an organic trifunctional ligand with appropriate geometry (see also ref 22). Due to its steric properties, it caps the $\{V^{IV}_3O_{13}\}$ unit nearly without strain and decreases its charge.

The anion $[(V^VO_4)V^{IV}_6V^V_{12}O_{45}]^{9-}$ (**1d**),[23] which was only very recently reported, has the same symmetry as **1a** and **1b** and is also formally generated by 18 $\{VO_n\}$ polyhedra ($n = 4, 5, 6$) with 12 V^V centers in tetrahedral and octahedral environments, surrounding an almost regular $\{VO_4\}$ tetrahedron. In contrast to **1a** and **1b**, the central tetrahedron appears not to be disordered in the crystal. The twisted pole units, mentioned above for **1a** and **1b**, are also present. However, it is of special interest that one of the two pole units is formed by three $\{VO_5\}$ square pyramids (instead of octahedra as in **1a** and **1b**) building a $\{V_3O_{12}\}$ unit (Figure 1c). The pole units are connected by three $\{V^VO_4\}$ tetrahedra and nine $\{V^{IV/V}O_6\}$ octahedra. A similar $\{V_{19}O_{49}\}$ cluster, as yet not well-characterized, was reported by Johnson.[24,25]

B. $\{Mn_2V_{22}\}$ with Two Decavanadate-Type Moieties

The anion $[(MnV_9O_{28})V_2O_4]_2^{10-}$ ($\{Mn_2V_{22}\}$, **2**) consists of two $\{Mn^{IV}V^V_9\}$ decavanadate-type moieties

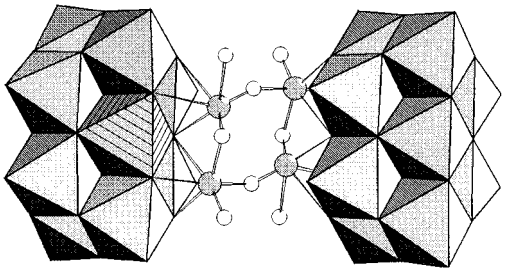

Figure 2. Structure of the cluster anion $[(MnV_9O_{28})\text{-}V_2O_4]_2^{10-}$ (**2**). The decavanadate $\{MnV_9\}$-type moieties are shown in polyhedral representation ($\{MnO_6\}$ octahedra, hatched; $\{VO_6\}$ octahedra, gray; bridging V centers, gray spheres; O atoms of the bridge, small white spheres).

capped and linked by two $\{V_2O_4\}$ groups.[26] The fragments are connected via two V−O−V bridges. All V atoms have a (distorted) octahedral coordination environment (Figure 2).

C. Structures Built up from $\{O{=}VO_4\}$ Pyramids: $\{V_{22}\}$ and $\{V_{34}\}$

In a novel type of reaction procedure cluster shells can be generated by linking fragments which depend to a large extent on size, shape, and charge of a template (in most cases anions) incorporated as guest in the final structure. The O=V···X interactions (*X* = nucleophilic template/anionic guest with small charge) do not direct the linking procedure strongly, so that the cluster shell can be considered as a kind of molecular container for only very weakly bonded guests. The V−O cluster-shell containers can be used as matrixes (cages) for anions with small charges.[5,27,28] Examples for related species are $[HV^{IV}_8V^{V}_{14}\text{-}O_{54}(ClO_4)]^{6-}$ (**3a**),[29] $[HV^{IV}_8V^{V}_{14}O_{54}(SCN)]^{6-}$ (**3b**),[28] and $[H_2V^{IV}_{10}V^{V}_{12}O_{54}(CH_3COO)]^{7-}$ (**3c**),[30] but also others of the $\{V_{18}O_{42}\}$ type with smaller anions as guests such as Cl^- and NO_3^- [5] (see also ref 31). The cluster shells of **3a**−**c**, which have approximate D_{2d} symmetry (Figure 3a,d) are formed by edge- and corner-sharing of tetragonal $\{O{=}VO_4\}$ pyramids, whereby ClO_4^-, SCN^-, CH_3COO^-, and $HMoO_4^-$ ions are encapsulated.

For this type of novel host−guest species the attractive and (the stronger) repulsive forces between the electrophilic (V^{n+}) and nucleophilic (O^{2-}) centers of the negatively charged shell and the enclosed guests only approximately balance each other. According to basic MO calculations of M. Bénard and co-workers on an ab initio level, the electrostatic potential inside related, overall negatively charged cluster cages is negative.[32] However, the consideration of the crystal environment[33] leads, due to the large number of cations in the crystal lattice, to positive values of the potential thus supporting our earlier intuitive assumption[5] that the cations of the crystal lattice have, at least for the highly charged anions, an important influence on the stabilization of this type of unusual polyoxovanadate host−guest system.

In **3a** the central ClO_4^- group is not disordered since very weak interactions of its O atoms with the V atoms of the shell seem to "fix" the "guest" ion. On the other hand, the SCN^- ion in **3b** (located on the S_4 axis) is disordered and appears to float within the carcerand, corresponding to the fact that the rather long V−(SCN) distances reveal only extremely weak interactions.[29,30]

A further important aspect of the relevant chemistry is that the templates can even be generated in the solutions themselves. A cubane-type "template" $\{(V_4O_4)O_4\}$ which has the same stoichiometry as amphoteric $V^{IV}O_2$ can be generated in situ in solution. As a (covalently bound) nucleus it strongly influences the type of linking of the $\{O{=}VO_4\}$ pyramids, and thus the generation of the cluster species $[\{(V^{IV}_4O_4)O_4\}V^{IV}_{12}V^{V}_{18}O_{74}]^{10-}$ (**4**). (The process is probably synergistic).[34] It displays approximate D_{2d} symmetry and consists of an ellipsoid-shaped $\{V_{30}O_{74}\}$ sheath, which is formed by linking 30 tetragonal $\{O{=}VO_4\}$ pyramids (see Figure 3b). The two identical $\{V_{15}O_{37}\}$ halves of the $\{V_{30}O_{74}\}$ shell are, as required by the geometry of the central $\{(V_4O_4)O_4\}$ unit, rotated by an angle of 90° with respect to each other. Each half contains 20 of the 24 O atoms spanning a complete O_{24} rhombicuboctahedron, a solid formed by the μ_2-O atoms of the α-Keggin ion and representing a basic building block in polyoxometalate chemistry. It comprises 12 square {110}

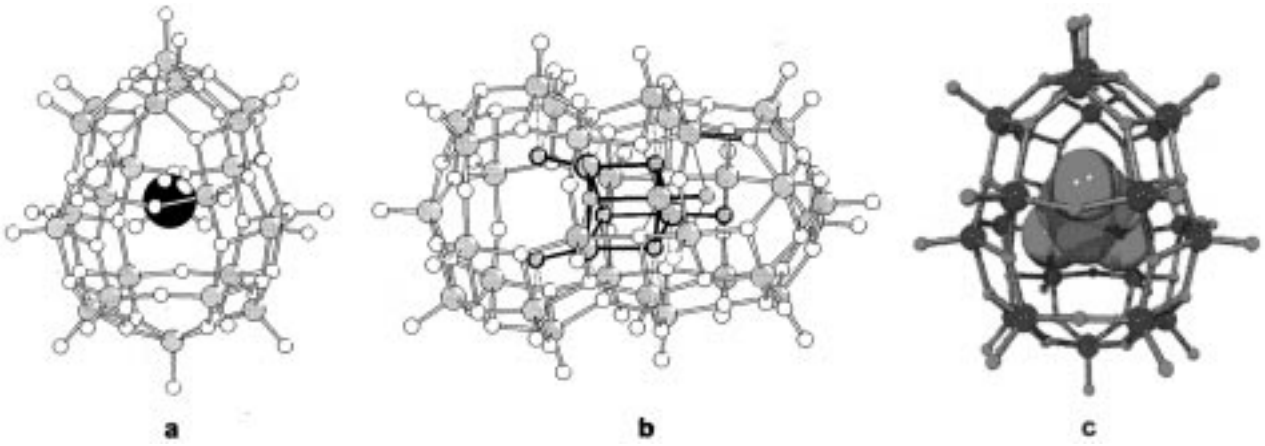

Figure 3. Ball-and-stick representation of the structure of $[HV_{22}O_{54}(ClO_4)]^{6-}$ (**3a**) (a, V centers, gray; O, white; Cl, black) and $[\{(V_4O_4)O_4\}V_{30}O_{74}]^{10-}$ (**4**) (b, code as in a; the central $\{(V_4O_4)O_4\}$ cube is emphasized by black lines). (c) Illustration of the host−guest character of **3a** with the central ClO_4^- guest shown in space-filling representation (V centers, blue; O, red; Cl, green).

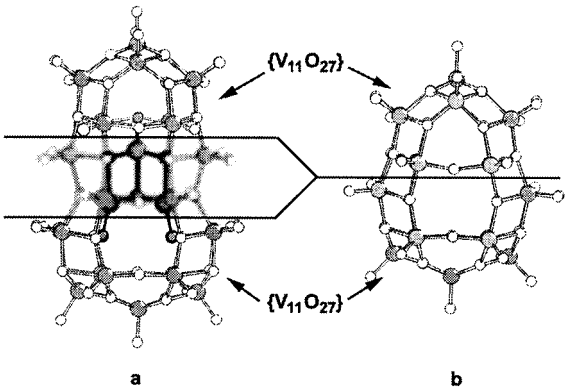

Figure 4. View of the structural correlation between the $\{V_{34}\}$ cluster **4** (a) and the $\{V_{22}\}$-type clusters **3a**−**c** (b). Formal removal of the two central {VO} layers of **4** (including the $\{(V_4O_4)O_4\}$ cube, visualized as blurred area), results in the two half-shells $\{V_{11}O_{27}\}$ of **3a**−**d**. For the $\{V_{22}\}$ cluster only the shell without guest is shown (b, V centers, gray; O, white).

and six {100} faces as well as eight {111} triangles.[35] Nine of the 12 {110} faces (all capped in the Keggin ion) and two of the unoccupied {100} faces of the rhombicuboctahedron are in **4** capped by a {V=O} group. Additionally, a novel type of capping occurs in **4**: above two {110} faces of the Keggin ion, each of which is flanked by two {111} triangles, the {V=O} group is replaced by an {O=V−O−V=O} unit.[34]

There is another type of interesting description: **4** consists of six almost planar V−O layers (with the exception of the $\{V_3O_7\}$ units at the poles), which are oriented perpendicular to the S_4 axis. The layers correspond to a distorted section of the NaCl lattice, whereby some central positions of the layers in the neighborhood of the poles are not occupied. Interestingly, by formal removal of the two middle layers ($\{V_{12}O_{28}\}$ fragments containing the central $\{(V_4O_4)O_4\}$ cube) with subsequent linking of the remaining $\{V_{11}O_{27}\}$ half shells, the shell of **3a**−**c** is formed (Figure 4), and the original (approximate) D_{2d} symmetry is retained. The relatively close packing of the O atoms here seems to be decisive for the stability of **3a**−**c** and especially of **4**.[29]

Note that the surfaces of different cluster shells formed from $\{O{=}VO_4\}$ pyramids (without terminal O atoms), e.g. those of $\{V_{22}O_{54}\}$ and $\{V_{30}O_{74}\}$ can be considered as segments of a layer of vanadium pentoxide (see Figure 5).[5,6] To some extent the pyramidal $\{O{=}VO_4\}$ unit dominates the structural hierarchy. Its mode of linking is in general partly directed by very weak O=V···X interactions (X = nucleophile) and results not only in molecular containers, but also in the layered structure of vanadium pentoxide (with the {V=O} groups as nucleophiles). A kind of template principle underlies the formation and stacking of the V_2O_5 layers: layer $n + 1$ forms on layer n through the weak O=V···O=V interactions. The corresponding interactions between the V_2O_5 layers are to some extent similar to those present in the container compounds of **3a**−**c**, although in these cases repulsive interactions between the negatively charged {V=O} groups certainly do influence the curvature of the shell. The interaction between the layers of the V_2O_5 lattice can also be

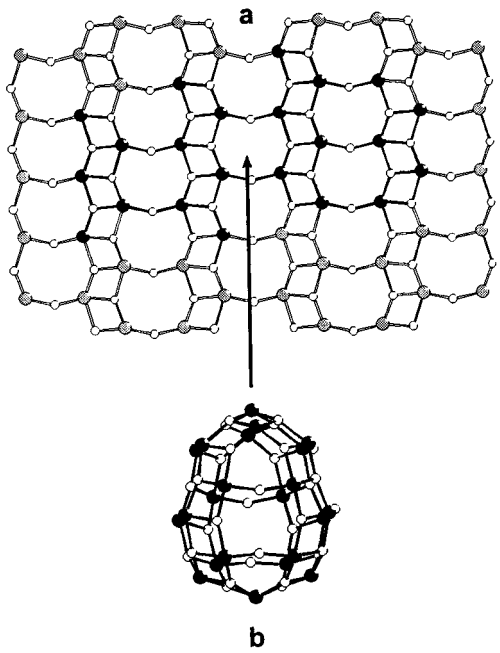

Figure 5. (a) View of a segment of a layer of V_2O_5 with the terminal oxygen atoms omitted (V centers, black and gray; O, white). Black lines and spheres show the $\{V_{22}\}$ sheet (see Figure 4) of the cluster shells of **3a**−**c**, which is presented separately in b.

compared with the $\{O_{term}{=}V(shell)\cdots O_{term}{=}V(cluster)\}$ interaction of the terminal atoms of the central $\{(V_4O_4)O_{4,term}\}$ cluster fragment with the shell of the anion of **4**.[27,30]

IV. Niobates

A. The $\{Al_2Eu_6Nb_{30}\}$ Cluster

In the cluster anion $[\{Eu^{III}{}_3O(OH)_3(OH_2)_3\}_2Al^{III}{}_2(Nb^{V}{}_6O_{19})_5]^{26-}$ ($\{Al_2Eu_6Nb_{30}\}$, **5**), which has approximate D_3 symmetry (Figure 6a), five hexaniobate groups $\{Nb_6O_{19}\}^{8-}$ ($\{Nb_6\}$) are interconnected by two $\{Eu_3O(OH)_3(OH_2)_3\}^{4+}$ ($\{Eu_3\}$) cluster fragments and two Al^{III} centers.[36a] Two types of $\{Nb_6\}$ groups are distinguishable: three equatorial groups on C_2 axes and two axial ones on the C_3 axis. The central core of the anion consists of two $\{Eu_3\}$ fragments arranged as parallel triangles in an antiprismatic way (Figure 6b) with the equatorial $\{Nb_6\}$ groups directly attached to four Eu centers of these triangles via Nb−O−Eu bridges. Each of the two axial $\{Nb_6\}$ groups is connected to one of the $\{Eu_3\}$ fragments via a bridging Al center, which is coordinated to three μ_2-O atoms of the $\{Nb_6\}$ and to three μ_2-O centers of the $\{Eu_3\}$ fragment. The isomorphous Er and Lu analogues of **5** have also been characterized.[36b,c]

V. Molybdates

These species—most of which are of the diamagnetic, mixed-valence type—show an extreme variety of complicated structures and therefore great significance is attached to structural details. If the ratio Mo^V/Mo^{VI} is high, structures are preferred with Mo^V−Mo^V pairs, while if it is smaller, highly delocalized systems with the characteristic dark-blue color (due to intervalence charge-transfer transitions) are favored.

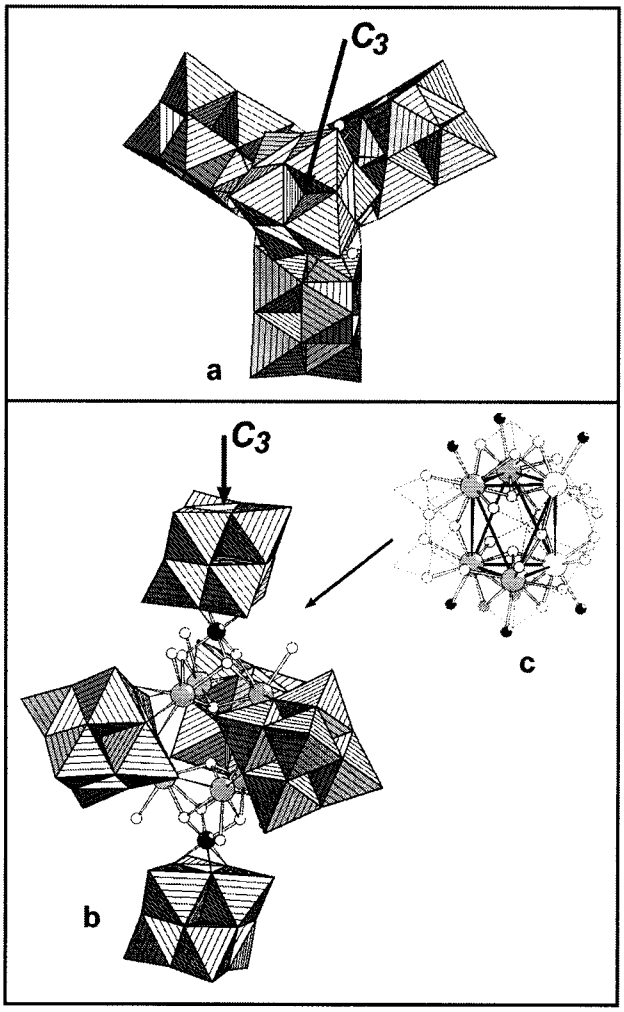

Figure 6. (a) Structure of the cluster $[\{Eu_3O(OH)_3\}(H_2O)_3\}_2Al_2(Nb_6O_{19})_5]^{26-}$ (**5**) with view along the C_3 axis showing four of the five $\{Nb_6\}$-type fragments. (b) View of the structure of **5** showing three "equatorial"$\{Nb_6\}$-type fragments connected to the central $\{Eu_3\}_2$ entity by Nb−O−Eu bridges and two "axial" $\{Nb_6\}$ fragments, which are linked to the central $\{Eu_3\}$-type fragment (see c) via an Al center ($\{NbO_6\}$ octahedra, hatched; Eu centers, gray spheres; Al, black spheres; O, white spheres). (c) Ball-and-stick model of the central $\{Eu_3\}_2$ core. The Eu centers form a trigonal antiprism depicted by black lines (code as in a, plus OH, small gray spheres; H_2O, small black spheres).

A. Clusters with $\{Mo_7\}$ Units: $\{Eu_4Mo_{29}\}$ and $\{Pr_8Mo_{58}\}$

The center of the cluster anion $[\{Eu^{III}(H_2O)_4\}_4(Mo^{VI}O_4)(Mo^{VI}{}_7O_{24})_4]^{14-}$ ($\{Eu_4Mo_{29}\}$, **6**) is built up by a distorted $\{MoO_4\}$ tetrahedron to the O atoms of which four Eu^{III} centers are coordinated.[37] These exhibit 9-fold coordination, whereby the different types of oxygen atoms form a tricapped trigonal prism. Besides the coordination to the central $\{MoO_4\}$ unit, each Eu center is further connected to three $\{Mo_7O_{24}\}$ ($\{Mo_7\}$) fragments as shown in Figure 7.

The anion $[Pr^{III}{}_4(Mo^{VI}O_4)(H_2O)_{13}(Mo^{VI}{}_7O_{24})_4]_2^{28-}$ ($\{Pr_8Mo_{58}\}$, **7**) can be considered as a "dimer" of $\{Pr_4Mo_{29}\}$ fragments, which are essentially equivalent to the $\{Eu_4Mo_{29}\}$ structure **6**. Compounds with different lanthanide cations (ranging from Ce to Dy, with the exception of Pm) and with Am centers have been synthesized to date; but only the Pr compound has been structurally characterized (Figure 8).[38,39] In the $\{Pr_4Mo_{29}\}$ fragment each Pr center exhibits 9-fold coordination and possesses four terminal H_2O ligands pointing outward and toward the cavity formed by two opposite $\{Mo_7\}$ fragments (Figure 8).

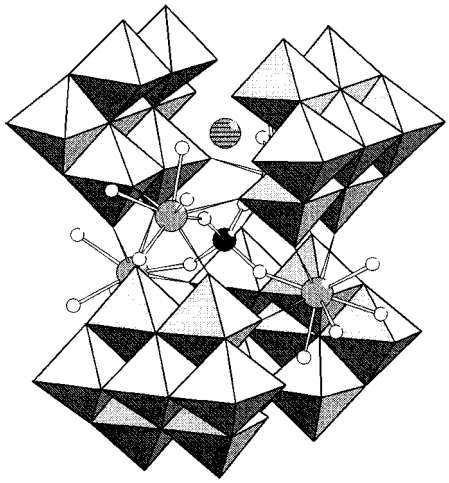

Figure 7. Structure of the anion $[\{Eu(H_2O)_4\}_4(MoO_4)(Mo_7O_{24})_4]^{14-}$ (**6**) with the heptamolybdate fragments in polyhedral representation (Mo center of the central MoO_4 unit, black sphere; Eu centers, gray; O, white; N center of NH_4^+ cation, hatched sphere). The $\{Mo_7\}$ fragments form two cavities occupied by NH_4^+ cations above and below the central MoO_4 group. The terminal oxygen ligands of the $\{EuO_9\}$ polyhedra are doubly protonated and point outward and to the cavity.

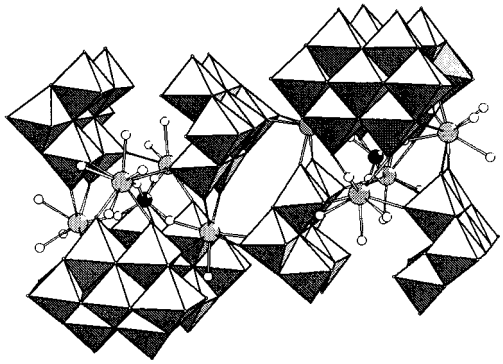

Figure 8. Structure of the cluster anion $[Pr_4(MoO_4)(H_2O)_{13}(Mo_7O_{24})_4]_2^{28-}$ (**7**) with heptamolybdate fragments ($\{Mo_7\}$) in polyhedral representation (Mo centers of the central $\{MoO_4\}$ tetrahedra, black; Pr centers, gray spheres). The two $\{Pr_4Mo_{29}\}$ fragments are linked via two Pr^{III} centers exhibiting 8-fold coordination. The cavity between the two $\{Pr_4Mo_{29}\}$ fragments, which are built up by four $\{Mo_7\}$ units, a central $\{MoO_4\}$ tetrahedron and four Pr centers, is occupied by H_2O molecules (not shown).

B. Clusters with Capped α-Keggin Cores: $\{Mo_{16}V_{14}\}$ and $\{(Mo_8V_7)_n\}$

The structure of the anion $[\{(V^VO_4)Mo^{VI}{}_8V^{IV}{}_4O_{36}(V^{IV}O)_2\}_2]^{14-}$ ($\{Mo_{16}V_{14}\}$, **8**) is based on the hypothetical α-Keggin ion $[(V^VO_4)Mo^{VI}{}_8V^{IV}{}_4O_{36}]^{11-}$ which has additional trans-capping $\{VO\}$ units.[40] Two of these units are condensed thus building the "dimer" **8** (see Figure 9a). Within **8**, layers spanned by four Mo and four V atoms respectively alternate. The distance between the V centers of the cap and those of the central V layer is ~4 Å, and that between the Mo

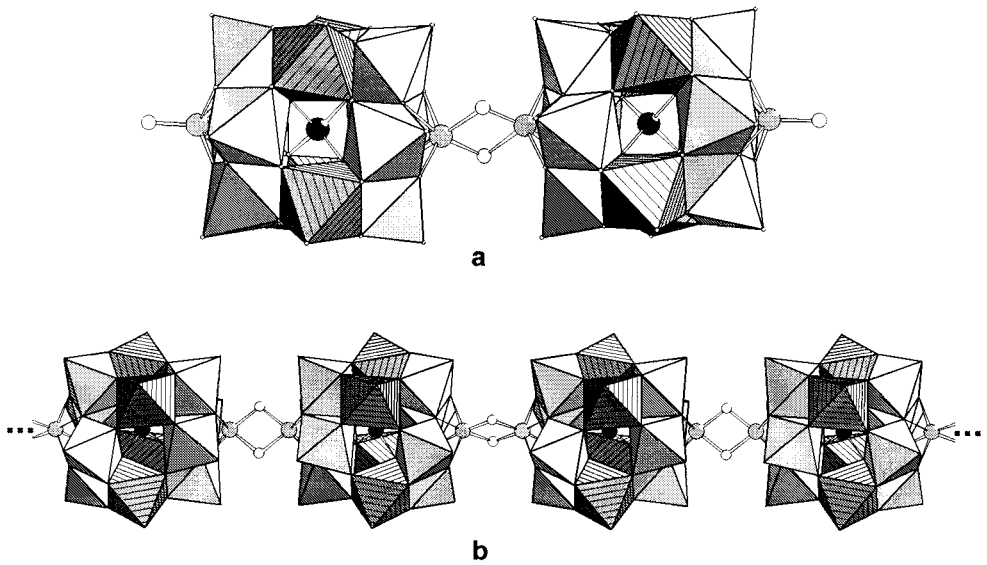

Figure 9. (a) Structure of the cluster anion $[\{(VO_4)Mo_8V_4O_{36}(VO)_2\}_2]^{14-}$ (**8**) in polyhedral representation ($\{MoO_6\}$ octahedra, gray; $\{VO_6\}$ octahedra, hatched; central V atoms, black spheres; V atoms of the caps, gray; O, white). (b) Structure of the related $\{[(VO_4)Mo_8V_4O_{36}(VO)_2]^{7-}\}_n$ (**9**), with the Keggin-type fragments (polyhedral representation) linked by $\{V_2O_2\}$ groups, showing four units of an infinite chain (code as above).

layers ~4.6 Å. The bridging V atoms are 2.9 Å apart. While all the Mo^{VI} centers have octahedral environments, the V centers exhibit tetrahedral (central V^V), square-pyramidal (the terminal {VO} caps), distorted trigonal-prismatic (bridging V centers), and distorted octahedral environments (all others).

The linkage of such units can correspondingly be extended to build an infinite chain as shown in the catena structure of $\{[(V^VO_4)Mo^{VI}{}_8V^{IV}{}_4O_{36}(V^{IV}O)_2]^{7-}\}_n$ ($\{Mo_8V_7\}_n$, **9**).[10] Here, in contrast to **8**, both {VO} caps are condensed thus leading to a chain formed by linking Keggin-type units. These units are connected via $\{V(O_2)V\}$ bridges as shown in Figure 9b.

C. Clusters Built up by Lacunary Keggin Fragments: $\{As_8Mo_{24}\}$ and $\{As_{10}Mo_{24}\}$

A fundamental, promising route toward the targeted synthesis of complex polyoxometalate structures appears to be the strategy of generating large, highly negatively charged (and therefore soluble) intermediates in solution, which can either be trapped and stabilized or coupled to each other in successive condensation reactions. Another possibility is to use synthons which have highly reactive functional groups such as $\{MoO_3\}$ or fragments which can be linked, as in the case of $[(AsOH)_3(MoO_3)_3(AsMo_9O_{33})]^{7-}$ ($\{As_4Mo_{12}\}$, **10**).[41] In **10** the lone electron pair at the As^{III} center of the basic $\{AsMo_9O_{33}\}^{13-}$ fragment prevents the adoption of a spherical structure, which can nevertheless be formed on oxidation of this As^{III} center to an As^V center with concomitant rearrangement of the whole cluster framework thus leading to α-Keggin-type anions with a central AsO_4^{3-} tetrahedron. The cluster anion **10** consists formally of the highly negatively charged $\{AsMo_9O_{33}\}^{13-}$ Keggin fragment mentioned above, which is capped by a six-membered ring comprising three electrophilic $\{AsOH\}^{2+}$ and three highly reactive facial $\{Mo^{VI}O_3\}$ units. These are arranged alternately and linked together as well as to the Mo atoms of the nucleophilic, lacunary $\{AsMo_9O_{33}\}^{13-}$ fragment through μ_3-O atoms (Figure 10). Within the crystal lattice, the $\{Mo^{VI}O_3\}$ units are stabilized through hydrogen bonds to the $\{AsOH\}^{2+}$ groups of neighboring anions.[41]

On lowering the pH value of the reaction solution in which **10** is formed from approximately 4.5 to 3.0, the "dimeric" cluster ion $[(AsOH)_6(MoO_3)_2(O_2Mo{-}O{-}MoO_2)_2(AsMo_9O_{33})_2]^{10-}$ ($\{As_8Mo_{24}\}$, **11**) is obtained. Condensation via the four highly reactive $\{Mo^{VI}O_3\}$ fragments and formation of two $\{O_2Mo{-}O{-}MoO_2\}$ bridges takes place after protonation. Consequently, the two six-membered rings of **11** retain in total two of their facial $\{Mo^{VI}O_3\}$ groups, each of which is stabilized by one hydrogen bond between one of its terminal oxygen atoms and the OH function of the opposite $\{AsOH\}^{2+}$ unit (see Figure 10).[41]

If a larger amount of As_2O_3 is added to the solution, a further linking with the remaining highly reactive $\{MoO_3\}$ units of **11** yields the cluster anion $[(AsOH)_4(AsO)_2(HOAs{-}O{-}MoO_2)_2(O_2Mo{-}O{-}MoO_2)_2(AsMo_9O_{33})_2]^{8-}$ ($\{As_{10}Mo_{24}\}$, **12**), which can be precipitated as trimethylammonium salt[41,42] (see Figure 10).

D. Clusters with an ϵ-Keggin-Type Core: $\{Mo_{37}\}$, $\{Mo_{42}\}$, and $\{Mo_{43}\}$

The reduction of the well-known α-Keggin cluster with T_d symmetry can in principle yield the highly nucleophilic ϵ-Keggin-type cluster $[H_xMo^V{}_{12}O_{40}]^{(20-x)-}$ (with six short $Mo^V{-}Mo^V$ contacts) as intermediate, which can be stabilized by protonation and by capture of four electrophilic $\{Mo^{VI}O_3\}$ groups, thus forming anions of the type $[H_xMo^V{}_{12}O_{40}(Mo^{VI}O_3)_4]^{(20-x)-}$. One of these occurs in salts ($[NH_4]^+$ and $[(CH_3)_2NH_2]^+$) of the anions $[H_2Mo_{16}(OH)_{12}O_{40}]^{6-}$ (**13**) and $[NaMo_{16}(OH)_{12}O_{40}]^{7-}$ (**14**), which have well-defined protonation.[43] On further reduction ($Mo^{VI} \rightarrow Mo^V$) the originally electrophilic $\{Mo^{VI}O_3\}$ groups on the surface of the $\{Mo_{16}\}$-type cluster themselves become nucleophilic and, in addition, seem to have a template-type function: they seem to induce the formation of

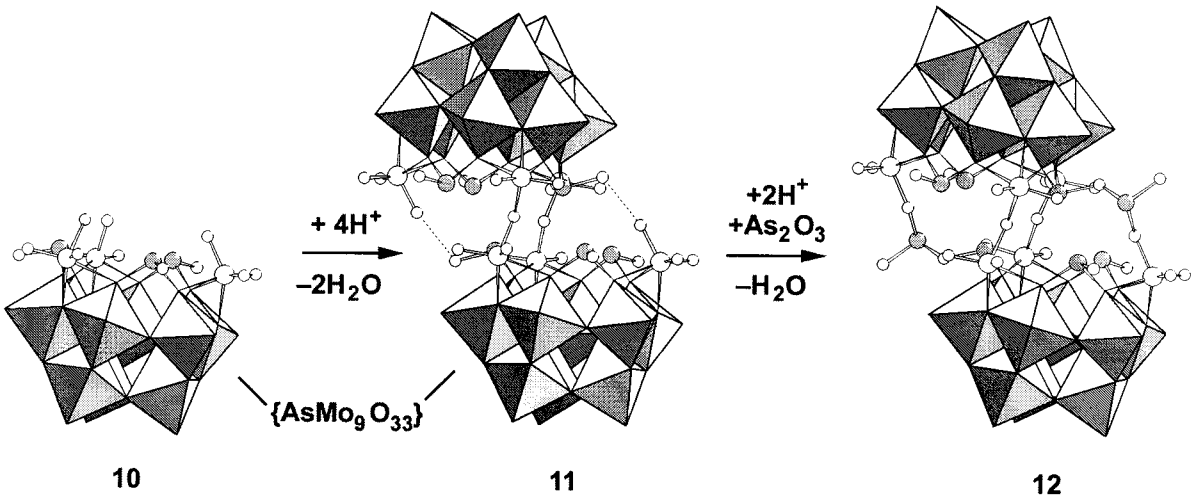

Figure 10. Structure of $[(AsOH)_3(MoO_3)_3(AsMo_9O_{33})]^{7-}$ (**10**) as well as the related clusters $[(AsOH)_6(MoO_3)_2(O_2MoOMoO_2)_2(AsMo_9O_{33})_2]^{10-}$ (**11**) and $[(AsOH)_4(AsO)_2(HOAsOMoO_2)_2(O_2MoOMoO_2)_2(AsMo_9O_{33})_2]^{8-}$ (**12**) with the same $\{AsMo_9\}$ fragments. In **10** the $\{AsMo_9\}$ unit (polyhedral representation) is capped by three $\{As^{III}OH\}$ and three $\{Mo^{VI}O_3\}$ groups ($\{MoO_6\}$ octahedra, gray; As^{III} centers, gray spheres; Mo, large white spheres; O, small white spheres). In the related "dimer" **11**, two $\{As_4Mo_{12}\}$ units (built up by the $\{AsMo_9\}$ unit and the three $\{AsOH\}$ as well as the three $\{MoO_3\}$ capping units) are connected by two $O_2Mo-O-MoO_2$ bridges and stabilized by two $As^{III}-OH\cdots O=Mo^{VI}O_2$ hydrogen bonds (dashed lines, code as above). Cluster **12** has two additional $O_2Mo^{VI}-O-As(OH)_{term}-O-As$ bridges between the units (code as above).

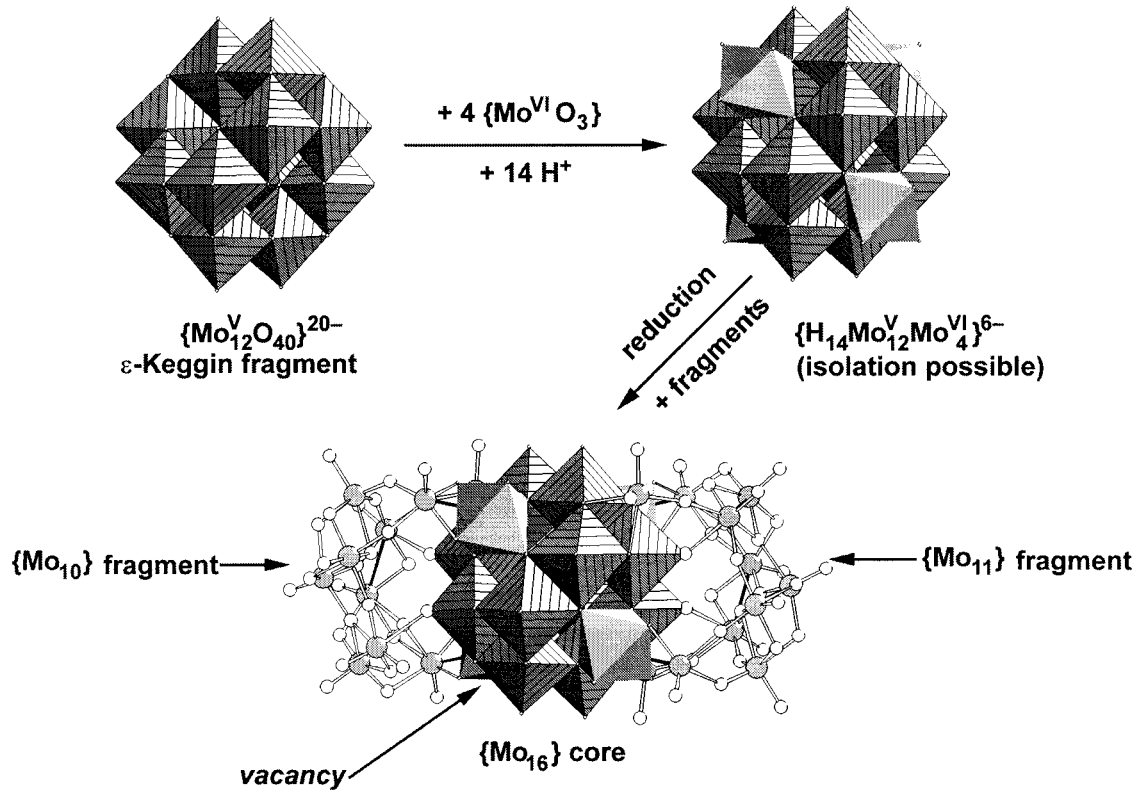

Figure 11. Structure of the cluster $[H_{14}Mo_{37}O_{112}]^{14-}$ (**15**) including its structural relation to the building blocks. The reduced ϵ-Keggin fragment (top, left) is capped with four $\{Mo^{VI}O_3\}$ units building the cluster anion $[H_2Mo_{16}(OH)_{12}O_{40}]^{6-}$ (**13**) (top, right). Further reduction of these caps ($Mo^{VI} \rightarrow Mo^{V}$) and condensation with an $\{Mo_{11}\}$ as well as an $\{Mo_{10}\}$ fragment leads under formal consideration to **15** (bottom). In the $\{Mo_{10}\}$ fragment, one Mo center is missing ($\{MoO_6\}$ octahedra of the central Keggin-type core, hatched; $\{MoO_6\}$ octahedra of the caps, gray; Mo centers of the $\{Mo_{10}\}$ and $\{Mo_{11}\}$ fragments, gray spheres; O, white spheres).

electrophilic polyoxometalate fragments with 10 and 11 molybdenum atoms thereby forming the racemic cluster anion $[H_{14}Mo_{37}O_{112}]^{14-}$ ($\{Mo_{37}\}$, **15**).[44]

The red anion **15** represents an unusual binary molecular species with a rather complicated structure containing no symmetry element. It formally consists of the central $\{H_6Mo^{V}{}_{12}O_{40}(Mo^{V}O_3)_4\}^{18-}$ core and the two similar but not identical "coordinated ligands" $\{Mo_{10}\}$ and $\{Mo_{11}\}$ (see Figure 11). The mentioned core is built up from an $\{Mo^{V}{}_{12}O_{40}\}$ ϵ-Keggin-type subcore, which is capped by four $\{Mo^{V}O_3\}$ groups.

The $\{H_5Mo^{V}{}_6Mo^{VI}{}_5O_{31}\}^{3+}$ ($\{Mo_{11}\}$) "ligand", which has approximately *m* symmetry, is mainly built up by two incomplete $\{Mo_3O_4\}$ cubes. Two $\{MoO_6\}$

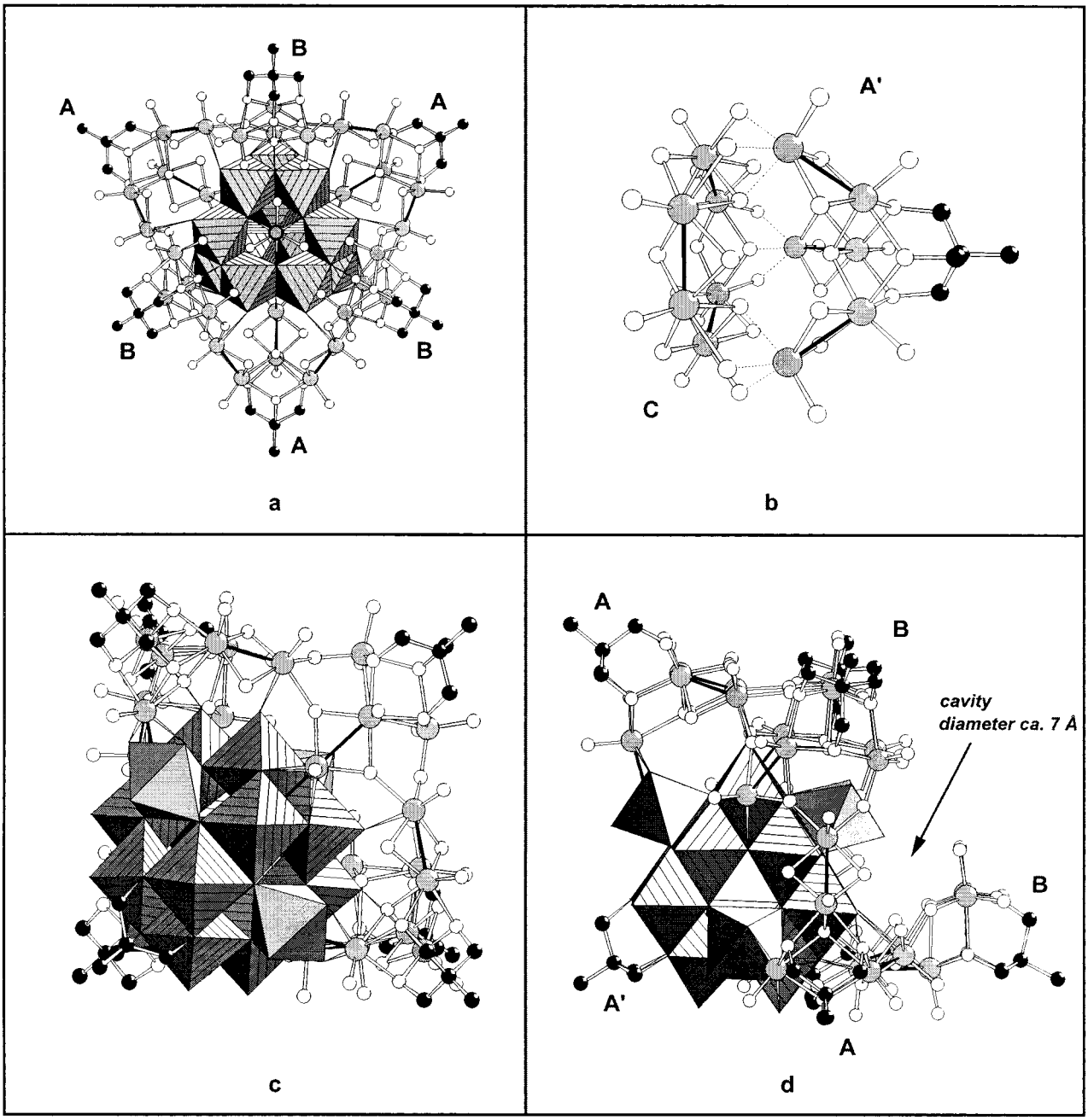

Figure 12. (a) Structure of the cluster anion $[H_xMo_{43}O_{112}\{(OCH_2)_3CR\}_7]^{y-}$ (**17**) with the central $\{Mo_{12}\}$ ϵ-Keggin core in polyhedral representation viewed along the molecular C_3 axis ($\{MoO_6\}$ octahedra of the Keggin-type core, hatched; Mo centers at the periphery, gray spheres; O, white spheres; carbon atoms of the organic ligands, black spheres). Each $\{Mo_6O_6\}$ face of the core is capped by an $\{MoO_3\}$ moiety but in the case of the $\{Mo_{42}\}$ cluster (**16**) one of these positions is occupied by a $\{Na(H_2O)_3\}^+$ moiety (emphasized sphere in the center of the anion). The core is surrounded by three A-type and three B-type fragments. (b) The $\{Mo_{12}\}$ core (including one organic ligand) is built up by a C-type and an A′-type fragment attached to an organic residue (Mo centers, gray spheres; O, white; C atoms of the organic ligands, black). (c) View of the structure of $\{Mo_{43}\}$ (**17**) with the $\{Mo_{16}\}$ core in polyhedral representation (code as in a, plus capping $\{MoO_6\}$ octahedra, gray). (d) View of the cavity produced by the three type B subunits, one of which is not clearly seen.

octahedra of one of the $\{Mo_3O_4\}$ units are connected via *edges* to neighboring $\{MoO_6\}$ octahedra; the third octahedron is correspondingly bonded to an $\{MoO_3\}$ cap of the central $\{H_6Mo^V_{12}O_{40}(Mo^VO_3)_4\}$ core. In this $\{Mo_3O_4\}$ unit all the molybdenum atoms are of the Mo^V type, whereby the three μ_2-O and the μ_3-O atoms are protonated. The three $\{MoO_6\}$ octahedra forming the second $\{Mo_3O_4\}$ unit are bonded to neighboring polyhedra via *corners*. This $\{Mo_3O_4\}$ unit contains exclusively Mo^{VI} centers, whereby only the μ_3-O atom is protonated thus leading to the same formal charge as the former $\{Mo_3O_4\}$ unit. The $\{Mo_{11}\}$ "ligand" contains a further Mo^V atom remarkably surrounded by five coordinating oxygen atoms forming an unusual square pyramid, which shares an edge with a second $\{MoO_3\}$ cap of the central core. Two further Mo^{VI} atoms of the "ligand" cap two $\{Mo_3O_4\}$ units of the central core thus completing the $\{Mo_4O_4\}$ "cubes".

In the $\{H_3Mo^V_4Mo^{VI}_6O_{29}\}^+$ ($\{Mo_{10}\}$) "ligand" one of these Mo^{VI} atoms is missing, thus leaving one $\{Mo_3O_4\}$ unit of the $\{H_6Mo^V_{12}O_{40}(Mo^VO_3)_4\}$ core uncapped and its three μ_2-O atoms protonated.[44]

It should be stressed that the reaction leading to **15** can be considered as a molecular step-by-step, symmetry-breaking process with decrease in molecular symmetry from T_d to C_1. This of course differs from the type of symmetry breaking in classical (first- and second-order) phase transitions, for instance during crystallization from solution or during a transition from a para- to a ferromagnet. In these cases, symmetry breaking refers to the whole system.

In contrast to the low symmetry of **15**, the related cluster anions $[Na(H_2O)_3H_xMo_{42}O_{109}\{(OCH_2)_3CCH_2OH\}_7]^{y-}$ ($x = 13$, $y = 9$; $x = 15$, $y = 7$) ($\{Mo_{42}\}$, **16**) and $[H_xMo_{43}O_{112}\{(OCH_2)_3CR\}_7]^{y-}$ ($x = 14$, R = CH_2OH, $y = 9$; $x = 13$, R = CH_3, $y = 10$) ($\{Mo_{43}\}$, **17**), with a $\{Mo_{16}O_{52}\}$ core have, due to the presence of triangular $\{Mo_3O_n[(OCH_2)_3CR]\}$ units, rather high C_{3v} symmetry of the core cluster.[22,45,46] The anions **16** and **17** exist with different degrees of protonation. These clusters are basically identical but in **16** an $\{Na(H_2O)_3\}^+$ group is coordinated to the central part of the cluster, while in **17** this is replaced by an $\{Mo^{VI}O_3\}$ group.

According to Khan and Zubieta[45b] the anions can be divided into four main types of basic structural building blocks A, A′, B, and C, three of which are bonded to organic residues (see Figure 12): (1) three hexanuclear fragments $\{Mo^{V}_6O_{22}[(OCH_2)_3CR]\}$ (A), (2) one identical fragment, which differs only in its relative, i.e., central, position within the cluster (A′), (3) three tetranuclear fragments $\{Mo^{V}_2Mo^{VI}_2O_{15}[(OCH_2)_3CR]\}$ (B), and (4) a hexanuclear ring $\{Mo^{V}_6O_{24}\}$ with no organic residues attached (C). Furthermore there is an additional moiety coordinated to the central part of the cluster: an $\{Na(H_2O)_3\}^+$ unit in the case of **16** and an $\{Mo^{VI}O_3\}$ group in the case of **17**. The fragments C and A′ form the completely reduced ϵ-Keggin core $\{Mo_{12}\}$ with an organic residue attached (Figure 12b), which regarded as a basic building block provides a further possible description (see also refs 46 and 47). Its hexagonal $\{Mo_6O_6\}$ faces are capped by three Mo^V centers belonging to the Mo^VO_3 groups of Mo^V-Mo^V dumbbells of fragment A and the $\{Na(H_2O)_3\}^+$ (for **16**) or $\{MoO_3\}$ (for **17**) group. In this way, in the case of **17**, an $\{Mo_{16}\}$ core similar to that in **15** is built up, but with one $Mo^{VI}O_3$ cap. Whereas the trigonal $\{Mo_3O_4\}$ faces (incomplete cubes) of the ϵ-Keggin core $\{Mo_{12}\}$ are capped by three Mo^V centers belonging to the Mo^V-Mo^V groups of fragment B, the fourth face is capped by an organic residue. The three B-type subunits point outward and produce a cavity of ca. 7 Å in diameter (Figure 12d). In contrast to **15**, where two distinct coordinated fragments are present, the $\{Mo_{16}\}$ core in **17** is surrounded by one fragment.

Alternatively, one could also identify the ϵ-Keggin unit as the core wrapped by an $\{Mo_{30}\}$ ring.

E. Clusters Containing $\{Mo_8\}$ Moieties: $\{Mo_{36}\}$, $\{Mo_{57}\}$, and $\{Mo_{154}\}$

1. $\{Mo_{36}\}$

The cluster anions $[Mo_{36}O_{112}(H_2O)_{16}]^{8-}$ ($\{Mo_{36}\}$, **18a**) and $[Mo_{36}(NO)_4O_{108}(H_2O)_{16}]^{12-}$ ($\{Mo_{36}(NO)_4\}$,

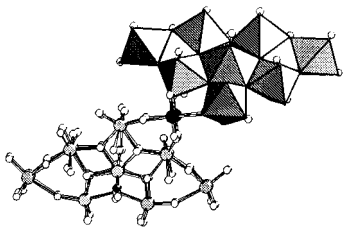

Figure 13. Structure of the anion $[Mo_{36}(NO)_4O_{108}(H_2O)_{16}]^{12-}$ (**18b**) viewed along a C_2 axis showing the $\{Mo_8\}$ unit (in polyhedral representation) which is the basic structural feature of **18b** and of several other clusters. Two pairs of $\{Mo_8\}$ fragments, which are linked by two $\{Mo_1\}$ bridges (not visible in the figure), build the $\{Mo_{17}\}$ units as described in the text ($\{MoO_6\}$ octahedra and $\{MoO_6(NO)\}$ bipyramid of the $\{Mo_8\}$ unit, gray; Mo centers, gray spheres; O, white; Mo centers of the bridging $\{MoO_2\}^{2+}$ groups, large black spheres; N, small black spheres). In many clusters the $\{MoNO\}^{3+}$ group in the bipyramid can be replaced by an $\{MoO\}^{4+}$ group. We refer in both cases to the $\{Mo_8\}$ unit.

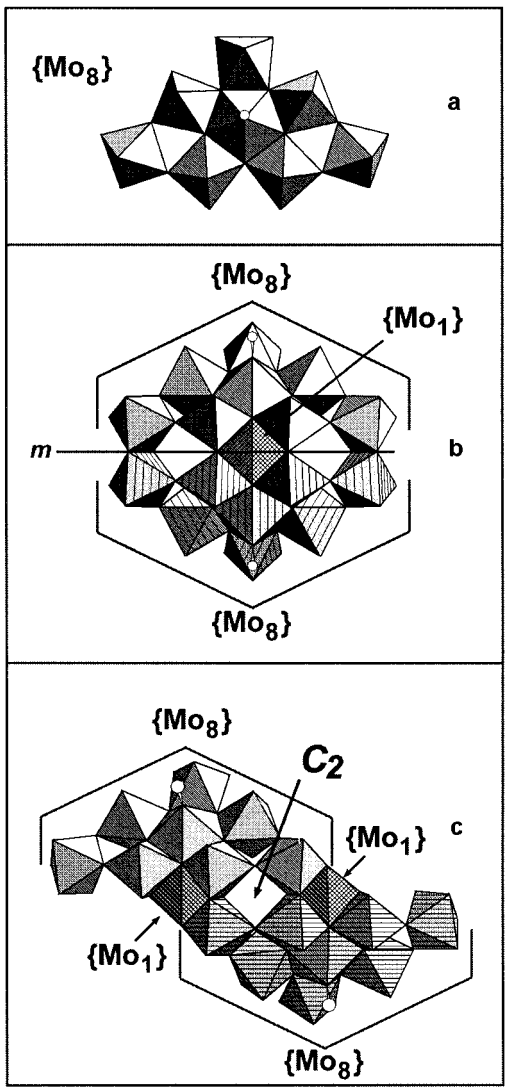

Figure 14. Structure of the $\{Mo_8\}$ unit (a) and larger subunits derived from it (b and c). Two $\{Mo_8\}$ units (code as in Figure 13, one unit is represented by hatched polyhedra) can be connected by an $\{Mo_1\}$-type center (crosshatched) to build an $\{Mo_{17}\}$ unit, present in **18a**, **18b**, **19a** and **19b** (b). A unit built up by two $\{Mo_8\}$ groups connected by two $\{Mo_1\}$-type centers (crosshatched), which is present in **20** and in several other large clusters (c).

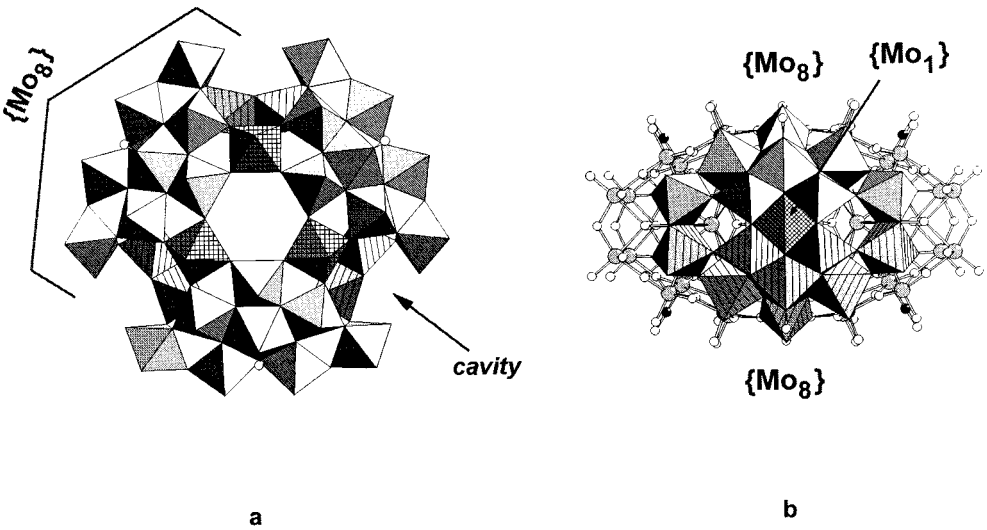

Figure 15. Structure of the $\{Mo_{57}M_6\}$-type clusters $[\{V(H_2O)O\}_6\{Mo(\mu\text{-}H_2O)_2(\mu\text{-}OH)Mo\}_3\{Mo_{15}(MoNO)_2O_{58}(H_2O)_2\}_3]^{21-}$ (**19a**) and $[\{Fe(H_2O)_2\}_6\{Mo(\mu\text{-}H_2O)_2(\mu\text{-}OH)Mo\}_3\{Mo_{15}(MoNO)_2O_{58}(H_2O)_2\}_3]^{15-}$ (**19b**). (a) View along the S_3 axis showing the $\{Mo_{17}\}$ units, built up by two $\{Mo_8\}$ (code as in Figure 13) and one $\{Mo_1\}$ group, in polyhedral representation ($\{MO_6\}$ octahedra (M = Fe, V), crosshatched; $\{Mo_2\}$ units, hatched). With this view of the model, one $\{Mo_8\}$ group of the $\{Mo_{17}\}$ and the connecting $\{Mo_1\}$ unit is hidden behind the rest (see also ref 57b). One of the surface cavities, which can be occupied by metal−oxygen fragments, is marked with an arrow (see text). (b) View perpendicular to the S_3 axis with the clear identification of one whole $\{Mo_{17}\}$ unit in polyhedral representation (code as in Figure 14).

18b)[11,48−54] exhibit a variety of different polyhedra: two $\{MoO_6\}$, four $\{(O{=})MoO_4(H_2O)\}$, eight $\{(O{=})_2MoO_3(H_2O)\}$, eight $\{(O{=})MoO_5\}$, and two $\{(O{=})_2MoO_4\}$ octahedra as well as four pentagonal $\{Mo(X)O_6\}$ bipyramids (X = O for **18a**, X = NO for **18b**) and four $\{Mo_2O_8(\mu\text{-}O)(\mu\text{-}H_2O)\}$ units consisting of edge-shared octahedra.[11] The anion **18b**, which was very probably first reported in ref 12, formally consists of two rather large $\{Mo^{VI}{}_{15}(MoNO)_2{}^{3+}O_{58}(H_2O)_2\}^{20-}$ ($\{Mo_{17}\}$) units (Figure 13), which are linked by two $\{MoO_2\}^{2+}$ groups, with the two (terminal) oxygen atoms in cis position.

The $\{Mo_{17}\}$ units can be described as being built up from two $\{Mo_8\}$ units fused via eight oxygen atoms and one Mo atom (see also Figure 14b). The centers of these $\{Mo_8\}$ units are formed by the pentagonal $\{MoXO_6\}$ bipyramid mentioned above, which is connected to five $\{MoO_6\}$ octahedra via edges. Four of these are connected to two other $\{MoO_6\}$ octahedra via corners (see Figure 14a). The substitution of the $\{MoNO\}^{3+}$ groups in the bipyramids or the $\{Mo_8\}$ groups by $\{MoO\}^{4+}$ leads directly to the nonreduced anion **18a**. Similar $\{Mo_8\}$ units can also be found in the solid-state structures Mo_5O_{14} and $Mo_{17}O_{47}$.[55]

The $\{Mo_{17}\}$ subunits can alternatively be described as being formally built up by central heptamolybdate-like $\{Mo_7\}$ entities containing two seven-coordinated molybdenum atoms in the form of two pentagonal $\{Mo(NO)O_6\}$ bipyramids.[11]

2. $\{Mo_{57}\}$

The structures of the unusual highly symmetrical (D_{3h}) cluster anions $[\{V^{IV}(H_2O)O\}_6\{Mo^{V}(\mu\text{-}H_2O)_2(\mu\text{-}OH)Mo^{V}\}_3\{Mo^{VI}{}_{15}(MoNO)_2O_{58}(H_2O)_2\}_3]^{21-}$ ($\{Mo_{57}V_6\}$, **19a**)[11] and $[\{Fe^{III}(H_2O)_2\}_6\{Mo^{V}(\mu\text{-}H_2O)_2(\mu\text{-}OH)Mo^{V}\}_3\{Mo^{VI}{}_{15}(MoNO)_2O_{58}(H_2O)_2\}_3]^{15-}$ ($\{Mo_{57}Fe_6\}$, **19b**)[7] are shown in Figure 15 (see also refs 56−59). These doughnut-shaped anionic species consist of 276 non-hydrogen atoms and also exhibit, corresponding to the $\{Mo_{36}\}$-type clusters, a variety of polyhedra. The anions are formally composed of *three* of the above-mentioned highly negatively charged $\{Mo_{15}(MoNO)^{3+}{}_2O_{58}(H_2O)_2\}^{20-}$ ($\{Mo_{17}\}$) units (see also section V.E.1), acting as bridging ligands for cationic centers: six $\{V^{IV}(H_2O)O\}^{2+}$ of these occur in **19a** and six $\{Fe^{III}(H_2O)_2\}^{3+}$ units in **19b**, as well as three dinuclear $\{Mo^{V}(\mu\text{-}H_2O)_2(\mu\text{-}OH)Mo^{V}\}^{9+}$ groups in both **19a** and **19b**.

The relatively large cavity inside the cluster anions is formally accessible through two "openings" in the cluster shell located along the S_3 axis. This cavity (with a diameter perpendicular to the S_3 axis of ∼0.9 and parallel to it of ∼0.5 nm neglecting the H atoms) is formed by a central $\{O_{33}\}$ polyhedron. The two openings are delimited by two almost planar and alternating Mo−O−M−O (M = V for **19a**; M = Fe for **19b**) 12-membered rings.[11]

An important structural feature of the chemistry is the presence of three rather large cavities located on the outer sphere of the clusters in the region between the $\{Mo_{17}\}$ fragments. These cavities are accessible to the coordination of further highly electrophilic metal−oxygen fragments such as $\{MoO\}^{4+}$ groups, thus resulting in a step-by-step growth so that all species of the type $\{Mo_{57+x}V_6\}$ ($x = 0-6$) can be formed. Each of the $\{MoO\}^{4+}$ groups binds formally to three oxygen atoms of the $\{Mo_{57}V_6\}$ core resulting in a tetrahedral coordination of the incorporated Mo atoms. The degree of occupation of the cavities can be correlated with the degree of reduction of the parent cluster **19a**. Its reduction increases the nucleophilicity and initiates this type of growth process whereby even up to six electrophilic $\{MoO\}^{4+}$ entities, as in the case of $[H_3Mo_{57}V_6(NO)_6O_{189}(H_2O)_{12}(MoO)_6]^{21-}$ (**19c**), can be incorporated.[44]

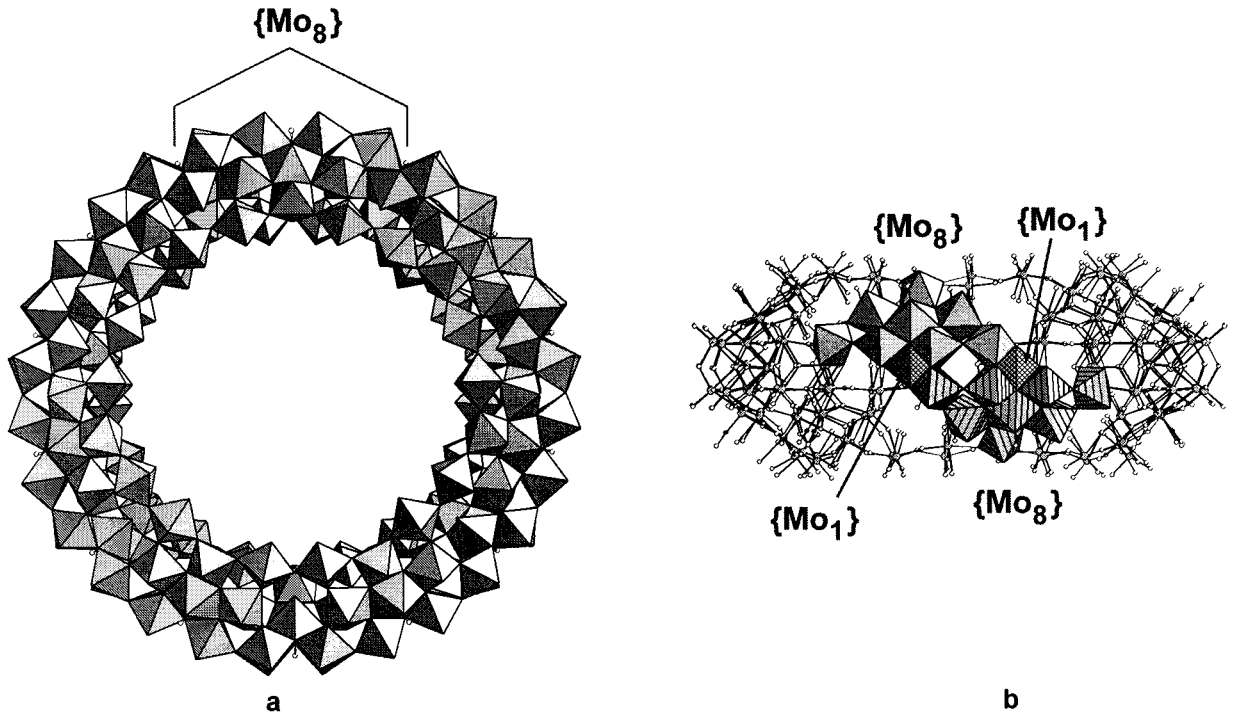

Figure 16. (a) Structure of the cluster anion $[Mo_{154}(NO)_{14}O_{420}(OH)_{28}(H_2O)_{70}]^{(25\pm5)-}$ (**20**) ("giant wheel") in polyhedral representation. (b) View perpendicular to panel a whereby two $\{Mo_8\}$ units and the two connecting $\{Mo_1\}$-type units are shown in polyhedral representation (code as in Figure 14).

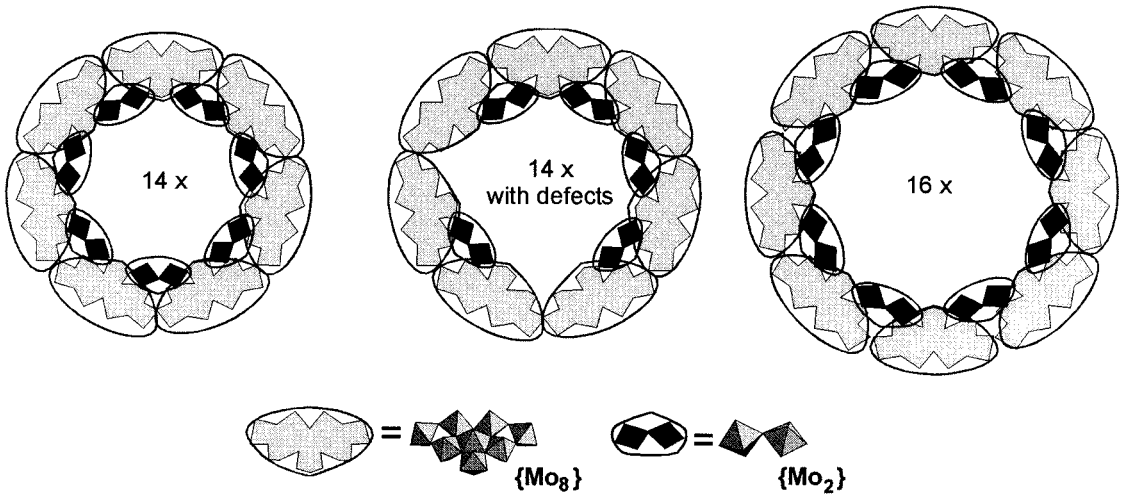

Figure 17. Schematic comparison of the ring-type clusters built up by the building blocks $\{Mo_1\}$, $\{Mo_2\}$, and $\{Mo_8\}$ (with central {MoO} or {MoNO} group of the pentagonal bipyramid). Clusters with a set of 14 and 16 of the mentioned building blocks, as well as some with defects in the $\{Mo_2\}$ units are known so far (see text).

3. {Mo154(NO)14} and Comparison to {Mo57}

From the same reaction system that leads to the clusters **18b**, **19a**, and **19b**, also the diamagnetic, deep-blue, mixed-valence, electron-rich species $[Mo_{154}(NO)_{14}O_{420}(OH)_{28}(H_2O)_{70}]^{(25\pm5)-}$ ($\{Mo_{154}(NO)_{14}\}$, **20**), can be isolated in the ammonium salt.[9] (The uncertainty regarding the cluster charge arises from the difficulty in determining the exact number of cations in the crystal lattice, owing to disorder problems with respect to the NH_4^+ ion positions as well as the crystal water positions.) The approximately ring-shaped anion consists of 140 $\{MoO_6\}$ octahedra and 14 $\{Mo(NO)O_6\}$ pentagonal bipyramids. The cavity, like a car tire, is broader at the equator and measures about 20 Å in diameter. The anion **20** can be described as a tetradecamer with approximate D_{7d} symmetry. Each of the 14 subunits has a pentagonal-bipyramidal $\{Mo(NO)O_6\}$ center to which seven other $\{MoO_6\}$ octahedra are linked by corner and edge sharing to form an $\{Mo_8\}$ fragment. These fragments are arranged above and below the equatorial plane of the cluster[9] (see Figure 16).

Equivalent $\{Mo_8\}$ building blocks (Figure 14a) also occur in the anions **18b**, **19a**, and **19b**. (In the following, $\{Mo_8\}$ units have a central pentagonal bipyramid containing an $\{MoNO\}^{3+}$, or an equivalent $\{MoO\}^{4+}$ group.) The fundamental difference between the two structural types (**18b**, **19a**, and **19b** on one hand, and **20** on the other hand) is that the $\{Mo_8\}$ fragments lie directly on top of each other in

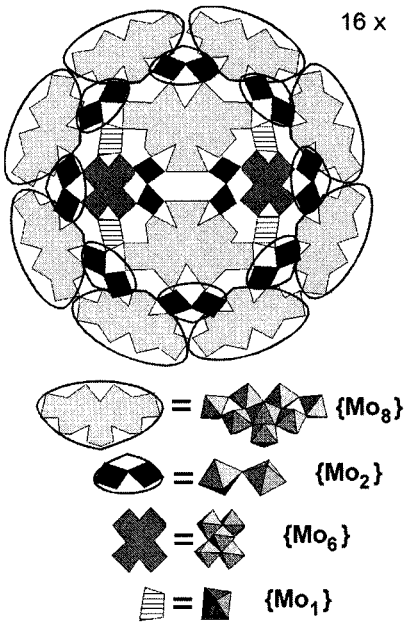

Figure 18. Schematic representation of the structure of the unusual wheel-shaped $\{Mo_{248}\}$ cluster which can formally be constructed by doubly capping the $\{Mo_{176}\}$ ring-type cluster. The two caps, forming a cavity inside, consist of $\{Mo_8\}$ and $\{Mo_2\}$ units (which are similar to those found in the rings), as well as $\{Mo_1\}$- and $\{Mo_6\}$-type groups. The latter units can be considered as lacunary fragments of the known octamolybdate structure.

19a and **19b** which means they are related to each other by the equatorial mirror plane, whereas in **20** they are twisted relative to each other by an angle of 360°/14 about the approximate C_7 (S_{14}) axis. In **19a** and **19b** the pentagonal bipyramids of each unit are linked to each other through *one* additional $\{Mo_1\}$ unit lying in the equatorial plane, and therefore formally "pseudo-discrete" $\{Mo_{17}\}$ ($2 \times 8 + 1$) fragments are abundant (see also section V.E.1). These can therefore be considered as *transferable ligands*, "isolated" from each other and linked through the cationic $\{V^{IV}O(H_2O)\}^{2+}$ or $\{Fe^{III}(H_2O)_2\}^{3+}$ as well as $\{Mo^{V}(\mu\text{-}H_2O)_2(\mu\text{-}OH)Mo^{V}\}^{9+}$ groups, respectively (see Figure 14b). In contrast, in **20** the shift of the $\{Mo_8\}$ units relative to each other means that in each case *two* equatorial $\{Mo_1\}$-type units are required to link two $\{Mo_8\}$ fragments (Figure 14c). Neighboring $\{Mo_8\}$ fragments above and below the equatorial plane are, additionally, linked together directly through a μ_3-O atom. The smaller curvature of the cluster-ion shell relative to that of **19a** and **19b** correlates with the fact that in the region of each of the cavities of the latter species sufficient space is available for a further linking of the $\{Mo_8\}$ units by an $\{Mo_2\} \equiv \{Mo^{VI}O_2(H_2O)(\mu\text{-}O)Mo^{VI}O_2(H_2O)\}^{2+}$ group. (In **19a** and **19b** they are linked by a V^{IV} or Fe^{III} center.[9]) According to a building-block principle, **20** can be formulated as $[\{Mo^{VI}_2O_5(H_2O)_2\}\{Mo_7Mo(NO)O_{25}(OH)_2(H_2O)_3Mo\}]_{14} \equiv [\{Mo_2\}\{Mo_8\}\{Mo_1\}]_{14}$.

A further characteristic of the structure of the anion **20** is the exceptionally high degree of protonation resulting from the high degree of reduction. Investigations reveal 28 singly and 70 formally doubly protonated oxygen atoms corresponding to H_2O ligands, whereby 28 equivalent μ_3-O atoms located in the equatorial plane show the single protonation. Of the terminal H_2O ligands, 42 are coordinated to the Mo atoms constituting the two 42-membered rings, which contain alternating molybdenum and oxygen atoms, and delimit the central cavity. In these rings the H_2O ligands are arranged both above and below the ring's plane, and an alternating (trans) orientation between two adjacent centers is favored.[9]

4. Beyond the $\{Mo_{154}\}$ Level

Recent attempts to synthesize analogues of the ring-type species without NO groups were also successful. An $\{Mo_{176}\}$-type electron-rich, ring-shaped cluster has been isolated, which can be described as a hexadecamer containing a set of 16 $[\{Mo_2\}\{Mo_8\}$-

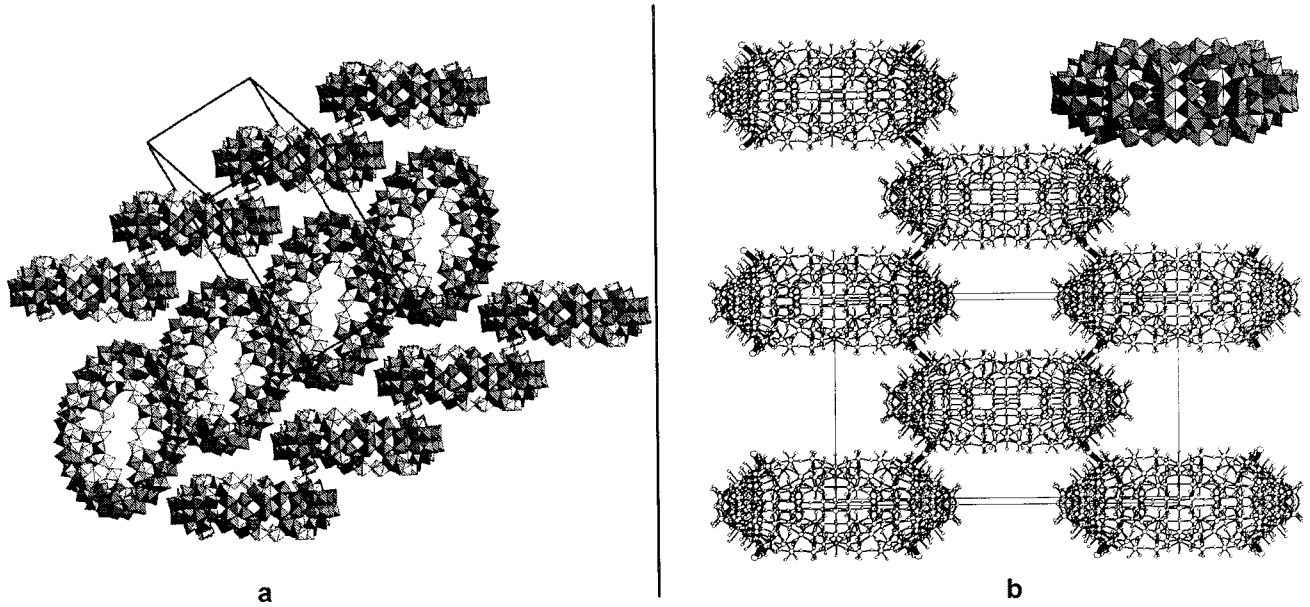

Figure 19. Examples for the linking potentiality of the giant ring clusters to form chains[62] (a) and layers[17] (b). The type and degree of condensation is related to the type of defect—that means is due to released $\{Mo_2\}$ groups.

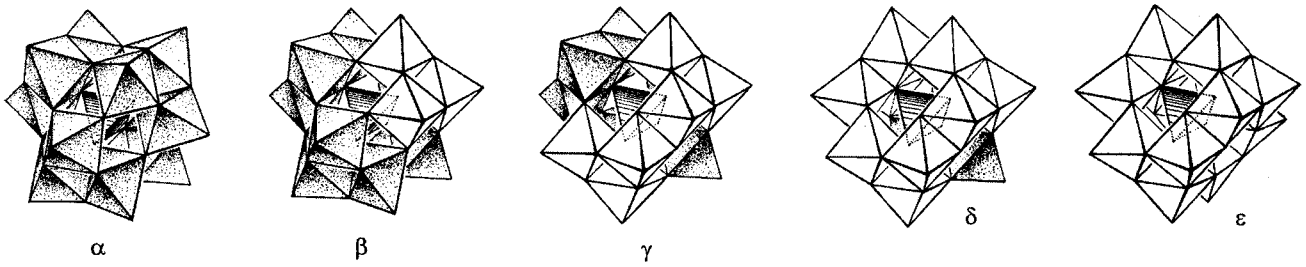

Figure 20. Polyhedral representation of the five skeletal isomers (α−ϵ) of the Keggin anion $[(XO_4)W_{12}O_{36}]^{n-}$, each corresponding to the "rotation"of one or more edge-shared $\{W_3O_{13}\}$ groups by π/3. Rotated groups are shown with unshaded octahedra.

$\{Mo_1\}$] groups (corresponding to the formula $[\{Mo_2O_5(H_2O)_2\}\ \{Mo_7Mo(NO)O_{25}(OH)_2(H_2O)_3Mo\}]$) instead of 14 as in the case of the $\{Mo_{154}\}$ cluster species discussed above, see Figure 17.[18] In another very unusual cluster with 248 Mo atoms the $\{Mo_{176}\}$-type ring is doubly capped with polyoxomolybdate sheets (see Figure 18).[60] All these types of species attract special interest because of their relevance to the soluble molybdenum blue compounds.[61]

Solid-state structures with chains and layers could be obtained by linking the large rings and in particular rings which have defects, which means missing $\{Mo_2\}^{2+}$ groups (corresponding to the lacunary-type Keggin species).[17,62] Some compounds exhibit channels due to stacking of the rings (see Figure 19). Furthermore, colloids with a hydrodynamic radius of ~80 nm can be proven to form from the $\{Mo_{154}\}$-type rings in organic solvents.[63]

VI. Tungstates

The structures of very large polytungstate anions may all be represented in terms of subunits based on lacunary fragments of the Keggin anion or its isomers.

Although some of these lacunary fragments (which occur in all the tungstates discussed) may not have an independent existence, and may not (or may) be mechanistically involved in the formation of the complete polyanions, dissection of the structures into such components does provide a convenient way to describe and classify the larger structures. It is therefore appropriate to begin this discussion with a review of these putative building blocks.

The five possible skeletal ("Baker-Figgis")[64] isomers, α−ϵ, of the Keggin anion are illustrated in polyhedral form in Figure 20. Examples of α, β, and γ structures are known for dodecatungstates, but the γ isomer is much less stable than the others, a possible consequence of a larger number of intraionic metal−metal repulsions between edge-shared $\{WO_6\}$ octahedra.[65] Lacunary versions of these structures result from the removal of one or more W atoms. Examples of three lacunary derivatives (one monovacant, two trivacant) of the α-Keggin anion are shown in Figure 21; structures of lacunary derivatives of the other isomers can easily be imagined. The two trivacant species in Figure 21 correspond to loss of a corner-shared group of $\{WO_6\}$ octahedra (A-type $\{XW_9\}$) or an edge-shared group (B-type $\{XW_9\}$). Note that in the B-type anion the central tetrahedrally

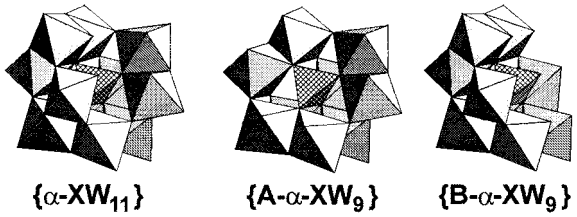

Figure 21. Polyhedral representation of three lacunary derivatives of the α-Keggin anion.

coordinated heteroatom has an unshared terminal oxygen atom. B-type structures are also commonly observed if the central atom has an unshared pair of electrons (e.g., As^{III}, Te^{IV}).

Fusion of two *A*-$[PW_9O_{34}]^{9-}$ units generates the well-known Wells−Dawson anion $[P_2W_{18}O_{62}]^{6-}$. Six isomers of this anion are in principle possible depending upon whether the half-units are derived from α- or β-Keggin species and whether they are combined in staggered (**S**) or eclipsed (**E**) fashion.[64] Four of these isomers have been observed for $[As_2W_{18}O_{62}]^{6-}$ and three for $[P_2W_{18}O_{62}]^{6-}$.[66] As for the Keggin anion, lacunary derivatives of the Wells−Dawson structure are known. The most significant of these are derived from the most common isomer (αα**E**, generally known as the α-Dawson anion) shown in Figure 22 together with two monovacant (α_1 and α_2) and trivacant lacunary derivatives.

A. Clusters Incorporating Different Numbers of Monovacant Lacunary $\{XW_{11}\}$-Type Building Blocks

1. $\{XW_{11}\}$: $\{Si_2W_{23}\}$

The anion $[Si_2W_{23}O_{77}(OH)]^{9-}$ ($\{Si_2W_{23}\}$, **21**) is formed when γ-$[SiW_{10}O_{36}]^{8-}$ ($\{SiW_{10}\}$) is treated with acidified tungstate. The anion comprises {γ-SiW_{10}} and {α-SiW_{11}} moieties linked by an unsymmetrical $\{W_2\}$ group (O═W···O═W−OH). The resulting structure has no element of symmetry (see Figure 23).[67]

2. $\{XW_{11}\}_2$ or $\{X_2W_{17}\}_2$: $\{MX_2W_{22}\}$ and $\{MX_4W_{34}\}$

In 1971 Peacock and Weakley[68] first reported that the monovacant lacunary anions (mla) $[PW_{11}O_{39}]^{7-}$, $[SiW_{11}O_{39}]^{8-}$, and $[P_2W_{17}O_{61}]^{10-}$ (the last subsequently known as the α_2 isomer) formed both 1:1 and 1:2 complexes with several lanthanide cations. Salts of the 1:2 complexes, $[Ln(mla)_2]^{n-}$, were isolated, and these species, $\{MX_2W_{22}\}$ (**22**) and $\{MX_4W_{34}\}$ (**23**), fall within the scope of this review. Weakley and Peacock

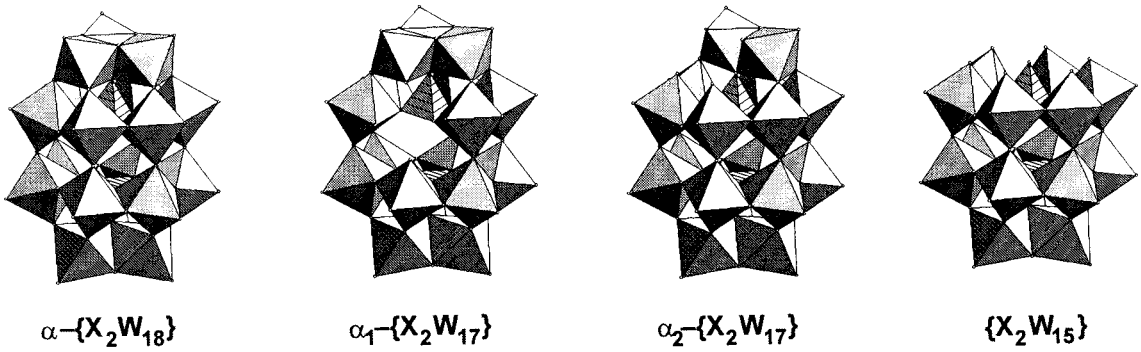

Figure 22. The α-Dawson structure $[X_2W_{18}O_{62}]^{n-}$, and three lacunary derivatives ({WO_6} octahedra, gray; {XO_4} tetrahedra, hatched). The monovacant derivatives have vacancies in the "belt"(α_1) or "cap"(α_2) positions.

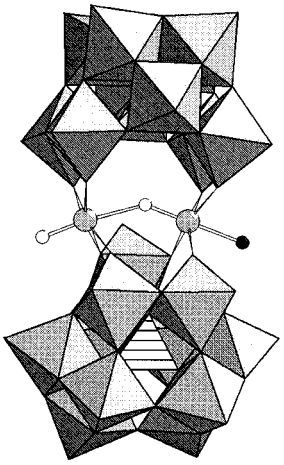

Figure 23. Structure of $[Si_2W_{23}O_{77}(OH)]^{9-}$ (**21**, {WO_6} octahedra, gray; central {SiO_4} tetrahedra, hatched; bridging W centers, gray spheres; O atoms, white spheres; OH ligand, black sphere).

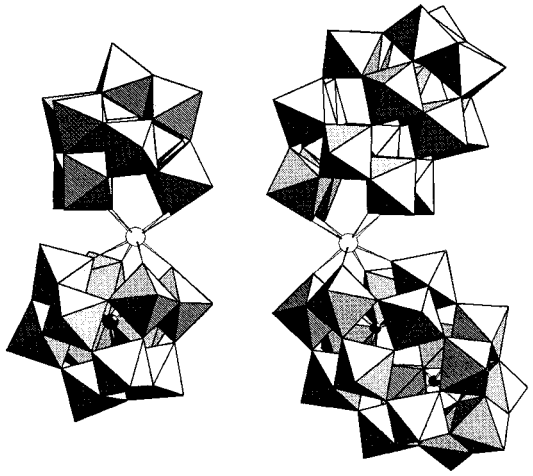

Figure 24. (a) Structure of $[U(\alpha\text{-}SiW_{11}O_{39})_2]^{12-}$ (**22**, {WO_6} octahedra, gray; Si atom, black sphere; U^{IV} center, white sphere). Conformation of {SiW_{11}} ligands is trans-oid. (b) Structure of $[U(\alpha_2\text{-}P_2W_{17}O_{61})_2]^{16-}$ (**23**). Conformation of {α_2-P_2W_{17}} ligands is cis-oid (code as above, except P atoms, black spheres).

suggested that the heteropolyanion ligands were tetradentate, binding to the lanthanide center through the four oxygen atoms that surrounded the tungsten vacancy, and generating a quasi-square antiprismatic coordination sphere for the lanthanide cation.

Many examples of analogues of the Peacock–Weakley anions have since been reported. Besides yttrium atoms, all the trivalent lanthanides, cerium(IV) and terbium(IV), and the tetravalent actinides (Th to Bk) have also been incorporated in such complexes. Although not all possible combinations of Ln/An and mla have been exhausted, the heteropolyanion ligands now include $[XW_{11}O_{39}]^{n-}$ (X = P[69–81] As[70,76,77,82–84] Si[69,70,37,76,83,85–88] Ge[69,70,76,89–91] B,[70,76,77,83,86,92–94] Ga,[95] Zr,[96] Cu[97]), α_1-$[P_2W_{17}O_{61}]^{10-}$,[98–100] α_2-$[P_2W_{17}O_{61}]^{10-}$,[69,70,75–78,101–106] α_2-$[As_2W_{17}O_{61}]^{10-}$,[70,83,107–110] $[XMo_{11}O_{39}]^{n-}$ (X = P,[73,111–114] As,[115] Si,[73,112–114,116–122] Ge[113,114,123]), $[X_2Mo_{17}O_{61}]^{10-}$ (X = P,[124,125] As[126]).

X-ray diffraction investigations of crystals of Cs_{12}-$[U^{IV}(GeW_{11}O_{39})_2]\cdot 13H_2O$,[127] $K_{11}H_2[Dy(SiMo_{11}O_{39})_2]\cdot xH_2O$,[113,120] $K_7H_6[Nd(GeMo_{11}O_{39})_2]\cdot 27H_2O$,[123] K_8H_5-$[La(SiW_2Mo_9O_{39})_2]\cdot 21H_2O$,[87] $K_{10}H_3[Pr(SiMo_{11}O_{39})_2]\cdot 18H_2O$,[79] $K_{10}H_3[Pr(SiW_5Mo_6O_{39})_2]\cdot 30H_2O$,[118] $K_{16}[Ce^{IV}$-$(\alpha_2\text{-}P_2W_{17}O_{61})_2]\cdot 50H_2O$,[128] $K_{17}[Lu(\alpha_2\text{-}P_2W_{17}O_{61})_2]\cdot xH_2O$,[129] and $K_{16}[U^{IV}(\alpha_n\text{-}P_2W_{17}O_{61})_2]\cdot xH_2O$, ($n$ = 1, 2)[100] confirm the proposal of Peacock and Weakley. The lacunary heteropolyanions function as tetradentate ligands generating an approximately square antiprismatic coordination environment for the lanthanide(actinide) cation. Since the polyanion ligands have only C_s symmetry, there are four possible conformations for the complexes corresponding to "cis-oid" and "trans-oid" enantiomeric pairs.[80] In the crystalline state all of the above Keggin-derived complexes are trans-oid, whereas $[M^n(\alpha_2\text{-}P_2W_{17}O_{61})_2]^{(20-n)-}$ (M = Ce^{IV}, Lu^{III}, U^{IV}) are cis-oid, see Figure 24. However, structures of potassium salts of the α_1-derived complexes $[M(\alpha_1\text{-}P_2W_{17}O_{61})_2]^{16-}$ (M = Th, U) and $[U(\alpha_1\text{-}P_2W_{17}O_{61})(\alpha_2\text{-}P_2W_{17}O_{61})]^{16-}$ reveal both cis- and trans-oid conformations, and, in solution, the existence of stereoisomers has been demonstrated.[100] With the exception of the latter three species, there is little reason to doubt that the conformers of the {XW_{11}} and {α_2-X_2W_{17}} complexes readily interconvert in solution, probably via rotation. ^{183}W NMR spectra of $[Ln(PW_{11}O_{39})_2]^{11-}$ show six lines for Ln = La to Eu (consistent with C_{2v} symmetry for the whole complex), but 11 lines for Ln = Tb to Lu.[71,72] Although these results were interpreted to reveal a change from cubic to square antiprismatic coordination for the smaller lanthanide cations, they may well simply reflect a smaller barrier to intramolecular rotation for the complexes of the larger lanthanides. Variable temperature measurements are indicated.

Table 1. Conditional Formation Constants for $[M(mla)_n]^{p-}$ ($n = 1, 2$)

	$\log \beta_1$	$\log \beta_2$	medium	ref
$[PW_{11}O_{39}]^{7-}$				
Ce^{III}	6.2 ± 0.2	10.2 ± 0.2	?	68
	8.7	15.4	1 M $LiNO_3$	99
Ce^{IV}	22.9	33.5	1 M $LiNO_3$	99
$[SiW_{11}O_{39}]^{8-}$				
Ce^{III}	9.4	15.6	1 M $LiNO_3$	99
Ce^{IV}	24.6	35.0	1 M $LiNO_3$	99
α_1-$[P_2W_{17}O_{61}]^{10-}$				
Ce^{III}	6.6	8.1	1 M $LiNO_3$	99
Ce^{IV}	21.7	27.9	1 M $LiNO_3$	99
α_2-$[P_2W_{17}O_{61}]^{10-}$				
Ce^{III}	8.8	14.8	1 M $LiNO_3$	99
	1.74 ± 0.05	0.3 ± 0.5	1 M HNO_3	99
Nd^{III}	1.54		2 M HNO_3	152
Am^{III}		5.4	1 M HNO_3	136
	1.9	3	2 M HNO_3	152
Ce^{IV}	23.1	33.6	1 M $LiNO_3$	99
	15.1 ± 0.3	19.6 ± 0.3	1 M HNO_3	99
U^{IV}	7	11.4	2 M HNO_3	152
Np^{IV}	≥ 7		2 M HNO_3	152
Pu^{IV}	≥ 8	≥ 13	2 M HNO_3	152
Am^{IV}		32	pH 0.5−6.0	136
		9	1 M HNO_3	141
Am^{V}		6	pH 0.5−6.0	136

Table 2. $Ce^{IV/III}$ Reduction Potentials, V vs NHE[99]

L	CeL	CeL_2
$[PW_{11}O_{39}]^{7-}$	0.90	0.67
$[SiW_{11}O_{39}]^{8-}$	0.84	0.59
α_1-$[P_2W_{17}O_{61}]^{10-}$	0.85	0.57
α_2-$[P_2W_{17}O_{61}]^{10-}$	0.89	0.62

The high negative charges of the heteropolyanion ligands in these complexes allow the stabilization of "unusual" oxidation states for the lanthanide or actinide cations. Thus the presence of Pr^{IV},[130] Tb^{IV},[81,101,130,131] U^{V},[80] Am^{IV},[81,106,131−140] Cm^{IV},[81,106] Am^{V},[141] and Bk^{IV} [103,142] has been reported in such complexes. Many of the investigations of actinide complexes of this type have concerned their use in analysis and in separations of transuranium elements.[103,134,142−150] The polytungstate of choice has been α_2-$[P_2W_{17}O_{61}]^{10-}$.

Few 1:1 complexes have been isolated,[99] and no structures of these have been reported. However luminescence lifetimes for the complexes of $[PW_{11}O_{39}]^{7-}$ and $[SiW_{11}O_{39}]^{8-}$ with Sm, Eu, Dy, Tb, and Cm indicate that the 1:1 complexes have 4−6 coordinated water molecules compared with 0.1−0.5 water molecules for the 1:2 complexes.[74,151,152]

Some conditional formation constants for these complexes have been measured and are listed in Table 1. Corresponding Ce^{IV}/Ce^{III} reduction potentials are given in Table 2.

3. $\{XW_{11}\}_2$: $\{XW_{11}\}_2\{Mo_3S_4\}_2$

Recently Müller et al.[153] have demonstrated that the monovacant lacunary anion $[SiW_{11}O_{39}]^{8-}$ reacts as an electrophile toward the nucleophilic $[Mo_3S_4(H_2O)_9]^{4+}$ to yield the bridged species $[(SiW_{11}O_{39})_2\{Mo_3S_4(H_2O)_3\}_2(\mu\text{-}OH)_2]^{10-}$ ($\{XW_{11}\}_2\{Mo_3S_4\}_2$, **24**) with the structure of C_{2v} symmetry shown in Figure 25. It is evident that other reactions of this type are possible.

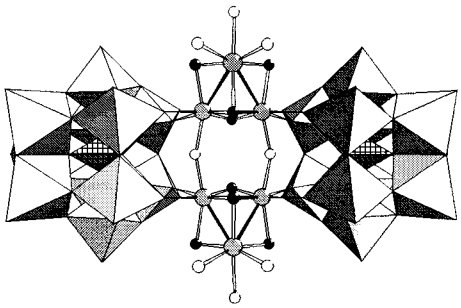

Figure 25. View of the structure of $[(SiW_{11}O_{39})_2\{Mo_3S_4(H_2O)_3\}_2\{\mu\text{-}OH\}_2]^{10-}$ (**24**). The lacunary Keggin-type fragments $\{\alpha\text{-}SiW_{11}\}$ are shown in polyhedral, the $\{Mo_3S_4\}$ units in ball-and-stick representation ($\{WO_6\}$ octahedra, gray; central $\{SiO_4\}$ tetrahedra, crosshatched; Mo atoms, gray spheres; S atoms, small black spheres; O atoms, small white spheres).

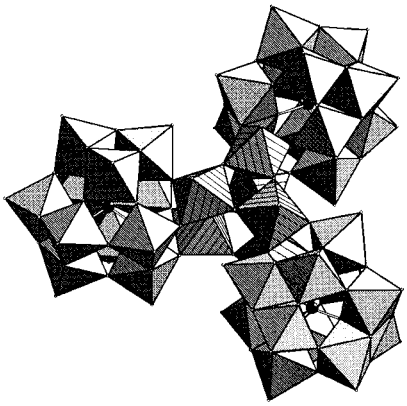

Figure 26. Structure of $[B_3W_{39}O_{132}]^{21-}$ (**25**, $\{WO_6\}$ octahedra of $\{\alpha\text{-}BW_{11}\}$ groups, gray; B centers, black spheres; $\{WO_6\}$ octahedra of central core, hatched).

4. $\{XW_{11}\}_3$: $\{B_3W_{39}\}$

The hexagonal form of tungstoboric acid,[154−157] long thought to be an isomer of the tetragonal form (which contains the Keggin anion), has recently been shown to have the composition $H_{21}[B_3W_{39}O_{132}]\cdot 69H_2O$ ($\{B_3W_{39}\}$, **25**).[158] The structure with C_{3h} symmetry, see Figure 26, is revealed to be an assemblage of three $\{BW_{11}\}$ anions linked by a central $\{W_6O_{27}\}$ group. The acid is stable in solution, and has been shown from viscosity measurements to have a hydrodynamic radius of 10.3 Å, consistent with that in the crystal.

B. Clusters Incorporating Different Types of Trivacant Lacunary Building Blocks

1. $[XW_9O_{34}]^{n-}$ (A- or B-Type)

a. $\{A\text{-}XW_9\}_2$: $\{X_2W_{21}\}$. Salts of the anion $[P_2W_{21}O_{71}]^{6-}$ ($\{P_2W_{21}\}$, **26**) have been known for over a century[159−161] and the more recently determined structure[162] reveals a sandwich-like arrangement of two $\{PW_9\}$ moieties enclosing three $\{WO_5(H_2O)\}$ octahedra (Figure 27). Although the crystal shows 3-fold rotational disorder of the anion, two positions are detected for the equatorial tungsten atoms. A careful NMR study shows that two of the tungsten atoms (W_{in}) are displaced toward the apparent 3-fold axis, and one (W_{out}) is displaced away from this axis.

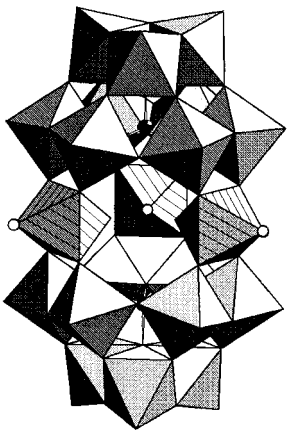

Figure 27. Structure of $[P_2W_{21}O_{71}]^{6-}$ (**26**, {*A*-α-PW_9} groups, gray; octahedra with P centers, black spheres; {$WO_5(OH_2)$} octahedra, hatched; H_2O, white spheres).

The center of the anion thus encloses two "terminal" oxo oxygen atoms and a H_2O molecule that is trans to the terminal oxygen atom of the third tungsten center. The central H_2O ligand undergoes slow exchange with solvent water molecules.[162] The analogous arsenate(V) anion has also been reported.[163]

The {P_2W_{21}} anion is generated by acidification of the lacunary species $[PW_{11}O_{39}]^{7-}$. Moderate acidification of the potassium salt of the latter anion (pH 2.0) leads to a lacunary derivative of {P_2W_{21}}, $[P_2W_{20}O_{70}(H_2O)_2]^{10-}$. An X-ray study of the corresponding salt is said to reveal a nondisordered anion in which a potassium cation occupies the unique equatorial tungsten (W_{out}) of the parent anion.[164] The arsenate(V) homologue has been reported.[165] Several examples of monosubstituted {XZW_{20}} complexes (Z = trivalent cation, VO^{2+}, Sn^{IV}, etc.) appear to exist.[164]

A quite different {P_2W_{20}} anion has been reported by Fuchs and Palm.[166] Treatment of a hot suspension of $K_3PW_{12}O_{40}$ with K_2CO_3 yields several products, one of which is $K_{13}[KP_2W_{20}O_{72}]\cdot 30H_2O$ ({P_2W_{20}}, **27**). As in the lacunary derivative of {P_2W_{21}}, the anion comprises two A-type {α-PW_9} units linked by two tungsten atoms, but the former are not eclipsed (with a common 3-fold axis) as in the {P_2W_{21}} family, and the linking tungsten centers each carry two cis terminal oxygen atoms. A potassium ion occupies the center of symmetry of the anion, which has nominal C_{2h} symmetry, see Figure 28.

The anion "$[P_2W_{19}O_{69}]^{14-}$" has been reported, and its behavior seemed to indicate that it was a divacant lacunary derivative of {P_2W_{21}}.[167,168] A more recent crystal structure confirms this, see Figure 29.[169] The anion appears to be unstable in solution, but crystallizes rapidly in the presence of potassium cations, two of which occupy equatorial sites in the anion.

b. {*B*-XW_9}$_3$: {$M_9P_5W_{27}$}. Salts of $[Co_9(OH)_3(H_2O)_6(HPO_4)_2(B\text{-}\alpha\text{-}PW_9O_{34})_3]^{16-}$ ({$Co_9P_5W_{27}$}, **28**) were obtained as byproducts in the synthesis of $[Co_4(H_2O)_2(PW_9O_{34})_2]^{10-}$. The structure of the anion is shown in Figure 30.[170] Three {α-PW_9Co_3} Keggin units are linked by corner sharing of the {Co_3} triads into an assembly of D_{3h} symmetry with capping axial phosphate groups. The magnetic properties of this complex and a Ni^{II} analogue have recently been reported.[171,172]

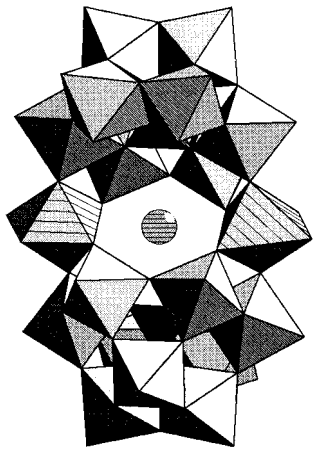

Figure 28. Structure of $[KP_2W_{20}O_{72}]^{13-}$ (**27**, {*A*-α-PW_9} groups, gray; octahedra with P centers, black spheres; bridging {WO_6} octahedra, hatched; enclosed K^+ cation, hatched sphere).

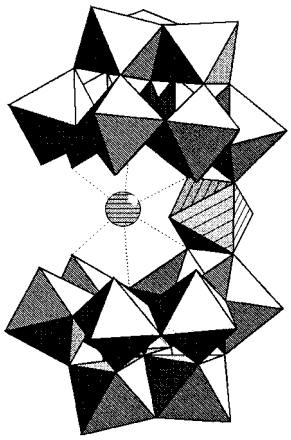

Figure 29. Structure of the divacant lacunary derivative of **26** (code as in Figure 27).

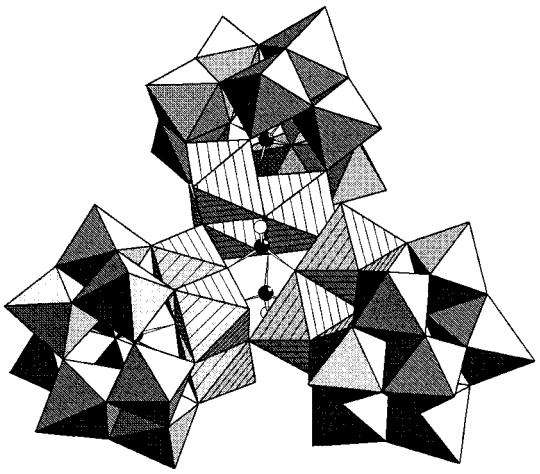

Figure 30. Structure of the cluster anion $[Co_9(OH)_3(H_2O)_6(HPO_4)_2(B\text{-}\alpha\text{-}PW_9O_{34})_3]^{16-}$ (**28**, {WO_6} octahedra, gray; {$Co^{II}O_6$} octahedra, hatched; P atoms, black spheres; OH ligands, small white spheres).

2. $[X^{III}W_9O_{33}]^{9-}$

a. {XW_9}: {Eu_3SbW_{24}}. The tungstoantimonate, $[Eu_3(H_2O)_3(Sb^{III}W_9O_{33})(W_5O_{18})_3]^{18-}$ ({Eu_3SbW_{24}}, **29**) has been reported by Yamase.[173] As indicated by the formula, the anion incorporates a {*B*-α-SbW_9} and

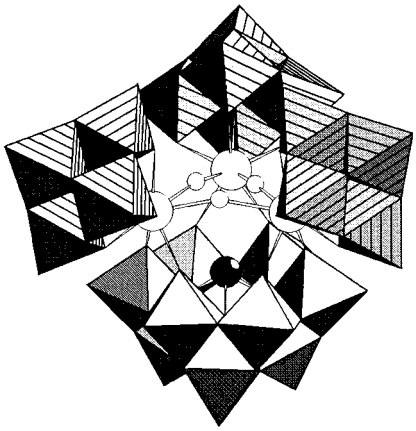

Figure 31. Structure of the cluster $[Eu_3(H_2O)_3(SbW_9O_{33})(W_5O_{18})_3]^{18-}$ (**29**), showing three $\{W_5O_{18}\}$ units (hatched octahedra) and a $\{B\text{-}\alpha\text{-}SbW_9\}$ group (gray octahedra). (Eu centers, large white spheres; Sb center, black sphere; H_2O, small white spheres).

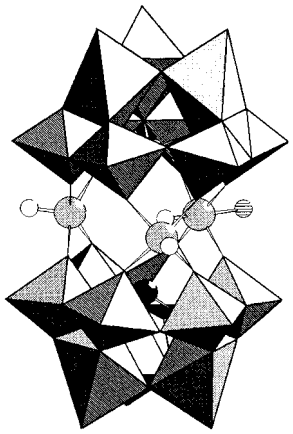

Figure 32. Structure of the anion $[As_2W_{21}O_{69}(H_2O)]^{6-}$ (**30**, $\{B\text{-}\alpha\text{-}AsW_9\}$ groups, gray; octahedra with As centers, black spheres; W centers, large gray spheres; O atoms, small white spheres; H_2O, small hatched sphere).

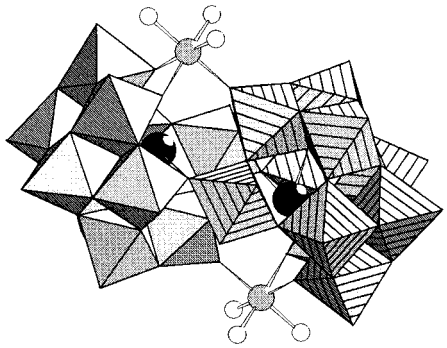

Figure 33. Structure of the anion $[Sb_2W_{22}O_{74}(OH)_2]^{12-}$ (**31**, $\{B\text{-}\beta\text{-}SbW_9\}$ groups and internal bridging $\{WO_6\}$ octahedra, gray and hatched; Sb centers, black spheres; external bridging W centers, large gray spheres; O atoms, small white spheres). The structure of $\{X_2W_{20}M_2\}$ anions (X = Sb, Bi; M = Fe^{III}, Co^{II}) is similar (M centers, large gray spheres; H_2O, small white spheres).

three $\{W_5\}$ groups (the latter may be viewed as lacunary derivatives of $[W_6O_{19}]^{2-}$). These are disposed in a roughly tetrahedral arrangement about a central $\{Eu_3\}$ triad, see Figure 31. Attempts to prepare analogues with $\{AsW_9\}$ and $\{BiW_9\}$ groups were unsuccessful. The photoluminescent behavior of the crystals of this complex was reported.[173]

b. $\{XW_9\}_2$: $\{X_2W_{21}\}$ and $\{X_2W_{22}\}$. The $\{As_2W_{21}\}$ anion and its lacunary derivatives $\{As_2W_{20}\}$ and $\{As_2W_{19}\}$ would appear to parallel the chemistry of the $\{P_2W_{21}\}$ family described in section VI.B.1a.[163,165,174] Unlike the tungstophosphates(V) the tungstoarsenates(III) were synthesized relatively recently. The structure of the parent anion, $[As_2W_{21}O_{69}(H_2O)]^{6-}$ ($\{As_2W_{21}\}$, **30**), based on a combination of single-crystal X-ray analysis and NMR spectroscopy[175,176] is indeed analogous to that of $\{P_2W_{21}\}$ but of course is based on B-type $\{AsW_9\}$ units as dictated by the lone pair of electrons on As^{III}. The arrangement of equatorial tungsten atoms is different also, two $\{W_{out}\}$ and one $\{W_{in}\}$ center, and this presumably is a consequence of the smaller dimensions, and the axial lone pairs, of the equatorial cavity produced by two $\{B\text{-}XW_9\}$ moieties. The $\{W_{out}\}$ atoms have nominal square-pyramidal coordination, although the terminal oxygen center of $\{W_{in}\}$ could be considered to function as a sixth "ligand" for the $\{W_{out}\}$ atoms, see Figure 32. Structures of the lacunary derivatives of $\{As_2W_{21}\}$ have not been reported, but those of $[As_2Co^{II}W_{20}O_{68}(H_2O)_2]^{8-}$ and the isomorphous zinc compound show that Co(Zn) have replaced a $\{W_{out}\}$ atom.[177]

Reports of "$\{XW_{11}\}$" anions (X = Sb^{III}, Bi^{III}) and their 1:1 complexes with di- and trivalent transition metal cations appeared in the early 1970s.[178−180] More recently these species have been revealed to be dimeric, based on structure determinations of salts of $[Sb_2W_{22}O_{74}(OH)_2]^{12-}$ (**31**), $[Sb_2W_{20}Fe^{III}_2O_{70}(H_2O)_6]^{8-}$, $[Sb_2W_{20}Co^{II}_2O_{70}(H_2O)_6]^{10-}$, and $[Bi_2W_{20}Fe_2O_{68}(OH)_2(H_2O)_6]^{6-}$.[181] The anion structure, see Figure 33, is seen to consist of two $\{B\text{-}\beta\text{-}XW_9\}$ groups linked by two additional tungsten atoms. Two more relatively weakly bound additional tungsten centers ($\{WO_6\}$ octahedra with three unshared vertexes) in the $\{W_{22}\}$ structure are replaced by $M^{II/III}$ cations in the substituted anions.

c. $\{XW_9\}_3$: $\{Ln_2As_3W_{29}\}$ and $\{(UO_2)_3As_3W_{29}\}$. Reaction of $\{B\text{-}XW_9\}$ anions with lanthanide and actinide cations which demand coordination numbers greater than six, yields a variety of polyoxoanions with unanticipated stoichiometries and structures.[182] The anions, $[Ln_2(H_2O)_7As_3W_{29}O_{103}]^{17-}$ (Ln^{III} = La, Ce; $\{Ln_2As_3W_{29}\}$, **32**), have the structure shown in Figure 34 which contains three $\{AsW_9\}$ fragments bridged by two additional tungsten atoms and two Ln^{III} cations, one eight- and one nine-coordinate. A similar trilobed structure is observed with the uranyl(VI) complex, $[(UO_2)_3(H_2O)_5As_3W_{29}O_{104}]^{19-}$ ($\{(UO_2)_3As_3W_{29}\}$, **33**), but differs in detail (*three* pentagonal-bipyramidal $\{UO_2\}^{2+}$ cations and a $\{W_2O_5\}$ bridging group (Figure 35).[183]

d. $\{XW_9\}_4$: $\{As_4W_{42}\}$, $\{Sb_8W_{36}\}$, and $\{Ln_4As_4W_{40}\}$. Three polyoxotungstate structures with four $\{B\text{-}XW_9\}$ building blocks have so far been identified. The first of these, $[As_4W_{40}O_{140}]^{28-}$ ($\{As_4W_{40}\}$, **34**), was reported in 1974 and it was shown to bind two additional transition metal cations.[174,184] A structure determination[176,185] of the cobalt(II) derivative revealed the cyclic anion, comprising four $\{\alpha\text{-}AsW_9\}$ units linked by additional tungsten atoms, shown in Figure 36.

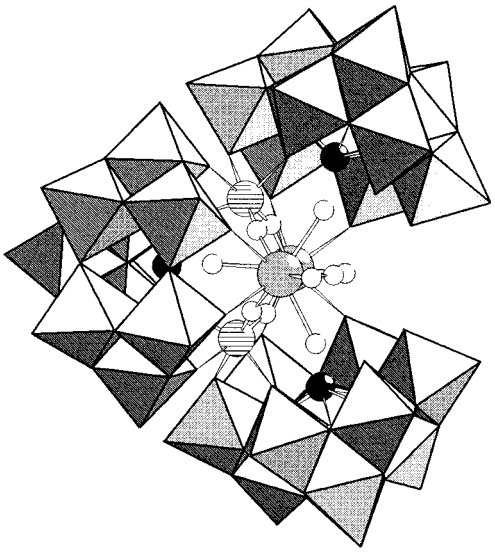

Figure 34. Structure of the anion type $[Ln_2(H_2O)_7As_3W_{29}O_{103}]^{17-}$ (**32**, {*A*-α-AsW_9} groups, gray; octahedra with As centers, black spheres; Ce(La) centers, large gray spheres; bridging W atoms, large hatched spheres; $O(H_2O)$, small white spheres).

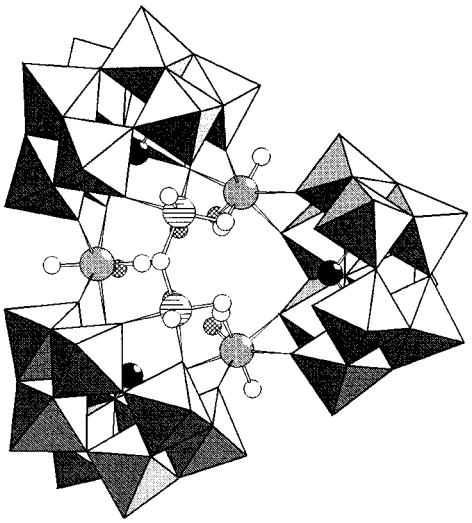

Figure 35. Structure of the anion $[(UO_2)_3(H_2O)_5As_3W_{29}O_{104}]^{19-}$ (**33**, {*A*-α-AsW_9} groups, gray; octahedra with As centers, black spheres; W centers, large hatched spheres; U centers, large gray spheres; O, small white spheres; H_2O, small hatched spheres).

The anion has a central cryptate site (S_1) and four lacunary sites (S_2). The S_1 sites can be occupied by alkali and alkaline earth cations (the order of stability is $Li^+ < Na^+ < K^+ > Rb^+ > Cs^+$ and $Mg^{2+} < Ca^{2+} < Sr^{2+} < Ba^{2+}$). These cations undergo slow exchange on the ^{183}W NMR time scale.[186] More recent work suggests that the S_1 sites can also accommodate lanthanide cations.[83,187] Two of the S_2 sites can be occupied by di- or trivalent metal cations, by Cu^I and by W^{VI}.[187−189] This has been attributed to an "allosteric" rearrangement of the structure resulting in enlargement of two of these sites when the other two are occupied by smaller metal cations.[185] Only in the case of Ag^I can all four S_2 sites become occupied. Metal cations in the S_2 sites have a single terminal aqua ligand which can be replaced by other ligands in aqueous[174] or nonaqueous solution.[190−192]

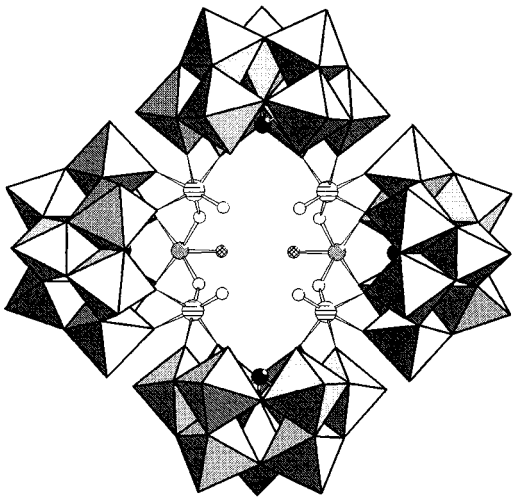

Figure 36. Structure of the dicobalt derivative of the anion $[As_4W_{40}O_{140}]^{28-}$ (**34**, code as for Figure 35 with Co centers, small gray spheres).

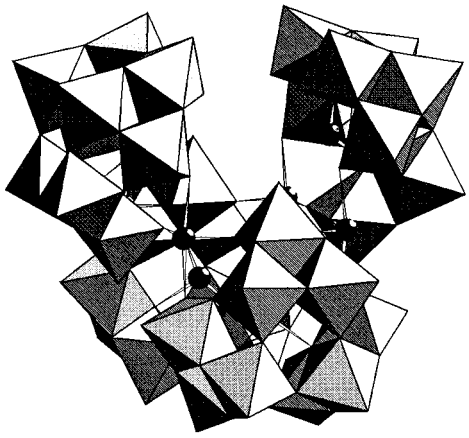

Figure 37. Structure of the anion $[Na_2Sb_8W_{36}O_{132}(H_2O)_4]^{22-}$ (**35**, {*B*-β-SbW_9} groups, shaded octahedra; Sb centers, black spheres).

The anion $[Na_2Sb_8W_{36}O_{132}(H_2O)_4]^{22-}$ ({Sb_8W_{36}}, **35**), see Figure 37, recently reported by Krebs and Klein[181] appears at first glance to be similar to {As_4W_{40}}. However the {SbW_9} groups have a β conformation and the bridging atoms are ψ-trigonal-bipyramidally coordinated Sb^{III} atoms rather than octahedrally coordinated W^{VI} centers. The central cavity contains two sodium cations and associated H_2O molecules; the anion appears not to be crystallizable in the absence of sodium cations, and establishes an equilibrium with other species in solution.

A third structure of this general {XW_9}$_4$ type has been reported.[182] Four {*B*-α-AsW_9} units in $[Ln_4As_4W_{40}O_{146}]^{28-}$ ({$Ln_4As_4W_{40}$}, **36**) are linked by eight-coordinate Ln^{3+} centers (Ln = La, Ce, Gd). Additional W^{VI} atoms occupy lacunary sites somewhat analogous to the S_2 sites in {As_4W_{40}}. Two of these sites are fully occupied and two have partial occupancy. An additional tungsten atom with trigonal-bipyramidal coordination occupies a unique axial position linking all four Ce atoms.

e. {XW_9}$_{12}$: {$Ln_{16}As_{12}W_{148}$}. The record-sized heteropolytungstate anions, $[Ln_{16}As_{12}W_{148}O_{524}(H_2O)_{36}]^{76-}$ ({$Ln_{16}As_{12}W_{148}$}, **37**), have recently been reported[7] and are shown to contain an assembly of 12 {α-AsW_9}

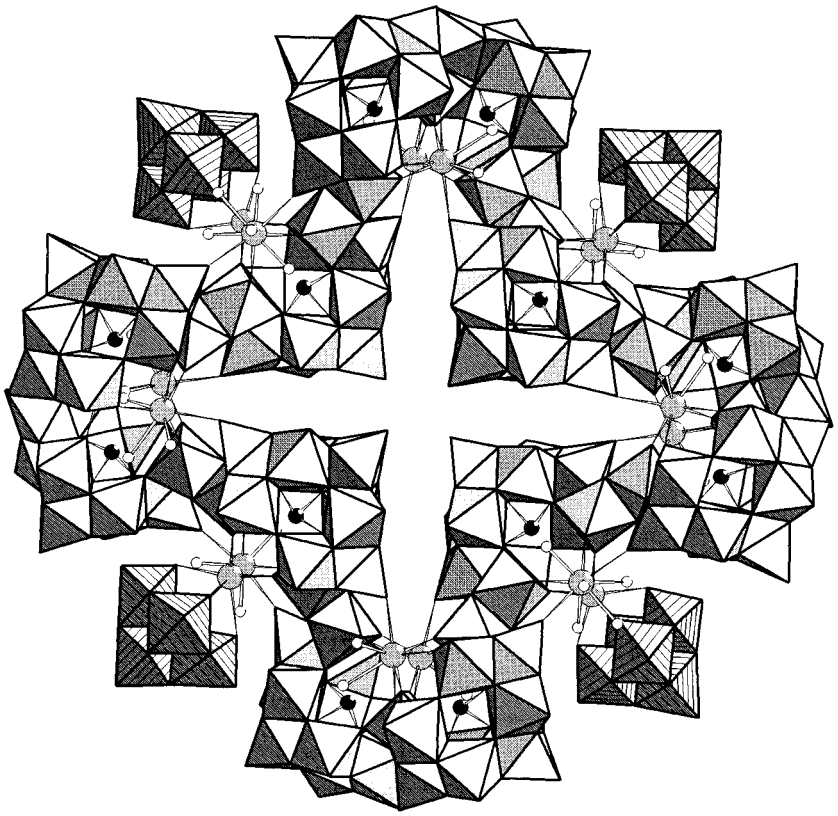

Figure 38. Structure of the anion $[Ln_{16}As_{12}W_{148}O_{524}(H_2O)_{36}]^{76-}$ (**37**) as a folded cyclic assembly of 12 {*B*-α-AsW_9} groups linked by additional tungsten centers (all shown in polyhedral representation) and four {LnW_5} groups. (Ce(La) centers, large gray spheres; As centers, small black spheres; H_2O, small white spheres).

groups linked by Ln^{III} cations (Ln = La, Ce, Nd, Sm, etc.) and additional tungsten atoms into a folded cyclic structure of D_{2d} symmetry. The anion structure is further embellished by four {W_5O_{18}} lacunary fragments, see Figure 38. The 16 Ln atoms carry a total of 36 aqua ligands which offer sites for further derivatization of the anion. Salts of these anions are formed in moderate (30%) yields starting either with preformed {AsW_9} groups or from solutions containing As^{III}, Ln^{III}, and WO_4^{2-}. The anions are stable in aqueous solution and give well-resolved ^{183}W NMR spectra. The solution and solid-state chemistry of these very large polyoxotungstates (relative molecular mass ~40 000, diameter 40 Å) is currently under investigation.

3. B-Type $[P_2W_{15}O_{56}]^{12-}$: {$M_4P_4W_{30}$} and {$P_4M_6W_{32}$}

The sandwich complexes of composition $[M^{II}_4(H_2O)_2(P_2W_{15}O_{56})_2]^{16-}$ ({$M_4P_4W_{30}$}, **38**) were first described by Finke and co-workers.[193,194] Their structures (Figure 39) were deduced, via ^{183}W NMR, to be analogous to those of $[M_4(H_2O)_2(PW_9O_{34})_2]^{10-}$ [195] (not considered in this review) and subsequently this was confirmed by crystallographic investigation of derivatives containing Cu,[196] Zn,[197] Mn, and Ni[198] atoms. The four divalent metal atoms which occupy adjacent edge-shared octahedra are antiferromagnetically coupled in the Mn^{II} complex, and ferromagnetically coupled in the Ni^{II} complex.[198] Recently the Fe^{III} derivative has been synthesized, structurally characterized, and evaluated as a catalyst for alkene oxidation.[199]

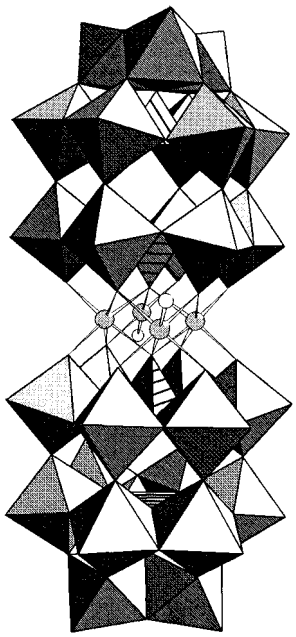

Figure 39. Structure of the anion type $[M_4(H_2O)_2(P_2W_{15}O_{56})_2]^{16-}$ (**38**). The lacunary {P_2W_{15}} fragments are shown in polyhedral, while the bridging metal centers are shown in ball-and-stick representation ({WO_6} octahedra, gray; {PO_4} tetrahedra, hatched; metal centers, gray spheres; H_2O centers, white spheres).

Salts of an anion formulated as $[P_4Ti_6W_{32}O_{132}]^{28-}$ ({$P_4M_6W_{32}$}, **39**) have recently been reported.[200] Although solids containing this anion have not been structurally characterized, crystals of an oxalate derivative **39a** contain a dimeric species [(P_2W_{18}-

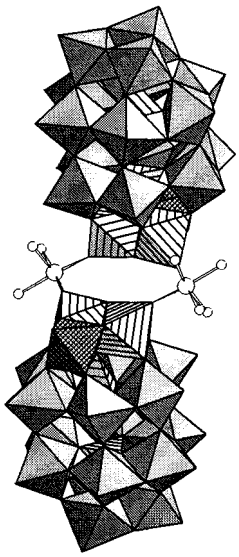

Figure 40. Structure of the dimeric species $[(P_2W_{18}Ti_2O_{62})_2(\mu\text{-}Ti(ox)_2)_2]^{28-}$ (**39a**). The two $\{P_2W_{16}Ti_2\}$ moieties are displayed in polyhedral representation ($\{WO_6\}$ octahedra, gray and crosshatched (see text); internal $\{PO_4\}$ tetrahedra and $\{TiO_6\}$ octahedra, hatched; bridging Ti centers, large white spheres; O atoms of the oxalato ligands, small white spheres; the C atoms of the oxalato ligands are omitted).

$Ti_2O_{62})_2(\mu\text{-}Ti(ox)_2)_2]^{28-}$, and it was assumed that **39** has an analogous structure with aqua or hydroxo ligands (see Figure 40). Independent confirmation of the dimeric nature of **39** is currently lacking however. The structure of **39a** is based on two lacunary $\{P_2W_{15}\}$ moieties that are "completed" by one tungsten and two titanium atoms, and these are bridged by two "external" bisoxalatotitanium groups through Ti−O−Ti bonds. The tetrabutylammonium salt of **39** has been shown to be an active photocatalyst for the oxidation of simple alcohols in acetonitrile solution.[200]

C. Clusters Incorporating Pentavacant Lacunary Building Blocks

1. {Sb_9W_{21}} and Related Anions

The tungstoantimonate(III) anion that was originally believed to have the composition $[Sb_2W_5O_{20}]^{4-}$ [180] was revealed to be $[NaSb_9W_{21}O_{86}]^{18-}$ ($\{Sb_9W_{21}\}$, **40**) from the structure determination of the ammonium salt.[201] The structure, see Figure 41, contains in agreement with the D_{3h} symmetry three $\{SbW_7\}$ groups linked to a central core of two $\{Sb_3O\}$ groups encapsulating a sodium cation. The $\{SbW_7\}$ units can be viewed as pentavacant lacunary derivatives of the hypothetical $\{\beta\text{-}SbW_{12}\}$ anion. The anion is formed at pH 7−8 from Sb_2O_3 and WO_4^{2-} or from $\{SbW_9\}$ species and Sb^{III}. An unstable analogue, $[NaSb_6As_3W_{21}O_{86}]^{18-}$, can be prepared in this way from $\{AsW_9\}$ at pH 8−9.[202] The selectivity of the central site for Na^+ ($>K^+ > Rb^+$, Cs^+; $> Li^+$) was determined by titration of the metastable ammonium derivative. Ca^{2+}, Sr^{2+},[186,202] and lanthanide derivatives have been reported.[83,203] Although two adjacent lacunary sites on each $\{SbW_7\}$ group should be occupiable by cations to give complete $\{\beta\text{-}SbW_7M_2\}$

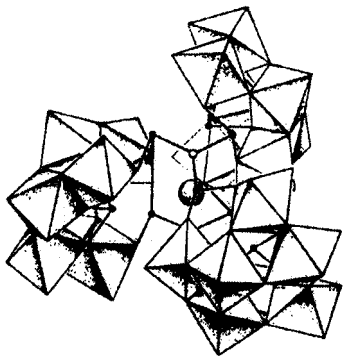

Figure 41. Structure of the anion $[NaSb_9W_{21}O_{86}]^{18-}$ (**40**). The three $\{SbW_7\}$ fragments are shown in polyhedral representation (Sb centers, black spheres; O atoms, white spheres; enclosed Na^+ cation, large sphere).

the experimental verification of this behavior is ambiguous at present. One study shows that the expected six cations ($M = Fe^{III}$ and VO^{2+}) can be added,[202] but another indicates that a total of only three ($M = Mn^{II}$, Fe^{III}, Co^{II}, Ni^{II}, Cu^{II}) are complexed.[204]

The ammonium salt of the $\{Sb_9W_{21}\}$ anion has achieved some notoriety as the antiviral agent HPA-23, which for a brief time was used for treatment of AIDS.[205] The discovery that large polytungstates showed in vitro and in vivo antiviral and antitumoral activity was made in the 1970s[206,207] and has spawned an immense literature (see e.g., refs 208−210) which is beyond the scope of the present review.

D. Clusters Incorporating Hexavacant Lacunary Building Blocks

1. {P_4W_{24}} and {P_8W_{48}}

Lacunary derivatives of the α-Dawson anion $[P_2W_{18}O_{62}]^{6-}$ ($\{P_2W_{18}\}$) include a metastable hexavacant species isolated as $K_{12}H_2P_2W_{12}O_{48}\cdot 24H_2O$ ($\{P_2W_{12}\}$).[211] The probable C_{2v} structure of the $\{P_2W_{12}\}$ anion was deduced from its reaction with molybdate(VI) to give a unique substitutional isomer (of C_{2v} symmetry) of α-$[P_2W_{12}Mo_6O_{62}]^{6-}$. Dilute solutions of $\{P_2W_{12}\}$ can be induced to yield crystals of $K_{28}Li_5H_7P_8W_{48}O_{184}\cdot 92H_2O$ ($\{P_8W_{48}\}$, **41**) with the cyclic structure shown in Figure 42.[176,212] The D_{4h} structure of the $\{P_8W_{48}\}$ anion can be regarded as a condensed tetramer of $\{P_2W_{12}\}$ groups. Alternatively, the anion is a cyclic fused octamer of $\{PW_6\}$ groups which are derived from the Keggin anion by removal of two corner-shared triads of $\{WO_6\}$ octahedra. The $\{P_8W_{48}\}$ anion is very stable in solution (pH 1−8; ^{31}P and ^{183}W NMR recorded) and the free acid can be prepared and titrated with 40 equiv of base. The crystal structure reveals that the central cavity of the anion contains a number of potassium cations.

A possible intermediate in the condensation process from $\{P_2W_{12}\}$ to $\{P_8W_{48}\}$ has been detected and isolated as $K_{16}Li_2H_6P_4W_{24}O_{94}\cdot 33H_2O$ ($\{P_4W_{24}\}$). Solutions containing the $\{P_4W_{24}\}$ anions are stable enough to permit observation of a ^{31}P NMR spectrum (two signals) which is consistent with structure(s) derived from a cis-oid and/or trans-oid condensation of two $\{P_2W_{12}\}$ moieties.[212]

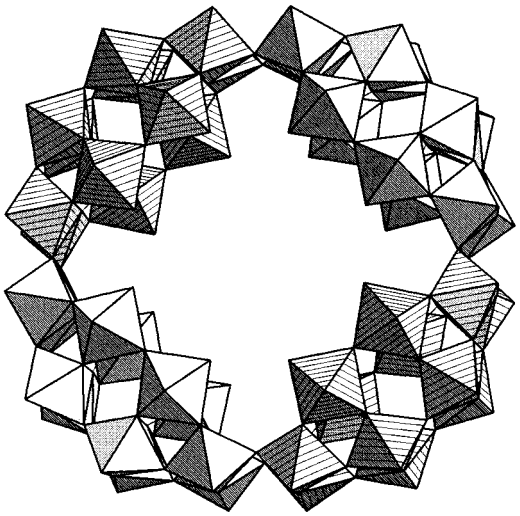

Figure 42. Structure of the anion $[P_8W_{48}O_{184}]^{40-}$ (**41**) as a cyclic assembly of four lacunary $\{P_2W_{12}\}$ groups. The internal $\{PO_4\}$ tetrahedra of the latter have been omitted ($\{WO_6\}$ octahedra, gray and hatched).

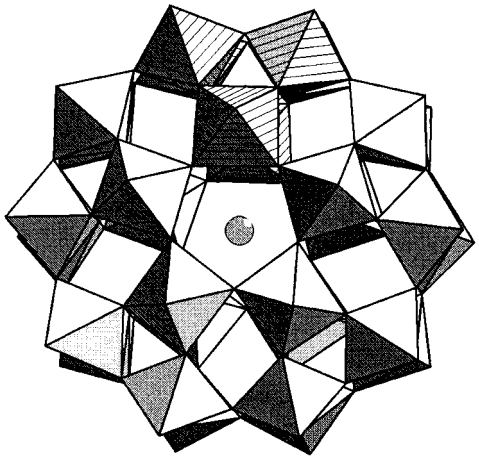

Figure 43. Structure of the anion $[NaP_5W_{30}O_{110}]^{14-}$ (**42**) as a cyclic assembly of five $\{PW_6\}$ groups (internal $\{PO_4\}$ tetrahedra omitted for clarity; Na center, large gray sphere).

2. {P_5W_{30}}

When sodium tungstate is boiled with an excess of phosphoric acid the main heteropolytungstate products are two isomers ($\alpha\alpha$**E** and $\alpha\beta$**E**) of the yellow Wells−Dawson anions, $[P_2W_{18}O_{62}]^{6-}$, and a smaller amount of a colorless species originally given the formula $[HP_3W_{18}O_{66}]^{8-}$.[213] A subsequent X-ray investigation of the ammonium salt showed the true composition of this anion to be $[NaP_5W_{30}O_{110}]^{14-}$ ($\{P_5W_{30}\}$, **42**) with the structure shown in Figure 43.[176,214] The unusual 5-fold symmetry of this anion is achieved by fusion of five $\{PW_6\}$ groups of the type noted above for the $\{P_8W_{48}\}$ species. The central sodium ion lies not on the equator of the anion but in a plane roughly defined by oxygen atoms of the phosphate groups. The sodium cation is nonlabile on the NMR time scale, and appears to be essential for the anion synthesis.[214] The presence of the sodium cation reduces the overall anion symmetry from D_{5h} to C_{5v}. The $\{P_5W_{30}\}$ anion is even more robust than the $\{P_8W_{48}\}$ one (pH stability range ~0−10). Under hydrothermal conditions (120−180 °C) the central Na^+ can be replaced by other cations of similar size, e.g., Ca^{2+}, most Ln^{III}, and U^{IV}.[215−218] Reduction of Eu^{III} to Eu^{II} in these complexes occurs within the potential range at which the polytungstate framework is reduced to heteropoly blues, and implies the possibility of generating an intermediate valence-state compound.[219,220] Structures of the Eu^{III} and U^{IV} derivatives have been reported, and show that these central cations are coordinated by a H_2O molecule that is enclosed in the central cavity.[221] The sodium derivative has been evaluated as a catalyst for the oxidation of H_2S to sulfur, and was the best of the polyoxometalates examined.[222]

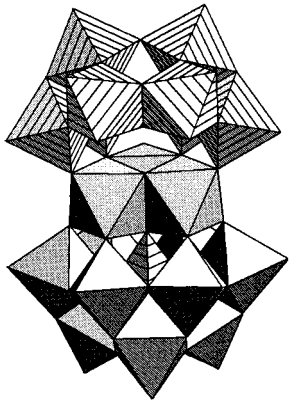

Figure 44. Structure of the cluster $[BW_{20}O_{66}]^{12-}$ (**43**) in polyhedral representation ($\{WO_6\}$ octahedra of the Keggin fragment, gray; central $\{BO_4\}$ tetrahedron, hatched; $\{WO_6\}$ octahedra of the $\{W_8\}$ group, hatched).

E. Mixed-Valence Clusters Derived from Heteropoly Browns {XW_{20}}

The six-electron-reduced Keggin heteropoly "browns", $[XW^{VI}_9W^{IV}_3O_{40}H_6]^{n-}$, X = H_2, B, Si, incorporate a trigonal $\{W^{IV}_3O_4(H_2O)_3\}$ cluster fragment.[223−225] In neutral solution these anions react with tungstate(VI) to yield an unsymmetrical sandwich-type anion $[H_3W_{20}O_{66}]^{12-}$ ($\{XW_{20}\}$, **43**).[226] The structure of this cluster retains the core of the original reduced Keggin anion with an additional $\{W_8\}$ group attached via the W^{IV} centers (see Figure 44). The structure is retained in aqueous solution according to well-resolved ^{183}W NMR spectra of the $\{H_2\}$ and B derivatives.[227] It is likely that more highly reduced heteropoly browns (6, 9, and 12 W^{IV}) can yield other large clusters with W^{IV} centers.

F. Structurally Uncharacterized Clusters

Two other polytungstate species might prove to be of a size to fall within the scope of this review. The first is a "$\{Se^{IV}W_6\}_x$" species,[228,229] for which $x \approx 4$ is based on ultracentrifugation. The second is a 2:2 complex of Ce^{III} (and also Ce^{IV}) with the trivacant lacunary anion $[P_2W_{15}O_{56}]^{12-}$ for which a sandwich-type structure has been proposed.[99]

VII. Magnetism of Polyoxometalates

Most polyoxometalates comprise d^0 ions, and therefore are not interesting from the magnetic point of

view. However recently there has been an increasing interest in the magnetic properties of new derivatives, which either contain d^1 centers, like the polyoxovanadates(IV), or encapsulate small clusters of magnetic metal ions, like cobalt(II), nickel(II), etc. The general interest for the properties of large metal ion clusters giving rise to magnetic interactions has had a dramatic increase in the past few years after it was shown that some of these clusters can indeed behave like tiny magnets.[230,231] In a very simple scheme one can imagine starting from an assembly of isolated magnetic ions: the system corresponds to a simple paramagnet. The individual ions can be induced to cluster in pairs, in triples and in increasingly complex aggregates. If there is some sort of interaction between the ions they will show up in the relevant emerging magnetic properties. If two d^1 ions are coupled, the energies of the lowest lying levels of the pair will correspond to a singlet and to a triplet state: if the former is lower in energy the system is said to be antiferromagnetically coupled, if the latter is lower the coupling is ferromagnetic.

The simplest approach to describe the magnetic interaction between the two ions is provided by the so-called Heisenberg−Dirac−van Vleck spin Hamiltonian.[232] It can be used for interacting pairs which have orbitally nondegenerate ground states. In this case the orbital coordinates can be replaced by spin coordinates, and the Hamiltonian expressed as

$$H = J\ \mathbf{S}_1 \cdot \mathbf{S}_2 \tag{1}$$

By applying this Hamiltonian to the basis of coupled functions $|S_1 M_1 S_2 M_2\rangle$ the eigenfunctions can be labeled using the total spin:

$$\mathbf{S} = \mathbf{S}_1 + \mathbf{S}_2 \tag{2}$$

where $|S_1 - S_2| \leq S \leq S_1 + S_2$. The energies of the total states are given by

$$E(S) = \frac{J}{2}[S(S+1) - S_1(S_1+1) - S_2(S_2+1)] \tag{3}$$

If $S_1 = S_2 = {}^1/_2$, $S = 1, 0$, and the energies of the triplet and the singlet are: $E(1) = {}^J/_4$, $E(0) = -{}^3/_4 J$, respectively. By using this convention the singlet−triplet separation is J, the singlet lying lowest for positive J.

This approach is a phenomenological one. J can be obtained from the fit of the experimental data, typically the temperature dependence of the magnetic susceptibility. The values of J so obtained are often compared with orbital models which justify their sign and intensity.[233] In extremely simplified terms the value of J depends on the orbitals which contain unpaired electrons, the magnetic orbitals. If they are orthogonal to each other the spins orient parallel to each other according to the Hund's rule, while if they have a nonzero overlap a weak bond is formed and the spins orient antiparallel to each other. The magnetic orbitals can be either in direct contact or interact through intervening doubly occupied orbitals of diamagnetic ligands (superexchange). Useful structural-magnetic correlations are now established for many pairs of metal ions.[233−235]

The extension of (1) to systems with a larger number of interacting centers can be done as shown

$$H = \sum_{i<j} J_{ij}\ \mathbf{S_i} \cdot \mathbf{S_j} \tag{4}$$

The energy levels can still be labeled with the total spin. For instance for three interacting $S = {}^1/_2$ spins, the levels will be two doublets and one quartet. On increasing the number of coupled spins the number of the states rapidly increases, as $(2S+1)^N$ for a cluster of N ions each with spin value S. Eventually the levels will merge into a continuum and the magnetic properties will become those of a bulk ferro-, ferri-, or antiferromagnet. In rigorous terms this occurs only when an infinite number of ions is assembled together, but this is clearly an abstraction. In practice when N becomes very large one can expect to pass from the regime of small clusters, where quantum mechanical effects are dominant, to that of bulk magnets, where classical treatments work well. The problem is therefore open as to how large N must be in order to observe this coexistence of quantum and classical effects. Clearly the problem is of large theoretical interest, because it gives information on the limits of validity of quantum theory itself and on the correspondence principle,[236,237] but it is also of large experimental interest because it may provide an answer to the question of which is the lower limit to the miniaturization of the magnets which are used for instance as memory elements.[238] The field of magnetism of clusters is therefore a meeting ground for solid-state physics and chemistry, and indeed this has happened in the past few years. Polyoxometalates, with their ability to form giant clusters, are indeed very promising systems in order to build tailor-made magnets.[239] Ideally one should tune the synthetic strategies in order to control the size of the clusters, the arrangement of the magnetic centers and the spin topology, and the magnetic anisotropy. This is certainly an exciting area for development and for chemical ingenuity.

Another very important feature of the magnetic properties of polyoxometalates is that in many cases they are mixed-valence species, with both possibilities: localized and delocalized. It has long been known that heteropoly anions can be reduced to mixed-valence species (heteropoly blues and browns) in which the excess electrons can be fully or partially delocalized, giving rise to delocalized−delocalized, delocalized−localized, and localized−localized interactions.[3] The problem of the interplay of exchange and delocalization effects is another popular topic at the moment, the interest ranging from the magnetic properties of metallo enzymes and metallo proteins, like iron−sulfur proteins[240] and the water oxidizing center of photosystem II of bacterial photosynthesis,[241] to colossal magnetoresistance effects observed in lanthanide manganites.[242] Again the possibility of fine-tuning the structural features of the polyoxometalates controlling the relative ratios of mixed-valence species and the nature of the interaction, corresponding to class II and class III of the Robin

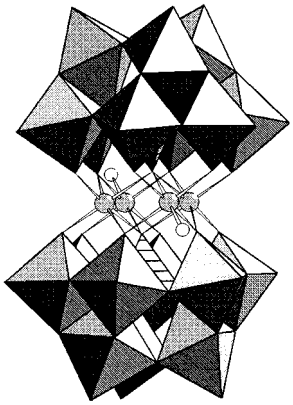

Figure 45. Sketch of the structure of the $[M_4(H_2O)_2(PW_9O_{34})_2]^{10-}$ anions in polyhedral representation.

and Day classification,[243] makes these materials ideal candidates for modeling these interactions and providing a testing grounds for theories.

Another relevant role of polyoxometalates in determining magnetic properties is that they can act as ligands toward other magnetic metal centers, encapsulating them.[172] In this way magnetic clusters are formed which can have different spin topologies, and in general are reasonably well separated from one another by the bulky nonmagnetic polyoxometalates. A typical structure[195] is shown in Figure 45, where an M_4 cluster ($M = Mn^{II}$, Fe^{II}, Co^{II}, Ni^{II}, Cu^{II}) is sandwiched by two $\{PW_9O_{34}\}$ groups to give an anion of formula $[M_4(H_2O)_2(PW_9O_{34})_2]^{10-}$.

Finally another important aspect associated with magnetic polyoxometalates is that they can be used as anions of organic charge-transfer systems, to investigate the interaction between moving electrons in the organic backbone and localized magnetic electrons in the polyoxometalates with the aim of obtaining new classes of molecular materials.[172] In fact the bulky anions have a variety of shapes and sizes, which can be used to modify the structure of the organic charge-transfer salts, thus tuning the physical properties of the materials.

In the following we will first treat the fully magnetic clusters, then the mixed-valence clusters and we will conclude with the polyoxometalate sandwiched clusters.

A. Polyoxovanadates(IV)

Polyoxovanadates(IV) represent an important class of magnetic polyoxometalates. We will consider them first, and in particular the systems which contain only oxovanadium(IV) centers. The building blocks of the clusters, relevant to the exchange pathways are shown in Figure 46.

In general in all these bridges antiferromagnetic coupling between the oxovanadium(IV) centers is observed,[239] even if the intensities of the interactions dramatically change with the nature of the bridges. It is certainly surprising that so far no satisfactory attempt to establish clear-cut relations between the structural features of the oxovanadium pairs and the magnetic coupling has been made, as was extensively done for instance for copper(II) complexes. An early attempt to collect the available information was made

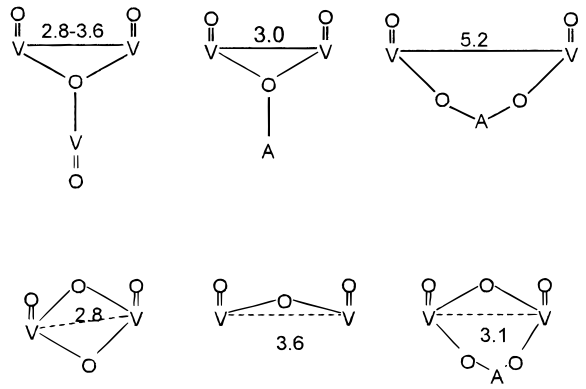

Figure 46. Scheme of the bridges most commonly found in polyoxovanadates(IV).

Table 3. Structural−Magnetic Correlations in Vanadium(IV) Pairs

type of bridge	V−V (Å)	V−O (bridge) (Å)	V−O−V (deg)	J	ref
$(OH)_2$	2.965	1.96	98	300	245
$(OH)_2$	3.033	1.956	101.2	354	246
$(OR)_2$	3.068	1.98	103	<300	247
$(OR)_2$	3.107	1.96	104.7	60	248
$(PO_4)_2$				9	249

by Syamal[244] but the number of well-characterized complexes was small, and no detailed conclusion could be reached, due to the lack of either structural or magnetic data. More recently some complexes were satisfactorily analyzed reporting all the necessary data[245−249] They are shown in Table 3. It is apparent that both the metal−metal distance and the angle at the bridging oxygen must play an important role.

So far the only attempt to use quantum mechanical treatments to calculate the exchange coupling constant has been reported by Plass,[245] who was interested in the conditions giving rise to ferromagnetic coupling between oxovanadium(IV) ions. In fact it has been found that in complexes such as oxovanadium tartrate, where the two {VO} groups are connected by bridges in a structure similar to that of copper acetate, a weak ferromagnetic coupling is operative.[250−255] Similar results were obtained in a dimer with a O=V−F−V=O linear bridge.[254] Now Plass reported[245] that in dimers with the structure shown in Figure 47 the coupling is weakly ferromagnetic ($J = -3$, -10 cm^{-1}). The use of density functional approaches yielded calculated values of the coupling constants of ~ -50 cm^{-1} which is in reasonable agreement with experiment. The origin of the ferromagnetic coupling was attributed to the interaction between an *xy* magnetic orbital on one center with an empty *yz* orbital on the other center.

More data are now available from the analysis of the magnetic properties of the polyoxovanadates.[239] The strongest coupling has been observed for di-μ-oxo bridges, and the weakest for the μ_2-OAO bridges, where $A = AsO_2$, PO_2. Some relevant data are shown in Table 4. The data in this table result from complex analysis of the magnetic properties of large clusters which will be described below, and as such some ambiguity in the determination of the values of the exchange parameters cannot be excluded.

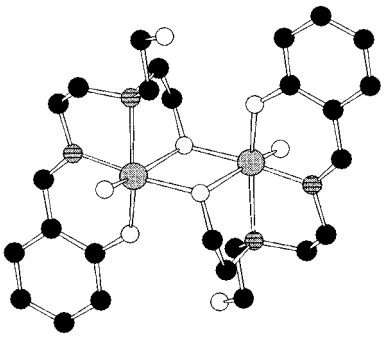

Figure 47. Molecular structure of $[VO(Hsabhea)]_2$, where H_3sabhea = *N*-salicylidene-2-(bis(2-hydroxyethyl)amino)-ethylamine (V atoms, gray spheres; O atoms, white spheres; N atoms, hatched spheres; C atoms, black spheres; H atoms omitted).

Table 4. Exchange Pathways and Coupling Constants in Some Polyoxovanadates(IV)[239]

bridge 1	bridge 2	V−V distance (Å)	J (cm^{-1})
μ_3-O	μ_3-O	2.9	>500
μ_3-O		3.7	50−200
μ_3-O	μ_2-OA	3.0	120
μ_2-OA	μ_2-OA	3.1	20
μ-OAO	μ-OAO	5.3−5.7	10

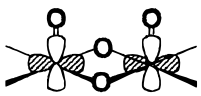

Figure 48. Magnetic orbitals for di-μ-oxo bridged oxovanadium(IV) pairs.

In principle the coupling between the oxovanadium(IV) centers is determined by the overlap between the *xy* magnetic orbitals. A possible scheme of interaction for di-μ-oxo bridges is shown in Figure 48. Given the relatively short distance between the two oxovanadium centers the interaction may be determined by both superexchange interactions through the orbitals of the bridging oxygen atoms and also by the direct exchange determined by the overlap of the *xy* orbitals which point to each other.

The largest oxovanadium(IV) polyoxometalates whose magnetic properties have been investigated so far comprise 14,[256] 15,[256,257] and 18[258] ions, respectively. We will label them in short as $\{V_{14}\}$, $\{V_{15}\}$, and $\{V_{18}\}$, respectively. Of these three clusters the magnetic properties of $\{V_{15}\}$ are the best understood, and we will start from that. $\{V_{15}\}$, $[V^{IV}{}_{15}As_6O_{42}(H_2O)]^{6-}$, has the trigonal structure[259] shown in Figure 49, with a trapped H_2O molecule in the middle of the cage. The oxovanadium ions can be grouped in three sets of six, three, and six, respectively. The two distorted hexagons on the outside of the anion have pairs of V ions separated by 2.87 Å and pairs separated by 3.05 Å. This structure in three layers has far-reaching consequences for the magnetic properties of the cluster.[256,257] In fact the room-temperature value of the effective magnetic moment, 4.0 μ_B, is much lower than expected for 15 unpaired electrons (6.7 μ_B), indicating that strong antiferromagnetic interactions are operative in the anion. This is confirmed by the temperature dependence of the effective magnetic moment, Figure 50, which gradually decreases on decreasing temperature and below 100 K it reaches a plateau at ~2.8 μ_B, slightly lower than the value expected for three unpaired electrons (3 μ_B). This is taken as an indication that the external hexagons are strongly antiferromagnetically coupled, and that they are in the ground nonmagnetic state $S = 0$ at relatively high temperature. The coupling is much weaker in the middle triangular layer, because the ions are not directly connected to each other. The interesting feature of the cluster is just this localization of the magnetic properties: at high temperature the three layers are all magnetic, while at low temperature only the middle layer is magnetically active. This shows that in principle one can build large clusters in which multimagnetic layers can be obtained. Given the current interest in nanostructured multimagnetic layers this may open exciting perspectives.

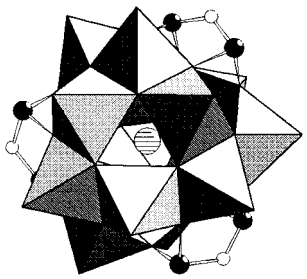

Figure 49. Sketch of the structure of the $[V^{IV}{}_{15}As_6O_{42}(H_2O)]^{6-}$ anion ({VO} polyhedra, gray; As atoms, black spheres; O atoms, white spheres; O atom of enclosed H_2O, hatched).

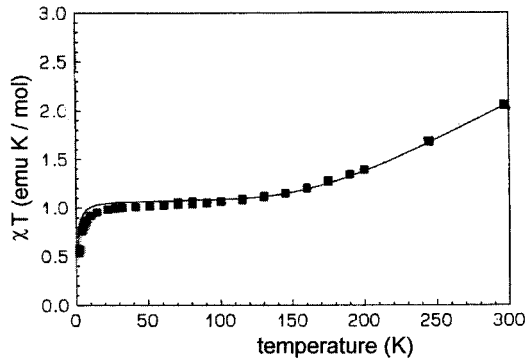

Figure 50. Temperature-dependence of the effective magnetic moment of $[V^{IV}{}_{15}As_6O_{42}(H_2O)]^{6-}$ $\{V_{15}\}$ and best fit with the parameters described in the text.

The magnetic properties of the cluster can be calculated by the Heisenberg Hamiltonian (4) which must be computed on the matrix of 2^{15} states originating from the interaction of the individual $S = {}^1/_2$ states. The size of the matrixes can be reduced by exploiting the symmetry, and this can be most effectively done using irreducible tensor operators.[260] In this way the matrix elements of (1) can be calculated simply by specifying the individual spins, S_i, the total spin, S, and the intermediate spins which are needed to specify how the individual spins are coupled. For instance one can couple S_1 to S_2 to give an intermediate spin S_{12}, then couple this to S_3 to give S_{123}, and continue the process up to $S_{12...14}$ to be coupled to S_{15} to give S. A given eigenfunction of (4) is completely identified by the set of numbers:

Table 5. Size of the Hamiltonian Matrices for $\{V_{15}\}$ Clusters

S	size	S	size
$^{15}/_2$	1	$^{7}/_2$	910
$^{13}/_2$	14	$^{5}/_2$	1638
$^{11}/_2$	90	$^{3}/_2$	2002
$^{9}/_2$	350	$^{1}/_2$	1430

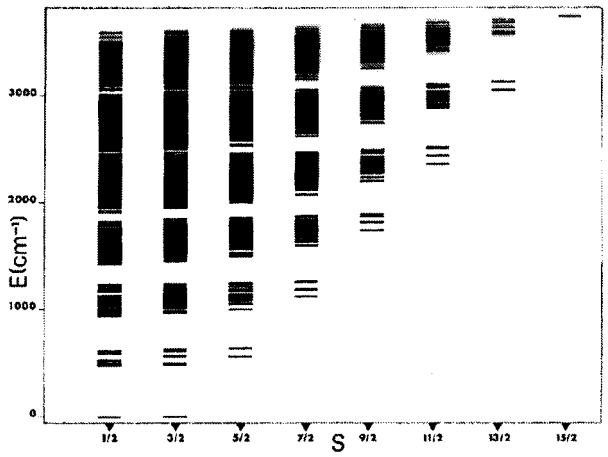

Figure 51. Calculated spin levels of $[V^{IV}{}_{15}As_6O_{42}(H_2O)]^{6-}$ $\{V_{15}\}$.

$|S_1S_2S_{12}S_3S_{123}...S_{123...14}S_{15}SM\rangle$, where $-S \le M \le S$. The intermediate spins and the total spin follow the usual vector coupling rules $|S_1 - S_2| \le S_{12} \le S_1 + S_2$. In the present case the use of symmetry reduces the size of the matrix from the original 32,768×32,768 to 8 matrixes (corresponding to $S = {}^1/_2$ up to $^{15}/_2$), with sizes ranging from 1 × 1 for $S = {}^{15}/_2$ to 2,002 × 2,002 for $S = {}^3/_2$, as shown in Table 5.

By using this approach it was possible to fit the experimental susceptibility of $\{V_{15}\}$ as shown in Figure 50. The best fit parameters require $J = 525$ cm^{-1} for the vanadium pairs bridged by two oxo groups. This is the interaction which quenches the magnetic moments of the two external layers of six oxovanadium(IV) ions. The calculated energy levels are shown in Figure 51. It is interesting to notice how the levels tend to merge into a continuum, as this must be expected on increasing the number of interacting centers. However the lowest lying states are well separated one from the other, showing that despite the complexity of the structure $\{V_{15}\}$ is still a paramagnet, whose properties are dominated by quantum effects. It is apparent that $\{V_{15}\}$ is not yet large enough to determine the transition from the quantum to the classic regime of the magnetic properties. It is interesting to notice that smaller clusters, comprising 12,[231] eight[261] or even four[262] spins already show incipient bulk magnetic behavior at low temperature. However these systems are formed by individual spins which are much larger than $^1/_2$ (namely $^3/_2$, 2, and $^5/_2$). It is apparent that assembling $S = {}^1/_2$ spins, which are the ones which have the largest quantum character it is necessary to assemble much larger numbers before superparamagnetic behavior starts to set in. This is clearly a challenge on the synthetic side, to learn how to make clusters with a very large number of spins.

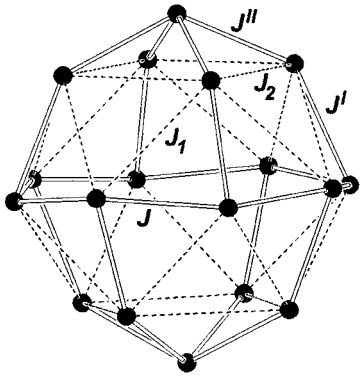

Figure 52. A limit polyhedron describing the structure of the $\{V_{18}O_{42}\}$ species and scheme of the possible important exchange pathways.

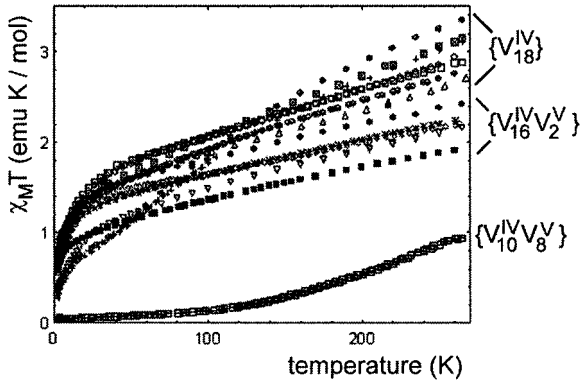

Figure 53. Temperature-dependence of χT for various $\{V_{18}O_{42}\}$ clusters.

A step forward from $\{V_{15}\}$ is represented by $\{V_{18}\}$.[258] This is a shorthand notation to indicate a series of clusters of general formula $[V^{IV}{}_{18}O_{42}]^{12-}$. The 24 μ_3-bridging oxygen atoms form either the edges of a distorted rhombicuboctahedron, the 14th Archimedean body,[263] or a polyhedron which can be generated by a 45° rotation of one-half of the rhombicuboctahedron around one of its S_4 axes, as shown in Figure 52.

The effective magnetic moment at high temperature is much lower than expected for uncoupled spins (1.2 vs 1.7 μ_B per V^{IV} ion), indicating an overall antiferromagnetic coupling. This is confirmed by the temperature dependence of χT, which decreases on lowering temperature, showing a marked decrease of slope around 40 K and the tendency to go through a plateau, as shown in Figure 53. Below 15 K a much faster decrease of χT is observed, approaching 0.4 emu mol^{-1} K at 2.8 K. A quantitative analysis is even more difficult in this case than in case of the $\{V_{15}\}$ system, because the overall states to be considered are 262 144. By using the same approach outlined above for the $\{V_{15}\}$ cluster a fit of the susceptibility was attempted. First of all a choice of the exchange coupling constants to be considered had to be made on the basis of the nature of the bridges, the bridge angles and the metal−metal distances. The five coupling constants which are schematically shown in Figure 52 are the minimum set which appeared to be necessary. Then, on the basis of the comparison with the data of other simpler systems, and the values of Table 3 and Table 4, it was assumed

J_1, $J_2 \ll J$, J^{I}, J^{II}. These parameters were allowed to vary in a rather limited range, to keep the computational demand at a reasonable level. A reasonable fit was obtained which of course is not unique, because a rigorous fitting procedure would require prohibitively long computer times, but it seems to be rather satisfactory that indeed the magnetic properties of relatively large clusters can at least be semiquantitatively interpreted, using parameters which compare well with those obtained from the analysis of simpler clusters.

The interesting feature of this cluster is that it can be partially oxidized, and clusters comprising variable numbers of V^{IV} and V^{V} centers can be synthesized. In this particular case the valences seem to be delocalized on the basis of the structural data. This leads to the necessity of tackling the properties of mixed-valent polyoxometalates, to be discussed below.

B. Mixed-Valence Clusters

The magnetic properties of mixed-valence clusters are more complex than those of localized valence species. In fact quite often the mixed-valence nature makes electron transfer from one center to the other comparatively easier and the resulting ground state of the pair depends on the interplay of electron transfer and Coulomb repulsion. The problems associated with mixed-valence systems have been thoroughly treated for dimers, trimers, and tetramers, but until recently there was no treatment available for larger clusters.

The first polyoxometalates in which the mixed-valence problem was tackled were the partially reduced Keggin and Wells−Dawson structures, in which variable numbers of electrons can be injected. The electrons are delocalized over a large number of atoms of the heteropoly framework. Furthermore, these structures can accommodate transition metal ions at specific sites which contain localized magnetic ions. Baker and co-workers elucidated the electron distribution in these materials[264−268] as well as the influence of electron delocalization on the magnetic properties of species containing paramagnetic metal ions. The main experimental result of these investigations has been the finding that a strong tendency to pairing the spins in a nonmagnetic ground state is operative in these materials. Recently Tsukerblat et al. worked out[269−271] a qualitative treatment of partially reduced Keggin and Wells−Dawson clusters using symmetry and introducing one- and two-electron-transfer processes, together with the Coulomb repulsion parameter U for putting two electrons on the same site. They found that spin pairing in the two-electron reduced heteropoly blues results from the simultaneous effects of single- and double-electron transfer processes. These processes are operative even when the two blue electrons are widely separated in the structure in order to minimize the Coulomb electron repulsion. Under these conditions the pairing through strong antiferromagnetic superexchange interactions can be ruled out.

A confirmation of this interpretation comes from the qualitative analysis[258] of the magnetic properties of the partially oxidized $\{V_{18}\}$ clusters, with different V^{V}/V^{IV} ratios. In fact clusters with 16 and 10 V^{IV} ions, respectively, were isolated, the complement to 18 being provided by V^{V} ions. A comparison of the effective magnetic moments at high temperature immediately shows that something which cannot be expected on the basis of superexchange only is going on. In fact the effective magnetic moment at room temperature per V^{IV} center is 0.8 μ_B for the $\{V^{IV}{}_{10}V^{V}{}_{8}\}$ cluster, and around 1.0 μ_B for the $\{V^{IV}{}_{16}V^{V}{}_{2}\}$ clusters. This can be compared with the value of 1.2 μ_B reported above for the fully reduced $\{V_{18}\}$ cluster. These data indicate that the antiferromagnetic coupling is larger in the clusters comprising smaller numbers of magnetic vanadium(IV) centers, while one would expect that on increasing the number of diamagnetic vanadium(V) ions the effective interactions should be weaker. This is confirmed by the temperature dependence of the magnetic susceptibility of the clusters, which shows that the $\{V_{10}{}^{IV}V_{8}{}^{V}\}$ system becomes diamagnetic at relatively high temperatures, while the other two types of clusters require lower temperatures. Since the geometries of the bridges are not substantially changed on introducing vanadium(V) centers it must be concluded that the stronger pairing of the spins in the delocalized species is the signature of the electron-transfer effects.

C. Polyoxometalates as Ligands to Magnetic Clusters

The last aspect of the magnetic properties of polyoxometalates we want to tackle is that of their use as ligands to magnetic clusters. A class of compounds of this type is based on the cluster $[PW_9O_{34}]^{9-}$. This diamagnetic anion is the lacunary fragment that results from the removal of a triad of W sites from the Keggin anion $[PW_{12}O_{40}]^{3-}$. The cluster acts as ligand toward divalent metal ions forming a reconstituted Keggin structure containing[272] the triangular $\{M_3O_{13}\}$ cluster fragment in $[PNi_3(H_2O)_3W_{10}O_{39}(H_2O)]^{7-}$. A second possibility is that two $\{PW_9O_{34}\}$ units encapsulate a rhomb-like tetranuclear $\{M_4O_{16}\}$ cluster like in $[(PW_9O_{34})_2M_4(H_2O)_2]^{x-}$ (M = Ni, Co, Cu, Mn).[194,195,273−277] When three $\{PW_9O_{34}\}$ units are involved in the reaction a nonanuclear cluster is encapsulated[171] which can be considered as formed by three triangular entities $\{M_3O_{12}\}$. The resulting cluster has the formula $[Co_9(OH)_3(H_2O)_6(HPO_4)_2(PW_9O_{34})_3]^{16-}$.

The magnetically active clusters in the three above-mentioned types of polyoxometalates are formed by $\{MO_6\}$ octahedra sharing edges in such a way that the M−O−M angles are close to 90°, thus favoring ferromagnetic coupling and eventually stabilizing large ground spin states. In fact the $\{Ni_3\}$ and $\{Ni_4\}$ clusters were shown to have $S = 3$ and $S = 4$ ground states, respectively, which are so far the largest spin states reported for polyoxometalates. An important feature of the approach is that it allows the formation of larger clusters using preformed building blocks.

A variant of this theme is provided by the clusters[278] $[\{V^{IV}(H_2O)O\}_6\{Mo^{V}(\mu\text{-}H_2O)_2(\mu\text{-}OH)Mo^{V}\}_3\{Mo^{VI}{}_{15}(MoNO)_2O_{58}(H_2O)_2\}_3]^{21-}$ ($\{(V^{IV}O)_6\}$), $[\{V^{IV}(H_2O)O\}_6$

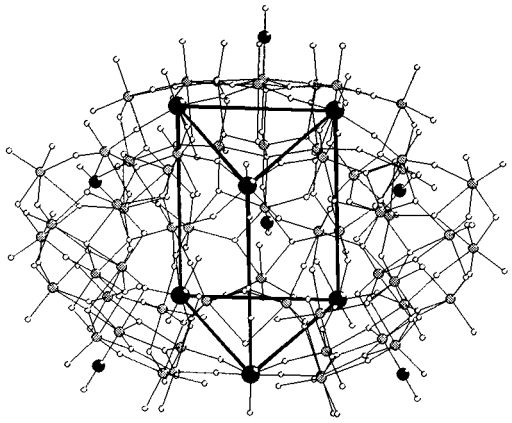

Figure 54. Structure of the $\{M_6\}$ clusters ($M = V^{IV}O$, Fe^{III}) (see text).

$\{Mo^{V}(\mu\text{-}H_2O)_2(\mu\text{-}O)Mo^{V}\}_3\{Mo^{VI}{}_{15}(MoNO)_2O_{58}(H_2O)_2\}_3]^{24-}$ ($\{(V^{IV}O)_6{*}\}$), and $[\{Fe^{III}(H_2O)_2\}_6\{Mo^{V}(\mu\text{-}H_2O)_2(\mu\text{-}OH)Mo^{V}\}_3\{Mo^{VI}{}_{15}(MoNO)_2O_{58}(H_2O)_2\}_3]^{15-}$ ($\{Fe^{III}{}_6\}$), in which three $\{Mo_{17}\}$ moieties bind three $\{MMo^{V}{}_2\}$ moieties, $M = V^{IV}O$, Fe^{III}.[7,11] In these giant clusters of 60 metal ions, the magnetic ions are the six M and the three $\{Mo^{V}{}_2\}$ groups ions, the others being nonmagnetic. From the magnetic ion point of view the role of the $\{Mo_{17}\}$ moieties is a structural one, i.e., it provides the structural frame for the magnetically active ones. The temptation to regard this giant cluster like a protein is therefore great. However the $\{Mo_{17}\}$ moiety has not only a structural role, but it actually participates in the transmission of the exchange interaction as shown below.

The molybdenum(V) centers presumably are not active because they are linked in pairs to each other giving rise to relatively short metal−metal distances. The comparison with simple compounds which have the same moieties suggests that all these pairs are nonmagnetic.[42] The magnetically active $\{M_6\}$ cluster fragments define a trigonal prism with metal−metal distances of 6.56, 6.54, and 6.40 Å in the triangular faces, and 9.60, 9.59, and 8.97 Å in the rectangular faces, respectively (see Figure 54). The metal centers are connected by $O-Mo^{VI}-O$ bridges in the triangular faces and by $O-Mo^{VI}-O-Mo^{V}-O$ bridges in the rectangular faces. The experimental measurement of the magnetic properties poses some problems: in fact one wants to obtain information on the magnetic properties of six centers embedded in molecules of relative molecular weight larger than 9 kDa, which leave a large uncertainty regarding the diamagnetic corrections. To reduce the experimental uncertainty the diamagnetic susceptibility of a cluster of formula $[Mo_{36}(NO)_4O_{108}(H_2O)_{16}]^{12-}$ was measured. Again the similarity with proteins is striking.

Given the long distances involved between the magnetic metal ions it is not surprising that both the intratriangle, J, and the intertriangle, J', interactions are weak in the iron cluster. The susceptibility was fitted with $J = 1.2$ cm^{-1} and $J' = 0.05$ cm^{-1}. On the contrary the magnetic properties of the oxovanadium(IV) clusters provide clear evidence of very strong intra- and inter-triangle interactions. In fact $J = 195$ cm^{-1}, $J' = 2.6$ cm^{-1} for $\{(V^{IV}O)_6\}$ and $J = 158$ cm^{-1}, $J' = 3.3$ cm^{-1} for $\{(V^{IV}O)_6{*}\}$.

The comparison of the J values with those usually observed in oxovanadium(IV) clusters, and with the values given in Table 3 and Table 4 is striking. In fact J is 1 order of magnitude larger than expected. The rationale for this unusual behavior was found in the peculiarity of the molybdate bridge, −O−Mo−O−, which, according to EHMO calculations, has frontier orbitals with energies which match quite well with those of the oxovanadium(IV) groups, thus giving rise to excellent conditions for efficient superexchange interactions.

The low-temperature magnetic data of $\{(V^{IV}O)_6\}$, and of $\{(V^{IV}O)_6{*}\}$ are not accurately reproduced by using only the isotropic exchange interactions. A definite improvement in the fit was obtained by introducing the antisymmetric exchange interaction. We remind here that the $\{M_6\}$ cluster fragments comprise two weakly coupled triangular arrays, and that a triangular array of antiferromagnetically coupled $S = {}^1/_2$ spins has a pair of degenerate $S = {}^1/_2$ states as the ground states.[279] This degeneracy in the ground state is often referred to as spin frustration.[280,281] These two states can be described as a ^2E in trigonal symmetry, to stress that they are related by some sort of orbital degeneracy. As in all cases of orbital degeneracy the system is intrinsically unstable to perturbations which remove the degeneracy. This symmetry breaking can occur either via spin−orbit coupling or via vibronic coupling. This is well-known for instance in single ions: the ^2E_g degeneracy of copper(II) is removed by vibronic coupling (Jahn−Teller effect), and that of $^4T_{1g}$ of high spin cobalt(II) by spin−orbit coupling. Something similar may occur in exchange coupled systems, like the ones we are considering. In this case spin−orbit coupling gives rise to the so-called antisymmetric exchange, which can be represented by the spin Hamiltonian:

$$H = \sum_{i<j} \mathbf{G_{ij}} \cdot [\mathbf{S_i} \times \mathbf{S_j}] \qquad (5)$$

where $\mathbf{G_{ij}}$ is a vector, which in a trigonal system is parallel to the unique axis, and whose modulus is usually approximated[282] as

$$G_{ij} \approx (\Delta g/g)\, J \qquad (6)$$

where $\Delta g = g - g_e$, g and g_e being the metal and the free electron gyromagnetic ratios, respectively. Inclusion of (5) in the Hamiltonian matrix removes the degeneracy of ^2E yielding two spin doublets separated by $3\sqrt{3}\, G_{ij}$. Therefore the inclusion of antisymmetric exchange dramatically changes the magnetic properties of the clusters at low temperature. In particular it introduces a temperature-dependent anisotropy, by varying the perpendicular component of the susceptibility and leaving the parallel one unchanged.

$\{(V^{IV}O)_6\}$ is a unique example of system where this effect could be unambiguously observed. In fact the magnetic anisotropy was measured and the best fit was found for $G_{ij} = 5$ cm^{-1}, which compares well with the value calculated with eq 6.

VIII. Outlook

Feynman's statement sums up entirely in one short sentence the future expectations in this area of chemistry: through a study and knowledge of elementary building blocks we can optimize our chemical procedures, and will succeed in the (targeted) production of more and more appropriate materials. Polyoxometalates, for which this statement represents a textbook example, form a class of inorganic compounds that is unmatched in terms of molecular and electronic structural versatility, reactivity, and relevance to analytical chemistry, catalysis, biology, medicine, geochemistry, materials science, and topology.[2,4] In this respect "chemistry" demands more and more an interest in multi-, inter-, and transdisciplinary research of complex systems, and complexity in general, with special emphasis on supramolecular chemistry. That some species may be used to model n-type semiconducting oxides and others display a reactivity with respect to oxygen transfer or play a key role as important transition metal−oxide-based catalysts are additional factors that will continue to stimulate research. This is mainly due to the fact that nanosized species (metal-based clusters even with much more than 200 metal atoms) can now be synthesized. Most important for the future will be to understand the intrinsic properties of the basic building block, mainly in reduced form, that lead to reaction in one particular way instead of another, to form for example high nuclearity species. The well-known high formation tendency of "spherical" polyoxometalates to optimize close-packing of oxygen atoms and minimize metal−metal repulsion is only one particular aspect.

In the future, we can anticipate the synthesis of ever larger clusters from known building blocks with known properties, perhaps even the targeted generation of nanosized molecular materials. An interesting subject will be the related magnetic properties which may "reach slowly" those of bulk magnets: how large must a cluster be, built up by paramagnetic centers, so that the coexistence of quantum and classical effects is observable?—A question of immense general and theoretical interest! The related research presents a challenge for *Chemistry—and Beyond*.[283]

IX. Acknowledgments

A.M. and F.P. thank B. Hauptfleisch for his assistance and the Deutsche Forschungsgemeinschaft as well as the Fonds der Chemischen Industrie for their financial support. M.P. thanks the National Science Foundation and the Department of Energy for research support. D.G. thanks MURST and CNR for funding.

X. Note Added in Proof

A very unusual supramolecular or host−guest compound could be obtained, which contains the $[Mo_{36}O_{112}(H_2O)_{16}]^{8-}$ cluster in the cavities of the chain built up by the $\{Mo_{154}\}$-type clusters but with defects in the form of missing $\{Mo_2\}^{2+}$ groups corresponding to the formula $[H_xMo_{148}O_{447}(H_2O)_{60}]^{n-}$ (see section V.E.4). The guests are fixed inside the host cavities (occupation 20%) by 16 hydrogen bonds (O···O: 2.8−2.9 Å). Four Na^+ cations located in between host and guest stabilize the system. The charge of the mixed-valence species is in general difficult to determine, e.g., because of disordered cations and the problem of determining the number of protons. Whereas the hexadecameric cluster with 176 Mo atoms (see section V.E.4) and stoichiometry $\{H_2(MoO_3)_{11}(H_2O)_5\}_{16}$ (protonated polymeric molybdenum trioxide with H_2O ligands) should be practically neutral and the tetradecameric cluster $\{H_2(MoO_3)_{11}(H_2O)_5\}_{14}$, too, the corresponding tetradecameric cluster **20** should, in contrast to the earlier reported value, preferably have a somewhat smaller charge (−14) due to the replacement of 14 $\{MoO\}^{4+}$ by 14 $\{MoNO\}^{3+}$ groups.

All compounds with nanosized ring-shaped anions, e.g., those in **20**, have the ability to take up varying, small amounts of alkali cations and small anions such as Cl^- from the reaction mixture, which again complicates the determination of the cluster anion charge.

XI. References

(1) Cited from: Siegel, R. W. *Physics Today* **1993**, *46*, 64.
(2) Pope, M. T.; Müller, A. *Angew. Chem., Int. Ed. Engl.* **1991**, *30*, 34.
(3) Pope, M. T. *Heteropoly and Isopoly Oxometalates*; Springer: Berlin, 1983.
(4) Pope, M. T., Müller, A., Eds. *Polyoxometalates: from Platonic Solids to Anti-retroviral Activity*; Kluwer: Dordrecht, 1994.
(5) Müller, A.; Reuter, H.; Dillinger, S. *Angew. Chem., Int. Ed. Engl.* **1995**, *34*, 2311.
(6) Klemperer, W. G.; Marquart, T. A.; Yaghi, O. M. *Angew. Chem., Int. Ed. Engl.* **1992**, *31*, 49.
(7) Müller, A.; Plass, W.; Krickemeyer, E.; Dillinger, S.; Bögge, H.; Armatage, A.; Proust, A.; Beugholt, C.; Bergmann, U. *Angew. Chem., Int. Ed. Engl.* **1994**, *33*, 849.
(8) Wassermann, K.; Dickman, M. H.; Pope, M. T. *Angew. Chem., Int. Ed. Engl.* **1997**, *36*, 1445.
(9) Müller, A.; Krickemeyer, E.; Meyer, J.; Bögge, H.; Peters, F.; Plass, W.; Diemann, E.; Dillinger, S.; Nonnenbruch, F.; Randerath, M.; Menke, C. *Angew. Chem., Int. Ed. Engl.* **1995**, *34*, 2122.
(10) Müller, A.; Koop, M.; Schiffels, P.; Bögge, H. *J. Chem. Soc., Chem. Commun.* **1997**, 1715.
(11) Müller, A.; Krickemeyer, E.; Dillinger, S.; Bögge, H.; Plass, W.; Proust, A.; Dloczik, L.; Menke, C.; Meyer, J.; Rohlfing, R. *Z. Anorg. Allg. Chem.* **1994**, *620*, 599.
(12) Jakób, W. F.; Jezowska, B. *Rocz. Chem.* **1931**, *11*, 229.
(13) Müller, A.; Eltzner, W.; Mohan, N. *Angew. Chem., Int. Ed. Engl.* **1979**, *18*, 168. Müller, A.; Eltzner, W.; Bögge, H.; Sarkar, S. *Angew. Chem., Int. Ed. Engl.* **1982**, *21*, 535.
(14) Müller, A.; Eltzner, W.; Sarkar, S.; Bögge, H.; Aymonino, P. J.; Mohan, N.; Seyer, U.; Subramanian, P. *Z. Anorg. Allg. Chem.* **1983**, *503*, 22. Sarkar, S.; Müller, A. *Angew. Chem., Int. Ed. Engl.* **1977**, *16*, 183. See also: Sarkar, S.; Müller, A. *Angew. Chem., Int. Ed. Engl.* **1977**, *16*, 468.
(15) (a) Wieghardt, K.; Backes-Dahmann, G.; Swiridoff, W.; Weiss, J. *Inorg. Chem.* **1983**, *22*, 1221. (b) Eltzner, W. Thesis, Bielefeld, 1984, p 105.
(16) Gouzerh, P.; Jeannin, Y.; Proust, A.; Robert, F. *Angew. Chem., Int. Ed. Engl.* **1989**, *28*, 1363. Zhang, S.; Liao, D.; Shao, M.; Tang, Y. *J. Chem. Soc. Chem. Commun.* **1986**, 835.
(17) Müller, A.; Krickemeyer, E.; Bögge, H.; Schmidtmann, M.; Peters, F.; Lu, C.; Beugholt, C. *Chem. Eur. J.*, submitted.
(18) Müller, A.; Krickemeyer, E.; Lu, C.; Bögge, H.; Schmidtmann, M.; Beugholt, C. *Angew. Chem.*, in press.
(19) Müller, A.; Penk, M.; Krickemeyer, E.; Bögge, H.; Walberg, H.-J. *Angew. Chem., Int. Ed. Engl.* **1988**, *27*, 1719.
(20) Müller, A.; Meyer, J.; Bögge, H.; Stammler, A. *Chem. Eur. J.*, in press.
(21) Müller, A.; Döring, J.; Bögge, H.; Krickemeyer, E. *Chimia* **1988**, *42*, 300. Müller, A.; Sessoli, R.; Krickemeyer, E.; Bögge, H.; Meyer, J.; Gatteschi, D.; Pardi, L.; Westphal, J.; Hovemeier, K.; Rohlfing, R.; Döring, J.; Hellweg, F.; Beugholt, C.; Schmidtmann, M. *Inorg. Chem.* **1997**, *36*, 5239.

(22) (a) Chen, Q.; Goshorn, D. P.; Scholes, C. P.; Tan, X.; Zubieta, J. *J. Am. Chem. Soc.* **1992**, *114*, 4667. (b) Khan, M. I.; Zubieta, J. *Progr. Inorg. Chem.* **1995**, *43*, 1.
(23) Suber, L.; Bonamico, M.; Fares, V. *Inorg. Chem.* **1997**, *36*, 2030.
(24) Johnson, G. K. Ph.D. Thesis, University of Missouri—Columbia, 1977; *Diss. Abstr.* **1978**, *38B*, 4801.
(25) See ref 3; p 39.
(26) Ichida, H.; Nagai, K.; Sasaki, Y.; Pope, M. T. *J. Am. Chem. Soc.* **1989**, *111*, 586.
(27) Müller, A. *J. Mol. Struct.* **1994**, *325*, 13.
(28) Müller, A.; Diemann, E.; Krickemeyer, E.; Che, S. *Naturwissenschaften* **1993**, *80*, 77.
(29) Müller, A.; Krickemeyer, E.; Penk, M.; Rohlfing, R.; Armatage, A.; Bögge, H. *Angew. Chem., Int. Ed. Engl.* **1991**, *30*, 1674.
(30) Müller, A.; Rohlfing, R.; Krickemeyer, E.; Bögge, H. *Angew. Chem., Int. Ed. Engl.* **1993**, *32*, 909.
(31) Müller, A. *Nature* **1991**, *352*, 115.
(32) Rohmer, M.-M.; Devémy, J.; Wiest, R.; Bénard, M. *J. Am. Chem. Soc.* **1996**, *118*, 13007.
(33) Blaudeau, J. P.; Rohmer, M. M.; Bénard, M. *Compt. Rend. Acad. Sci. Ser. C*, in press.
(34) Müller, A.; Rohlfing, R.; Döring, J.; Penk, M. *Angew. Chem., Int. Ed. Engl.* **1991**, *30*, 588.
(35) Müller, A.; Penk, M.; Döring, J. *Inorg. Chem.* **1991**, *30*, 4935.
(36) (a) Ozeki, T.; Yamase, T.; Naruke, H.; Sasaki, Y. *Inorg. Chem.* **1994**, *33*, 409. (b) Naruke, H.; Yamase, T. *Acta Crystallogr.* **1996**, *C52*, 2655. (c) Naruke, H.; Yamase, T. *J. Alloys Compd.* **1997**, *255*, 183.
(37) Naruke, H.; Ozeki, T.; Yamase, T. *Acta Crystallogr.* **1991**, *C47*, 489.
(38) Fedoseev, A. M.; Grigor′ev, M. S.; Yanovskii, A. I.; Struchkov, Yu. T.; Spitsyn, V. I. *Dokl. Akad. Nauk SSSR (Engl. Transl.)* **1987**, *297*, 111.
(39) Pope, M. T. In *From Simplicity to Complexity in Chemistry − and Beyond. Part I.*; Müller, A., Dress, A., Vögtle F., Eds.; Vieweg: Braunschweig, 1996; p 137.
(40) Zhang, Y.; Haushalter, R. C.; Clearfield, A. *J. Chem. Soc., Chem. Commun.* **1995**, 1149.
(41) Müller, A.; Krickemeyer, E.; Dillinger, S.; Meyer, J.; Bögge, H.; Stammler, A. *Angew. Chem., Int. Ed. Engl.* **1996**, *35*, 171.
(42) Müller, A.; Krickemeyer, E.; Penk, M.; Wittneben, V.; Döring, J. *Angew. Chem., Int. Ed. Engl.* **1990**, *29*, 88.
(43) Khan, M. I.; Müller, A.; Dillinger, S.; Bögge, H.; Chen, Q.; Zubieta, J. *Angew. Chem., Int. Ed. Engl.* **1993**, *32*, 1780.
(44) Müller, A.; Meyer, J.; Krickemeyer, E.; Beugholt, C.; Bögge, H.; Peters, F.; Schmidtmann, M.; Kögerler, P.; Koop, M. J. *Chem. Eur. J.*, in press.
(45) (a) Khan, M. I.; Zubieta, J. *J. Am. Chem. Soc.* **1992**, *114*, 10058. (b) Khan, M. I.; Chen, Q.; Salta, J.; O′Connor, C. J.; Zubieta, J. *Inorg. Chem.* **1996**, *35*, 1880.
(46) Chae, H. K.; Klemperer, W. G.; Marquart, T. A. *Coord. Chem. Rev.* **1993**, *128*, 209.
(47) Müller, A.; Dillinger, S.; Krickmeyer, E.; Bögge, H.; Plass, W.; Stammler, A.; Haushatter, R. C. *Z. Naturforsch.* **1997**, *52b*, 1301.
(48) Krebs, B.; Paulat-Böschen, I. *Acta Crystallogr.* **1982**, *B38*, 1710.
(49) Krebs, B.; Stiller, S.; Tytko, K. H.; Mehmke, J. *Eur. J. Solid State Inorg. Chem.* **1991**, *28*, 883.
(50) Tytko, K. H.; Glemser, O. *Adv. Inorg. Chem. Radiochem.* **1976**, *19*, 239.
(51) Paulat-Böschen, I. *J. Chem. Soc., Chem. Commun.* **1979**, 780.
(52) Tytko, K. H.; Schönfeld, B. *Z. Naturforsch.* **1975**, *B30*, 471.
(53) Tytko, K. H.; Schönfeld, B.; Buss, B.; Glemser, O. *Angew. Chem., Int. Ed. Engl.* **1973**, *12*, 330.
(54) Pope, M. T. *Progr. Inorg. Chem.* **1991**, *39*, 181.
(55) (a) Kihlborg, L. *Acta Chem. Scand.* **1960**, *14*, 1612. (b) Kihlborg, L. *Ark. Kemi* **1963**, *21*, 427.
(56) Zhang, S.; Huang, G.; Shao, M.; Tang, Y. *J. Chem. Soc., Chem. Commun.* **1993**, 37. Huang, G.; Zhang, S.; Shao, M. *Polyhedron* **1993**, *12*, 2067.
(57) (a) Müller, A.; Plass, W. *J. Mol. Struct.* **1994**, *321*, 215. (b) Müller, A.; Beugholt, C. *Nature* **1996**, *383*, 296.
(58) Müller, A.; Plass, W.; Krickemeyer, E.; Dillinger, S.; Bögge, H.; Armatage, A.; Beugholt, C.; Bergmann, U. *Monatsh.* **1994**, *125*, 525.
(59) Müller, A.; Bögge, H.; Krickemeyer, E.; Dillinger, S. *Bull. Pol. Acad. Sci. Chem.* **1994**, *42*, 291.
(60) Müller, A.; et al. To be published.
(61) Müller, A.; Meyer, J.; Krickemeyer, E.; Diemann, E. *Angew. Chem., Int. Ed. Engl.* **1996**, *35*, 1206.
(62) Müller, A.; Krickemeyer, E.; Bögge, H.; Schmidtmann, M.; Peters, F.; Menke, C.; Meyer, J. *Angew. Chem., Int. Ed. Engl.* **1997**, *36*, 484.
(63) Müller, A.; Eimer, W.; Diemann, E.; Serain, C. To be published.
(64) Baker, L. C. W.; Figgis, J. S. *J. Am. Chem. Soc.* **1970**, *92*, 3794.
(65) Knoth, W. H.; Harlow, R. L. *J. Am. Chem. Soc.* **1981**, *103*, 1865.
(66) Contant, R.; Thouvenot, R. *Inorg. Chim. Acta* **1993**, *212*, 41.
(67) Tézé, A.; Michelon, M.; Hérve, G. *Inorg. Chem.* **1997**, *36*, 5666.
(68) Peacock, R. D.; Weakley, T. J. R. *J. Chem. Soc., A* **1971**, 1836.
(69) Haraguchi, N.; Okaue, Y.; Isobe, T.; Matsuda, Y. *Inorg. Chem.* **1994**, *33*, 1015.
(70) Zubairi, S. A.; Ifzal, S. M.; Malik, A. *Inorg. Chim. Acta* **1977**, *22*, L29.
(71) Fedotov, M. A.; Maksimov, G. M.; Matveev, K. I. *Sov. J. Coord. Chem., Engl. Transl.* **1990**, *16*, 117.
(72) Fedotov, M. A., Pertsikov, B. Z., Danovich, D. K. *Polyhedron* **1990**, *9*, 1249.
(73) Yusov, A. B.; Fedoseev, A. M. *Radiokhimiya* **1992**, *34*, 70.
(74) Yusov, A. B.; Fedoseev, A. M. *Zh. Prikl. Spektrosk.* **1988**, *49*, 929; *Chem. Abstr.* **1989**, *111*, 67023p.
(75) Marcu, G.; Rusu, M.; Botar, A. *Rev. Roum. Chim.* **1989**, *34*, 207.
(76) Tourné, C.; Tourné, G. *Rev. Chim. Miner.* **1977**, *14*, 83.
(77) Saprykin, A. S.; Spitsyn, V. I.; Orlova, M. M.; Zhuravleva, O. P.; Krot, N. N. *Sov. Radiochem.* **1978**, *20*, 207.
(78) Marcu, G.; Rusu, M.; Botar, A. *Stud. Univ. Babes-Bolyai, Chem.* **1986**, *31*, 76; *Chem. Abstr.* **1988**, *108*, 30739p.
(79) Lee, C. W.; So, H. *Taehan Hwahakhoe Chi* **1982**, *26*, 160; *Chem. Abstr.* **1983**, *98*, 100101a.
(80) Termes, S. C.; Pope, M. T. *Transition Met. Chem.* **1978**, *3*, 103.
(81) Saprykin, A. S.; Shilov, V. P.; Spitsyn, V. I.; Krot, N. N. *Dokl. Phys. Chem. (Engl. Transl.)* **1976**, *226*, 114.
(82) Liu, J.; Rong, C.; Wang, E. *Gaodeng Xuexiao Huaxue Xuebao* **1986**, *7*, 565; *Chem. Abstr.* **1987**, *106*, 112528s.
(83) Liu, J. F.; Wang, W. Q.; Meng, L.; Liu, Y. *Gaodeng Xuexiao Huaxue Xuebao* **1996**, *17*, 179; *Chem. Abstr.* **1996**, *124*, 305451s.
(84) Liu, J.; Wang, W.; Wang, G.; Zhao, B.; Sun, S. *Polyhedron* **1994**, *13*, 1057.
(85) Qu, L.; Niu, Z.; Liu, J.; Chen, Y.; Zhao, B.; Peng, J. *Gaodeng Xuexiao Huaxue Xuebao* **1991**, *12*, 1434; *Chem. Abstr.* **1993**, *118*, 159754a.
(86) Ballardini, R.; Chiorboli, E.; Balzani, V. *Inorg. Chim. Acta* **1984**, *95*, 323.
(87) Ly, B.; Shan, Y.; Wu, Y.; Ying, Y.; Lin, Y.; Bai, S. *Jiegou Huaxue* **1996**, *15*, 301; *Chem. Abstr.* **1996**, *125*, 211163t.
(88) Zhu, Z.; Liu, J.; Zhao, B. *Wuji Huaxue Xuebao* **1991**, *7*, 409; *Chem. Abstr.* **1993**, *118*, 203950n.
(89) Wu, Q.; Xu, S.; Song, Y. *Chin. Chem. Lett.* **1994**, *5*, 59; *Chem. Abstr.* **1994**, *121*, 72339g.
(90) Rong, C.; Liu, J.; Chen, X.; Wang, E. *Inorg. Chim. Acta* **1987**, *130*, 265.
(91) Liu, S.; Xu, L.; Wang, E. *Zhongguo Xitu Xuebao* **1994**, *12*, 366; *Chem. Abstr.* **1995**, *122*, 329089q.
(92) Wang, E.; Liu, L.; Shen, E.; Wang, Z. *Gaodeng Xuexiao Huaxue Xuebao* **1991**, *12*, 1576; *Chem. Abstr.* **1993**, *118*, 159753z.
(93) Rusu, M.; Botar, A.; Trocan, C. *Stud. Univ. Babes-Bolyai, Chem.* **1981**, *26*, 58; *Chem. Abstr.* **1982**, *97*, 137564j.
(94) Rusu, M.; Botar, A. V. *Stud. Univ. Babes-Bolyai*, [*Ser.*] *Chem.* **1986**, *31*, 84; *Chem. Abstr.* **1987**, *107*, 108052k.
(95) Liu, J.; Zu, Z.; Zhao, B.; Liu, Z. *Inorg. Chim. Acta* **1989**, *164*, 179.
(96) Wang, W.; Zhu, X.; You, W.; Liu, J. *Wuji Huaxue Xuebao* **1993**, *9*, 347; *Chem. Abstr.* **1994**, *121*, 72334b.
(97) Wu, Q.; Wang, E.; Liu, J. *Polyhedron* **1993**, *12*, 2563.
(98) Qu, L.; Wang, S.; Peng, J.; Chen, Y.; Wang, G. *Polyhedron* **1992**, *11*, 2645.
(99) Ciabrini, J. P.; Contant, R. *J. Chem. Res. (S)* **1993**, 391; *J. Chem. Res. (M)* **1993**, 2720.
(100) Ostuni, A.; Bachman, R. E.; Pope, M. T. Manuscript in preparation.
(101) Shilov, V. P. *Koord. Khim.* **1981**, *7*, 1654.
(102) Yusov, A. B.; Fedoseev, A. M. *Radiokhimiya* **1992**, *34*, 61.
(103) Malikov, D. A.; Milyukova, M. S.; Kuzovkina, E. V. *Sovrem. Metody Razdeleniya i Opredeleniya Radioaktiv. Elementov*, M. **1989**, 99; from: *Ref. Zh., Khim.* **1990**, Abstr. No. 1V233; *Chem. Abstr.* **1990**, *112*, 241827m.
(104) Fedoseev, A. M. *Radiokhimiya* **1985**, *27*, 381.
(105) Nikitenko, S. I.; Dzyubenko, V. I. *Radiokhimiya* **1989**, *31*, 36.
(106) Kosyakov, V. N.; Timofeev, G. A.; Erin, E. A.; Andreev, V. *Sov. Radiochem. (Engl. Transl)* **1977**, *19*, 418.
(107) Liu, J.; Wang, G.; Zhao, B. *Chem. Res. Chin. Univ.* **1993**, *9*, 175; *Chem. Abstr.* **1994**, *121*, 67927t.
(108) Xi, X.; Wang, G.; Liu, B.; Dong, S. *Electrochim. Acta* **1995**, *40*, 1025.
(109) Liu, J.; Chen, X.; Wang, E.; Yan, D.; Liu, Z. *Huaxue Xuebao* **1988**, *46*, 1168; *Chem. Abstr.* **1989**, *110*, 241757x.
(110) Wang, W.; Liu, J. *Zhongguo Xitu Xuebao* **1995**, *13*, 365; *Chem. Abstr.* **1996**, *124*, 271035s.
(111) Xiao, Z.; Chen, Q.; Chen, C. *Fujian Shifan Daxue Xuebao, Ziran Kexueban* **1986**, *2*, 77; *Chem. Abstr.* **1987**, *106*, 130622x.
(112) Chen, H.; Chen, Q.; Chen, C. *Fujian Shifan Daxue Xuebao, Ziran Kexueban* **1986**, *2*, 69; *Chem. Abstr.* **1987**, *106*, 226257h.
(113) Wang, E.; Shan, Y.; Liu, Z.; Liu, J.; Zhang, B. *Huaxue Xuebao* **1991**, *49*, 774; *Chem. Abstr.* **1992**, *116*, 119632m.
(114) Wang, E.; Ren, Q.; Wang, Z.; Lu, X.; Zhang, S.; Zan, R.; Liu, G. *Wuji Huaxue Xuebao* **1993**, *9*, 65; *Chem. Abstr.* **1994**, *121*, 72311s.
(115) Chen, Q.; Cai, X. *Fujian Shifan Daxue Xuebao, Ziran Kexueban* **1989**, *5*, 55; *Chem. Abstr.* **1990**, *113*, 203742t.

(116) Zhang, X. M.; Cheng, L.; Xi, X. D.; Liu, B. F.; Dong, S. J. *Chin. Chem. Lett.* **1996**, *7*, 81; *Chem. Abstr.* **1996**, *124*, 214410m.
(117) Liu, M.; Dong, S. *Electrochim. Acta* **1995**, *40*, 197.
(118) Zhou, B.; Shan, Y.; Liu, Z.; Zhang, X. *Gaodeng Xuexiao Huaxue Xuebao* **1991**, *12*, 1425; *Chem. Abstr.* **1993**, *118*, 93136s.
(119) Cheng, L.; Zhang, X.; Xi, X.; Liu, B.; Dong, S. *J. Electroanal. Chem.* **1996**, *407*, 97.
(120) Shan, Y.; Liu, Z.; Wang, E.; Jin, Z.; Wei, G.; Liu, Y. *Jiegou Huaxue* **1990**, *9*, 159; *Chem. Abstr.* **1991**, *114*, 239243r.
(121) Shan, Y.; Liu, Z.; Jin, Z.; Wei, G.; Liu, Y.; Wang, E. *Sci. China, Ser. B* **1991**, *34*, 513; *Chem. Abstr.* **1991**, *115*, 293496j.
(122) Wang, H.; Yu, Z.; Wang, E. *Wuli Huaxue Xuebao* **1995**, *11*, 242; *Chem. Abstr.* **1995**, *122*, 250435r.
(123) Shan, Y.; Liu, Z.; Jin, Z.; Wei, G. *Huaxue Xuebao* **1992**, *50*, 357; *Chem. Abstr.* **1992**, *117*, 61562r.
(124) Wang, E.; Yu, W.; Liu, J.; Hu, C. *Gaodeng Xuexiao Huaxue Xuebao* **1991**, *12*, 1279; *Chem. Abstr.* **1993**, *118*, 159752y.
(125) Wang, E.; Zhang, L.; Wang, Z.; Huang, R.; Zhang, B.; Zhan, R.; Liu, Y. *Huaxue Xuebao* **1993**, *51*, 352; *Chem. Abstr.* **1993**, *119*, 84559a.
(126) Wang, E.; Hu, C.; Zhou, Y.; Liu, J. *Gaodeng Xuexiao Huaxue Xuebao* **1990**, *11*, 340; *Chem. Abstr.* **1990**, *113*, 203791h.
(127) Tourné, C. M.; Tourné, G. F.; Brianso, M. C. *Acta Crystallogr.* **1980**, *B36*, 2012.
(128) Molchanov, V. N.; Kazanskii, L. P.; Torchenkova, E. A.; Simonov, V. I. *Sov. Phys. Crystallog. (Engl. Transl.)* **1979**, *24*, 96.
(129) Bartis, J.; Sukal, S.; Dankova, M.; Kraft, E.; Kronzon, R.; Blumenstein, M.; Francesconi, L. C. *J. Chem. Soc., Dalton Trans.* **1997**, 1937.
(130) Yusov, A. B.; Fedoseev, A. M.; Spitsyn, V. I.; Krot, N. N. *Dokl. Phys. Chem. (Engl. Transl.)* **1986**, *289*, 777.
(131) Saprykin, A. S.; Spitsyn, V. I.; Krot, N. N. *Dokl. Phys. Chem. (Engl. Transl.)* **1976**, *231*, 1038.
(132) Milyukova, M. S.; Litvina, M. N.; Myasoedov, B. F. *Sov. Radiochem. (Engl. Transl.)* **1985**, *27*, 683.
(133) Litvina, M. N.; Milyukova, M. S.; Myasoedov, B. F. *J. Radioanal. Nucl. Chem.* **1988**, *121*, 355.
(134) Kremlyakova, N. Y.; Novikov, A. P.; Myasoedov, B. F.; Katargin, N. V. *J. Radioanal. Nucl. Chem.* **1990**, *145*, 183.
(135) Erin, E. A.; Kopytov, V. V.; Vasil′ev, V. Y.; Rykov, A. G. *Radiokhimiya* **1981**, *23*, 727.
(136) Milyukova, M. S.; Litvina, M. N.; Myasoedov, B. F. *Sov. Radiochem. (Engl. Transl.)* **1983**, *25*, 665.
(137) Erin, E. A.; Kopytov, V. V.; Vasil′ev, V. Y. *Radiokhimiya* **1986**, *28*, 737.
(138) Milyukova, M. S.; Varezhkina, N. S.; Kuzovkina, E. V.; Malikov, D. A.; Myasoedov, B. F. *Sov. Radiochem. (Engl. Transl.)* **1988**, *30*, 312.
(139) Milyukova, M. S.; Kuzovkina, E. V.; Malikov, D. A.; Varezhkina, N. S. *Sovrem. Metody Razdeleniya i Opredeleniya Radioaktiv. Elementov, M.* **1989**, 95; from: *Ref. Zh. Khim.* **1989**, Abstr. No. 24V800; *Chem. Abstr.* **1990**, *112*, 241830g.
(140) Malikov, D. A.; Milyukova, M. S.; Kuzovkina, E. V.; Myasoedov, B. F. L. *Sov. Radiochem. (Engl. Transl.)* **1992**, *34*, 106.
(141) Erin, E. A.; Kopytov, V. V.; Vasil′ev, V. Y.; Rykov, A. G. R. *Radiokhimiya* **1983**, *25*, 51.
(142) Milyukova, M. S.; Malikov, D. A.; Kuzovkina, E. V.; Myasoedov, B. F. *J. Radioanal. Nucl. Chem.* **1986**, *104*, 81.
(143) Kulyako, Yu. M.; Trofimov, T. I.; Frenkel, V. Ya.; Lebedev, I. A.; Myasoedov, B. F. *J. Anal. Chem. USSR (Engl. Transl.)* **1981**, *36*, 1691.
(144) Kulyako, Y. M.; Lebedev, I. A.; Frenkel, V. Y.; Trofimov, T. I.; Myasoedov, B. F. *Sov. Radiochem. (Engl. Transl.)* **1981**, *23*, 671.
(145) Molochnikova, N. P.; Frenkel, V. Y.; Myasoedov, B. F.; Lebedev, I. A. *Sov. Radiochem. (Engl. Transl.)* **1982**, *24*, 250.
(146) Molochnikova, N. P.; Frenkel, V. Y.; Myasoedov, B. F. *J. Radioanal. Nucl. Chem.* **1988**, *121*, 409.
(147) Milyukova, M. S.; Varezhkina, N. S.; Myasoedov, B. F. *Sov. Radiochem. (Engl. Transl.)* **1990**, *32*, 361.
(148) Molochnikova, N. P.; Frenkel, B. Y.; Myasoedov, B. F. *Radiokhimiya* **1989**, *31*, 65.
(149) Adnet, J. M.; Brossard, P.; Bourges, *J. Proc. Int. Conf. Technol. Expo. Future Nucl. Syst.: Emerging Fuel Cycles Waste Disposal Options* **1993**, *2*, 1008; *Chem. Abs.* **1994**, *120*, 146793d.
(150) Fedoseev, A. M.; Tananaeuv, I. G. *Radiokhimiya* **1994**, *36*, 422.
(151) Francesconi, L. C. Private communication 1997.
(152) Adnet, J. M. Thesis, Institut National Polytechnique de Toulouse 1991.
(153) Müller, A.; Fedin, V.; Fenske, H.-D.; Baum, G.; Peters, F. To be published.
(154) Klein, D. *Ann. Chim. Phys.* **1883**, *28*, 350.
(155) Rosenheim, A. *Z. Anorg. Chem.* **1911**, *70*, 418.
(156) Souchay, P. *Ann. Chim.* **1945**, *20*, 96.
(157) Souchay, P. *Bull. Soc. Chim. Fr.* **1951**, *5*, 365.
(158) Tézé, A.; Michelon, M.; Hervé, G. *Inorg. Chem.* **1997**, *36*, 505.
(159) Kehrmann, F. *Z. Anorg. Chem.* **1892**, *1*, 423.
(160) Kehrmann, F.; Freinkel, M. *Ber. Dtsch. Chem. Ges.* **1892**, *25*, 1966.
(161) Souchay, P. *Ann. Chim.* **1947**, *2*, 203.
(162) Tourné, C. M.; Tourné, G. F.; Weakley, T. J. R. *J. Chem. Soc., Dalton Trans.* **1986**, 2237.
(163) Contant, R.; Fruchart, J. M.; Hervé, G.; Tézé, A. *C. R. Acad. Sci., Ser. C* **1974**, *278*, 199.
(164) Tourné, G. F.; Tourné, C. M. In *Polyoxometalates: from Platonic Solids to Anti-retroviral Activity*; Pope, M. T., Müller, A., Eds.; Kluwer: Dordrecht 1994; p 59.
(165) Contant, R.; Hervé, G.; Thouvenot, R. Polyoxometalate Workshop, St.-Lambert-de-Bois, 1983.
(166) Fuchs, J.; Palm, R. *Z. Naturforsch.* **1984**, *39B*, 757.
(167) Tourné, C.; Revel, A.; Tourné, G.; Vendrell, M. *C. R. Acad. Sci., Ser. C* **1973**, *277*, 643.
(168) Tourné, C.; Revel, A.; Tourné, G. *Rev. Chim. Miner.* **1977**, *14*, 537.
(169) Tourné, C. M.; Tourné, G. F. *J. Chem. Soc., Dalton Trans.* **1988**, 2411.
(170) Weakley, T. J. R. *J. Chem. Soc., Chem. Commun.* **1984**, 1406.
(171) Galán-Mascarós, J. R.; Gómez-García, C. J.; Borrás-Almenar, J. J.; Coronado, E. *Adv. Mater.* **1994**, *6*, 221.
(172) Coronado, E.; Gómez-García, C. J. *Comments Inorg. Chem.* **1995**, *17*, 255.
(173) Yamase, T.; Naruke, H.; Sasaki, Y. *J. Chem. Soc., Dalton Trans.* **1990**, 1687.
(174) Leyrie, M.; Martin-Frère, J.; Hervé, G. *C. R. Acad. Sci., Ser. C* **1974**, *279*, 895.
(175) Jeannin, Y.; Martin-Frère, J. *J. Am. Chem. Soc.* **1981**, *103*, 1664.
(176) Jeannin, Y. *J. Cluster Sci.* **1992**, *3*, 55.
(177) Weakley, T. J. R. *Inorg. Chim. Acta* **1984**, *87*, 13.
(178) Souchay, P.; Leray, M.; Hervé, G. *C. R. Acad. Sci., Ser. C* **1970**, *271*, 1337.
(179) Michelon, M.; Souchay, P.; Massart, R.; Hervé, G. *C. R. Acad. Sci., Ser. C* **1971**, *273*, 1117.
(180) Michelon, M.; Hervé, G. *C. R. Acad. Sci., Ser. C* **1972**, *274*, 209.
(181) Bösing M.; Loose, I.; Pohlmann, H.; Krebs, B. *Chem. Eur. J.* **1997**, *3*, 1232.
(182) Wei, X.; Wassermann, K.; Dickman, M. H.; Pope, M. T. *Compt. Rend. Acad. Sci. Ser. C*, in press.
(183) Kim, K.; Pope, M. T. Manuscript in preparation.
(184) Hervé, G.; Tézé, A. *Inorg. Synth.* **1990**, *27*, 118.
(185) Robert, F.; Leyrie, M.; Hervé, G.; Tézé, A.; Jeannin, Y. *Inorg. Chem.* **1980**, *19*, 1746.
(186) Thouvenot, R.; Michelon, M.; Tézé, A.; Hervé, G. In *Polyoxometalates: from Platonic Solids to Anti-retroviral Activity*; Pope, M. T., Müller, A., Eds.; Kluwer: Dordrecht, 1994; p 177.
(187) Liu, J.; Guo, J.; Zhao, B.; Xu, G.; Li, M. *Transition Met. Chem. (London)* **1993**, *18*, 205.
(188) Leyrie, M.; Hervé, G. *Nouv. J. Chim.* **1978**, *2*, 233.
(189) Marcu, G.; Mironov, V. *An. Univ. Bucuresti, Chim.* **1992**, 1, 21.
(190) Liu, J.; Guo, J.; Li, J.; Zhao, B.; Xu, G. Gaodeng *Xuexiao Huaxue Xuebao* **1992**, *13*, 1352.
(191) Liu, J.; Guo, J.; Zhao, B.; Xu, G.; Cui, X. *Wuji Huaxue Xuebao* **1993**, *9*, 155; *Chem. Abs.* **1994**, *120*, 337695h.
(192) Leyrie, M.; Thouvenot, R.; Tézé, A.; Hervé, G. *New J. Chem.* **1992**, *16*, 475.
(193) Finke, R. G.; Droege, M. W. *Inorg. Chem.* **1983**, *22*, 1006.
(194) Finke, R. G.; Droege, M. W.; Domaille, P. J. *Inorg. Chem.* **1987**, *26*, 3886.
(195) Weakley, T. J. R.; Evans, H. T.; Showell., J. S.; Tourné, G. F.; Tourné, C. M. *J. Chem. Soc., Chem. Commun.* **1973**, 139.
(196) Weakley, T. J. R.; Finke, R. G. *Inorg. Chem.* **1990**, *29*, 1235.
(197) Finke, R. G.; Weakley, T. J. R. *J. Chem. Crystallogr.* **1994**, *24*, 123.
(198) Gómez-García, C. J.; Borrás-Almenar, J. J.; Coronado, E.; Ouahab, L. *Inorg. Chem.* **1994**, *33*, 4016.
(199) Zhang, X.; Chen, Q.; Duncan, D. C.; Campana, C. F.; Hill, C. L. *Inorg. Chem.* **1997**, *36*, 4208.
(200) Crano, N. F.; Chambers, R. C.; Lynch, V. M.; Fox, M. A. *J. Mol. Catal. A: Chemical* **1996**, *114*, 65.
(201) Fischer, J.; Ricard, L.; Weiss, R. *J. Am. Chem. Soc.* **1976**, *98*, 3050.
(202) Michelon, M.; Hervé, G.; Leyrie, M. *J. Inorg. Nucl. Chem.* **1980**, *42*, 1583.
(203) Liu, J.; Liu, S.; Qu, L.; Pope, M. T.; Rong, C. *Transition Met. Chem. (London)* **1992**, *17*, 311.
(204) Liu, J.; Liu, S.; Qu, L.; Pope, M. T. *Transition Met. Chem. (London)* **1992**, *17*, 314.
(205) Rozenbaum, W.; Dormont, D.; Spire, B.; Vilmer, E. *Lancet* **1985**, *1*, 450.
(206) Jasmin, C.; Chermann, J. C.; Hervé, G.; Tézé, A.; Souchay, P.; Boy-Loustau, C.; Raybaud, N.; Sinoussi, F.; Raynaud, M. *J. Nat. Cancer Inst.* **1974**, *53*, 469.
(207) Schönfeld, B.; Glemser, O. *Z. Naturforsch.* **1975**, *30B*, 827.
(208) Hill, C. L.; Kim, G. S.; Prosser-McCartha, C. M.; Judd, D. In *Polyoxometalates: from Platonic Solids to Anti-retroviral Activity*; Pope, M. T., Müller, A., Eds.; Kluwer: Dordrecht, 1994; p 359.

(209) Blasecki, J. W. In *Polyoxometalates: from Platonic Solids to Anti-retroviral Activity*; Pope, M. T., Müller, A., Eds.; Kluwer: Dordrecht, 1994; p 373.
(210) Clayette, P.; Dormont, D. In *Polyoxometalates: from Platonic Solids to Anti-retroviral Activity*; Pope, M. T., Müller, A., Eds.; Kluwer: Dordrecht, 1994; p 387.
(211) Contant, R.; Ciabrini, J. P. *J. Chem. Res. (M)* **1977**, *222*, 2601.
(212) Contant, R.; Tézé, A. *Inorg. Chem.* **1985**, *24*, 4610.
(213) Preyssler, C. *Bull. Soc. Chim. Fr.* **1970**, 30.
(214) Alizadeh, M. H.; Harmalker, S. P.; Jeannin, Y.; Martin-Frère, J.; Pope, M. T. *J. Am. Chem. Soc.* **1985**, *107*, 2662.
(215) Creaser, I.; Heckel, M. C.; Neitz, R. J.; Pope, M. T. *Inorg. Chem.* **1993**, *32*, 1573.
(216) Antonio, M. R.; Soderholm, L. *Inorg. Chem.* **1994**, *33*, 5988.
(217) Antonio, M. R.; Malinsky, J.; Soderholm, L. *Mater. Res. Soc. Symp. Proc.* **1995**, *368*, 223.
(218) Soderholm, L.; Liu, G. K.; Muntean, J.; Malinsky, J.; Antonio, M. R. *J. Phys. Chem.* **1995**, *99*, 9611.
(219) Antonio, M. R.; Soderholm, L. *J. Cluster Sci.* **1996**, *7*, 585.
(220) Antonio, M. R.; Soderholm, L. *J. Alloys Compd.* **1997**, *250*, 541.
(221) Dickman, M. H.; Gama, G. J.; Kim, K. C.; Pope, M. T. *J. Cluster Sci.* **1996**, *7*, 567.
(222) Harrup, M. K.; Hill, C. L. *Inorg. Chem.* **1994**, *33*, 5448.
(223) Jeannin, Y.; Launay, J. P.; Seid Sedjadi, M. A. *Inorg. Chem.* **1980**, *19*, 2933.
(224) Piepgrass, K. W.; Pope, M. T. *J. Am. Chem. Soc.* **1987**, *109*, 1586.
(225) Yamase, T.; Ishikawa, E. *J. Chem. Soc., Dalton Trans.* **1996**, 1619.
(226) Dickman, M. H.; Ozeki, T.; Rong, C.; Evans, H. T.; Jameson, G. B.; Pope, M. T. *Book of Abstracts*; American Chemical Society National Meeting; Washington, DC, 1990; American Chemical Society: Washington, DC, 1990; INOR 184.
(227) Dickman, M. H.; Ozeki, T.; Evans, H. T.; Pope, M. T.; Rong, C.; Jameson, G. B. Manuscript in preparation.
(228) Shakhova, Z. F.; Morosanova, S. A.; Zakharova, V. F.; Kurenkova, O. N. *Russ. J. Inorg. Chem. (Engl. Transl.)* **1969**, *14*, 1609.
(229) Viossat, B.; Volfovsky, C.; Cadiot, M. *C. R. Acad. Sci., Ser. C* **1971**, *273*, 1637.
(230) Gatteschi, D.; Caneschi, A.; Pardi, L.; Sessoli, R. *Science* **1994**, *265*, 1054.
(231) Sessoli, R.; Gatteschi, D.; Caneschi, A.; Novak, M. A. *Nature* **1993**, *365*, 141.
(232) Carlin, R. L. *Magnetochemistry*; Springer: Berlin, 1986.
(233) Kahn, O. *Molecular Magnetism*; VCH: Weinheim, 1993.
(234) Gatteschi, D., Kahn, O., Miller, J. S., Palacio, F., Eds.; *Magnetic Molecular Materials*; NATO ASI Series E 198; Kluwer: Dordrecht 1991.
(235) Willett, R. D.; Gatteschi, D.; Kahn, O.; Eds.; *Magneto-Structural Correlations in Exchange Coupled Systems*; NATO ASI Series C 140; Reidel: Dordrecht, 1984.
(236) Leggett, A. J. *Phys. Rev. B* **1984**, *30*, 1208.
(237) Stamp, P. C. E.; Chudnovsky, E. M.; Barbara, B. *Int. J. Mod. Phys.* **1992**, *6*, 1355.
(238) Awschalom, D. D.; DiVincenzo, D. P.; Smyth, J. F. *Science* **1992**, *258*, 414.
(239) Gatteschi, D.; Pardi, L.; Barra, A.-L.; Müller, A. In *Polyoxometalates: from Platonic Solids to Anti-retroviral Activity*; Pope, M. T., Müller, A., Eds.; Kluwer: Dordrecht, 1994; p 219.
(240) Blondin, G.; Girerd, J.-J. *Chem. Rev. (Washington, D.C.)* **1990**, *90*, 1359.
(241) Dismukes, G. C. In *Mixed Valency Systems: Applications in Chemistry, Physics and Biology*; Prassides, K., Ed.; Kluwer: Dordrecht, 1990.
(242) Rao, C. N. R. *Eur. J. Chem.* **1996**, *2*, 1499.
(243) Robin, M. B.; Day, P. *Adv. Inorg. Chem. Radiochem.* **1967**, *10*, 247.
(244) Syamal, A. *Coord. Chem. Rev.* **1975**, *16*, 309.
(245) Plass, W. *Angew. Chem., Int. Ed. Engl.* **1996**, *35*, 627.
(246) Neves, A.; Wieghardt, K.; Nuber, B.; Weiss, J. *Inorg. Chim. Acta* **1988**, *150*, 183.
(247) Wieghardt, K.; Bossek, U.; Volckmar, K.; Swiridoff, W.; Weiss, J. *Inorg. Chem.* **1984**, *23*, 1387.
(248) Carrano, C. J.; Nunn, C. M.; Quan, R.; Bonadies, J. A.; Pecoraro, V. L. *Inorg. Chem.* **1990**, *29*, 944.
(249) Castro, S. L.; Cass, M. E.; Hollander, F. J.; Bartley, S. L. *Inorg. Chem.* **1995**, *34*, 466.
(250) Wrobleski, J. T. *Inorg. Chem.* **1988**, *27*, 946.
(251) Carlisle, G. O.; Simpson, G. D. *J. Mol. Struct.* **1975**, *25*, 219.
(252) Hanson, M. V.; Smith, C. B.; Carlisle, G. O. *Inorg. Nucl. Chem. Lett.* **1975**, *11*, 865.
(253) Crawford, V. H.; Hatfield, W. E.; Tapscott, R. E. *J. Mol. Struct.* **1977**, *38*, 141.
(254) Wrobleski, J. T.; Thompson, M. R. *Inorg. Chim. Acta* **1988**, *150*, 269.
(255) Mohan, M.; Bond, M. R.; Otieno, T.; Carrano, C. J. *Inorg. Chem.* **1995**, *34*, 1233.
(256) Barra, A.-L.; Gatteschi, D.; Pardi, L.; Müller, A.; Döring, J. *J. Am. Chem. Soc.* **1992**, *114*, 8509.
(257) Gatteschi, D.; Pardi, L.; Barra, A.-L.; Müller, A.; Döring, J. *Nature* **1991**, *354*, 463.
(258) Müller, A.; Sessoli, R.; Krickemeyer, E.; Bögge, H.; Meyer, J.; Gatteschi, D.; Pardi, L.; Westphal, J.; Hovemeier, K.; Rohlfing, R.; Döring, J.; Hellweg, I.; Beugholt, C.; Schmidtmann, M. *Inorg. Chem.*, in press.
(259) Müller, A.; Döring, J. *Angew. Chem., Int. Ed. Engl.* **1988**, *27*, 1721.
(260) Gatteschi, D.; Pardi, L. *Gazz. Chim. Ital.* **1993**, *123*, 231.
(261) Barra, A.-L.; Debrunner, P.; Gatteschi, D.; Schulz, C. E.; Sessoli, R. *Europhys. Lett.* **1996**, *35*, 133.
(262) Aubin, S. M. J.; Wemple, M. W.; Adams, D. M.; Tsai, H.-L.; Christou, G.; Hendrickson, D. N. *J. Am. Chem. Soc.* **1996**, *118*, 7746.
(263) Day, V. W.; Klemperer, W. G.; Yagi, O. M. *J. Am. Chem. Soc.* **1989**, *111*, 5959.
(264) Casañ-Pastor, N.; Baker, L. C. W. *J. Am. Chem. Soc.* **1992**, *114*, 10384.
(265) Kozik, M.; Baker, L. C. W. *J. Am. Chem. Soc.* **1990**, *112*, 7604.
(266) Kozik, M.; Casañ-Pastor, N.; Hammer, C. F.; Baker, L. C. W. *J. Am. Chem. Soc.* **1988**, *110*, 7697.
(267) Kozik, M.; Baker, L. C. W. *J. Am. Chem. Soc.* **1987**, *109*, 3159.
(268) Kozik, M.; Hammer, C. F.; Baker, L. C. W. *J. Am. Chem. Soc.* **1986**, *108*, 2748.
(269) Borrás-Almenar, J. J.; Clemente, J. M.; Coronado, E.; Tsukerblat, B. S. *Chem. Phys.* **1995**, *195*, 1.
(270) Borrás-Almenar, J. J.; Clemente, J. M.; Coronado, E.; Tsukerblat, B. S. *Chem. Phys.* **1995**, *195*, 29.
(271) Borrás-Almenar, J. J.; Clemente, J. M.; Coronado, E.; Tsukerblat, B. S. *Chem. Phys.* **1995**, *195*, 17.
(272) Gómez-García, C. J.; Coronado, E.; Ouahab, L. *Angew. Chem., Int. Ed. Engl.* **1992**, *31*, 649.
(273) Evans, H. T.; Tourné, C. M.; Tourné, G. F.; Weakley, T. J. R. *J. Chem. Soc., Dalton Trans.* **1986**, 2699.
(274) Gómez-García, C. J.; Coronado, E.; Borrás-Almenar, J. J. *Inorg. Chem.* **1992**, *31*, 1667.
(275) Casañ-Pastor, N.; Bas-Serra, J.; Coronado, E.; Pourroy, G.; Baker, L. C. W. *J. Am. Chem. Soc.* **1992**, *114*, 10380.
(276) Gómez-García, J. C.; Coronado, E.; Borrás-Almenar, J. J.; Aebersold, M.; Güdel, H. U.; Mutka, H. *Physica B* **1992**, *180*−*181*, 238.
(277) Gómez-García, J. C.; Coronado, E.; Gómez-Romero, P.; Casañ-Pastor, N. *Inorg. Chem.* **1993**, *32*, 3378.
(278) Gatteschi, D.; Sessoli, R.; Plass, W.; Müller, A.; Krickemeyer, E.; Meyer, J.; Sölter, D.; Adler, P. *Inorg. Chem.* **1996**, *35*, 1926.
(279) Tsukerblat, B. S.; Belinski, M. I.; Fainzil′berg, V. E. *Sov. Chem. Rev.* **1987**, *9*, 399.
(280) Vannimenus, J.; Toulouse, G. *J. Phys. C: Solid State Phys.* **1977**, *10*, L537.
(281) McCusker, J. K.; Schmitt, E. A.; Hendrickson, D. N. In *Magnetic Molecular Materials*; Gatteschi, D., Kahn, O., Miller, J. S., Palacio, F.; Eds.; NATO ASI Series E198; Kluwer: Dordrecht, 1991; p 297.
(282) Moriya, T. *Phys. Rev.* **1960**, *117*, 635.
(283) Müller, A., Dress, A., Vögtle F., Eds. *From Simplicity to Complexity in Chemistry − and Beyond. Part I.*; Vieweg: Braunschweig, 1996.

CR9603946